Thermal evolution of the metamorphism in the eastern Taiwan Central Range: implications for Yuli Belt exhumation

ABSTRACT

The Yuli Belt of the eastern Taiwan Central Range encloses high pressure (HP) mafic–ultramafic blocks and hosts intensely deformed greenschist-facies metasediments. It is still debated if the Chulai Formation to the east is part of the Yuli Belt. To solve this problem, we provide new maximum metamorphic temperature in both units using Raman spectroscopic geo-thermometry in relation to structural deformation. The new peak metamorphic temperatures compiled with published data support systematic spatial variations across the eastern Taiwan Central Range. The Yuli Belt shows peak temperatures of ca. 400–550 °C higher than those of adjacent units. Temperatures > 500 °C in the Yuli Belt are close to three HP blocks. The temperature difference between the Yuli Belt and Chulai Formation reaches over 100 °C. It is likely that the contact between both units is a fault and that they underwent the same deformation history after its E-vergent backfolding phase.

Keywords: Taiwan; Yuli Belt; geothermometer; RSCM; blueschists

1 INTRODUCTION AND GEOLOGICAL SETTING

The collision between the Eurasian passive continental margin and the Luzon volcanic arc of the overriding Philippine Sea Plate formed the Taiwan Central Range since ca. 4–6 Ma (e.g., Chang and Chi, 1983; Suppe, 1984). Five roughly N-S oriented major morphotectonic units make up the Taiwan mountain belt (Fig. 1a). The Longitudinal Valley Fault (F4) separates units to the west derived from the Eurasian Plate, and the Coastal Range of the Philippine Sea Plate to the east. The Backbone Slates comprises a metamorphosed Cenozoic sedimentary cover unconformably overlying the Mesozoic metamorphic basement (the Tailuko Belt of the Tananao Complex) (Fig. 1a). The outcropping stratigraphy of the Backbone Slates consists of the prehnite–pumpellyite to greenschist facies Pilushan phyllite (incl. Heiyenshan and Tayuling formations) of Eocene (to Miocene) age as well as the prehnite–pumpellyite facies Lushan slate of Miocene age in the western range, and the greenschist facies Chulai Formation of

Eocene age in the eastern range from the southern Cross-island highway to around Juisui area (e.g., Chow and Lin, 1974; Stanley et al., 1981; Ho, 1986).

The Tananao Complex crops out as a narrow belt on the eastern side of Taiwan's Central Range (Fig. 1a) and bears evidence of polymetamorphism and multiple deformations (e.g., Ernst and Jahn 1987). Traditional classification subdivides the Tananao Complex into the western pre-Cenozoic Tailuko Belt and the eastern Cretaceous to Miocene Yuli Belt (e.g., Ho, 1986; Chen et al., 2017), separated by the Shoufeng Fault (Yen, 1963, F3 in Fig. 1), a possibly mega-backthrusting fault (e.g., Zhang et al., 2020). The Tailuko Belt consists of Permian Chiuchu marbles and variegated Mesozoic Kuyuan greenschists (Liou, 1981; Fig. 2). The Yuli Belt contains lithologically heterogeneous blueschist-facies rocks in what is referred to as high-pressure (HP) tectonic or exotic blocks (e.g., Liou et al., 1975) surrounded by an intensely deformed schistose unit of lower metamorphic grade (Fig. 1b). Three larger exposures of these blocks are the Wanjun, Juisui, and Chinsui Hsi areas (Yen, 1963; Liou et al., 1975). Some petrological pressure-temperature-timing studies and structural analyses (e.g., Yang and Wang,1985; Tsai et al., 2013; Sandmann et al., 2015; Conand et al., 2020) suggest an allochthonous HP blueschist nappe (~550 °C, 10–12 kbar) emplaced on top of the lower-grade metasedimentary unit along a thrust during a first deformation phase D1 (Zhang et al., 2020). The Yuli Belt's eastern contact with the Chulai Formation of the Backbone Slates (Fig. 1b) is strongly deformed and the sharp boundary in terms of lithology and metamorphic grade was interpreted as an unconformity (Stanley et al., 1981; Ho, 1986). However, based on recent detrital zircons ages, from the Yuli Belt metasediments and the northern part of the Chulai Formation, as young as Upper Miocene (e.g., 11.2 ± 0.2 Ma, Mesalles et al., 2020), an alternative trace of Shoufeng Fault has been depicted and the Chulai Formation has been reinterpreted as part of the Yuli Belt (e.g., Chen et al., 2017, 2019; Conand et al., 2020; Zhang et al., 2020; Fig. 1b).

Raman spectroscopy of carbonaceous material (RSCM) has been substantially used as a quantitative geothermometer to estimate maximum metamorphic temperature of the host sediments (e.g., Wopenka and Pasteris,1993; Yui et al., 1996; Beyssac et al., 2002; Lahfid et al., 2010; Henry et al. 2019). Beyssac et al. (2007) was a pilot study using RSCM at a continuous thermal gradient from the Backbone Slates to the Tananao Complex in Taiwan (Fig. 1b). The study encouraged a wider use of RSCM as

geothermometer (e.g., Chim et al., 2018; Chen et al., 2019; Conand et al., 2020). However, most past efforts have focused on the central part of the island, and little attention has been paid to the eastern side (Fig. 1b). Kouketsu et al. (2019)'s three samples from the Yuli Belt suggested that the results relate not only to peak metamorphic temperature, but also to the pre-metamorphic history and the duration of metamorphic heating. Two samples taken from the Chulai Formation (in Lakulaku and Xinwuliu areas; Fig. 1b) have been estimated via RSCM (ca. 370°C; Beyssac et al., 2007; Chim et al., 2018). The temperature is much lower than those of the adjacent Yuli Belt (ca. 450~500°C; Fig. 1b), which shows a significant gap between these two units. It is likely that the contact as a fault. These results and conclusions need to be tested with a larger sample set.

The purpose of this study is to investigate the thermodynamic evolution of the metamorphism in the Yuli Belt of Taiwan based on new RSCM data combined with interpretations of the structural deformation of the Yuli Belt and adjacent units. We also discussed the potential influence of our new data on the working tectonic model of the Taiwan arc-continent collision.

2 SAMPLING AND METHODOLOGY

To fill the gap in eastern Taiwan, our data complement previous RSCM data from transects of two cross-island highways (Beyssac et al., 2007), southern Taiwan (Conand et al., 2020), northern Taiwan (Chen et al., 2019), the Coastal Range (Chim et al., 2018), and the Yuli Belt (Syu, 2009; Kouketsu et al., 2019). Temperatures over 330°C were calibrated using the equation proposed by Beyssac et al. (2002) and low temperatures (200°C < T < 330 °C) were obtained using Lahfid et al. (2010) (Fig. 1b). Data of Chim et al. (2018) are plotted as arithmetic means of a larger population of data at the estimated localities shown. Our sixteen black metapelites/phyllites samples were collected along selected transects in the Yuli Belt and the Chulai Formation of eastern Taiwan (Fig. 1b; Table 1; representative microscopic features, Fig.S1). At each sampling site, a careful examination of structural deformation was carried out to systematically measure and characterize ductile deformation by the direction of stretching lineation and associated sense of shear whenever possible (Figs. 2, 3).

RSCM was used to quantify the degree of thermal alteration of carbonaceous material (CM) within the sampled metasediments. Raman spectra were obtained using corundum polished standard petrographic thin sections, with a thickness of ca. 30 μm.

RSCM analyses were performed at the Friedrich Schiller University of Jena using the Horiba LabRam HR Evolution with a focal length of 800 mm and a 532 nm Spectra Physics argon laser. Grains of CM were selected and analyzed one by one with an Olympus microscope mounted on the Raman spectrometer. 31 to 107 particles of CM (with an average of 66.4 for all samples) were collected per sample (Tables 1, S1). The spectra were baseline corrected via LabSpec Spectral Software using a linear baseline in the spectral range of 1100–1800 cm^{-1}, and decomposed to the G-band (1580 cm^{-1}), D1-band (1350 cm^{-1}) and D2-band (1620 cm^{-1}). We evaluated the crystallinity of CM using the parameter R2, which is the area ratio of D1/(G + D1 + D2). According to the calibration of Beyssac et al. (2002), the R2-ratio shows a linear correlation to peak metamorphic temperature (T) in the range of 330 °C to 640 °C. Standard errors are given for temperature with 1σ. Details on data processing and representative Raman spectra of CM in each sample are provided in supporting materials, respectively (Table S1; Fig.S2). Despite the use of the same calibration method, RSCM data obtained by different authors may show slight discrepancies in view of diverse analytical setups and differences in data handling.

3 RESULTS

RSCM temperature contours are generally along the NNE-strike in the eastern Taiwan Central Range (Fig. 4). Compared with RSCM temperatures of other major morphotectonic units in Taiwan (Fig. 1a), the Tananao Complex shows higher temperatures between ca. 350 and 550 °C (Fig. 1b). The western Tailuko Belt shows average temperatures of c. 450 °C. In its northern part that hosts numerous granitoids intrusions (Fig. 1b), temperatures can reach over 500 °C. The peak metamorphic temperatures along the Central and Southern cross island highways show a general eastward increasing trend in the Tailuko Belt (Figs. 1b, 3). We interpret the Tailuko Belt to be an eastward backfolding and thrusting structure in the orogenic retro-wedge, evidenced by the new developing W-dipping foliations (D3) overprinting earlier E-dipping foliated planes during crenulation (Fig. 3,4). The eastern Yuli Belt shows generally maximum metamorphic temperatures between ca. 400 and 550 °C, which is higher than in adjacent units. The peak metamorphic temperatures in the Yuli Belt are complicated due to the intensely multi-deformed schist formations (Fig. 2). In places, maximum temperatures in the Yuli Belt exceed 500 °C, specifically in close proximity to three HP metamorphic exotic blocks (Figs.1b, 2). We interpret higher temperatures

to indicate antiformal structures, and lower temperatures to be synforms in the mostly NW-dipping schistose unit of the Yuli Belt (Figs. 2, 3). In the Yuli Belt, the northwest-dipping dominant (D3) foliation (Fig. 2) refolded the earlier (D2) compositional layering (Fig.S3(a)(c)), and simple shear deformed schists with top-to-the-SE/S kinematic (Fig.S4(i)(j)), considered to have accommodated eastward backfolding and thrusting during D3. Temperature transitions across the Shoufeng Fault (e.g., along Shoufeng Hsi and Xinwuliu Hsi, Figs. 1b, 3) are gradual, which is in agreement with lithological and fabric transitions in the field. Dip direction and dip of schistose foliations are mostly W- to NW in the Yuli and Tailuko belts and remain constant across the fault (Figs. 2, 3). Thus, the juxtaposition of the two belts across the Shoufeng Fault may form during an early W-directed transport (D2) before eastward backfolding and thrusting (D3).

By contrast, samples from the Backbone Slates, including the western Pilushan Formation and the eastern Chulai Formation, contain much lower RSCM temperatures between 295 and 372 °C (Figs. 1b, 2, 3). The Chulai Formation is significantly different from the adjacent Yuli Belt but shares a number of key features to the Pilushan Formation. (1): The Chulai Formation shows average temperatures of c. 360 °C, within the temperature range of the Pilushan Formation, between 330 and 450°C. (2): Both Chulai and Pilushan formations contain pervasive silvery gray, quartz-rich phyllites and slates with NE/N-dipping in the field (S2 foliation in Fig.S3; Figs. 2, 3). Therefore, we propose a stratigraphic correlation linking Chulai Formation and Pilushan Formation together in the Backbone Slates (Fig. 3). (3): The temperature difference between the Chulai Formation and the Yuli Belt reaches ca. 100 °C (e.g., in the cross sections A-B and E-F, Figs. 2, 3), indicating the contact between these two units as a fault, namely the Chuisui Fault in this study (F2; Figs. 1, 2, 3). The Yuli Belt schist has experienced greenschist to amphibolite facies metamorphism at deeper levels, with higher estimated temperatures than the phyllitic Chulai Formation. On the basis of surface structural data and RSCM data, we interpret the whole Yuli Belt to be a nappe that emplaced on top of the lower-grade Chulai Formation along the Chuisui Fault during a second deformation phase D2. In the field metapsammitic to metapelitic sediments of the ductile contact zone are intensely deformed, with gradational textural and metamorphic change (Fig.S4(a)(b)). The eastward transport direction (D3) is observed in the contact zone, showing deformation structures indicative of top-to-the SE shear (Fig.S4),

kinematically similar to the Shoufeng Fault. It suggests both the Yuli Belt and the Chulai Formation may experience the same deformation history after D2 deformation.

4 Evolution in the eastern Taiwan Central Range

The tectonic evolution and structural position of the Yuli Belt as part of the Taiwan mountain belt is a key element for to understand the preceding subduction and the ongoing arc-continent collision. Metamorphic overprinting and age relations (e.g., Sandmann et al., 2015), RSCM data (e.g., this study; Fig. 4), and structural analyses (e.g., Zhang et al., 2020) suggest that the eastern Taiwan Central Range formed during four successive deformation stages, termed D1, D2, D3 and D4 in the following. A kinematic evolutionary shoe-box cartoon (Figs. 5, S5) is proposed to illustrate the relationship between cooling and erosion during exhumation of the eastern Taiwan Central Range.

D1: HP rock exhumation phase. The HP, blueschist-facies blocks within the Yuli Belt show Mid-Miocene protolith ages (three samples weighted mean of 15.6 ± 0.3 Ma; Chen et al., 2017), about when the South China Sea ceased spreading (ca. 15.5 Ma, Taylor and Hayes, 1983; Sibuet et al., 2002) and started subducting under the Philippine Sea Plate (Huang et al., 2006). The crystallization ages perhaps provide the single most solid maximum age for Taiwan mountain building initiation. HP blocks subducted reaching peak-P-T conditions (e.g., Beyssac et al., 2008; Tsai et al., 2013) and exhumed portions of crust and mantle along the HP thrust on top of the lower-grade metasedimentary unit of the Yuli Belt (F1; Zhang et al., 2020; Fig. 5). The higher RSCM temperatures of the metasediments surrounding the HP blocks (Fig. 4) are a result of additional thermal overprint either by the HP metamorphic blocks or by a retrograde overprint under amphibolite- to higher greenschist-facies conditions along the exhuming F1 thrust. Both possibilities suggest that the post-D1 metamorphic history of the Yuli Belt and the HP metamorphosed blocks is similar.

D2: W-ward folding and thrusting phase. Recent chronological constraints argue for the Yuli Belt metasedimentary unit and the Chulai Formation share the same continental affinity zircon U-Pb age populations as young as Upper Miocene (ca. 11 Ma, Chen et al., 2017; Mesalles et al., 2020). However, different lithologies and different maximum metamorphic temperatures (Figs. 4) between the Yuli Belt and the Chulai Formation contradict this interpretation. In this study, the correlation with the Eocene to Upper

Miocene age has been assigned to the sediments in Chulai and Pilushan Formations. Rift-related half-grabens generally accumulated via Eocene-Miocene fluvial to outer shelf deposits over 6 km thick, and derived from the Eurasian continent (Yu et al., 2013) (Fig. S5). RSCM temperatures, lithological-, and fabric- transitions are constant across the Shoufeng Fault (Fig. 1b, 4; Zhang et al., 2020). This indicates that the juxtaposition of the Yuli Belt and the Tailuko Belt (unconformably covered by Pilushan Formation) across the Shoufeng Fault formed during early W-directed transport (D2 phase; Fig. 5, S5). The Yuli Belt including the former allochthonous HP metamorphic material was thrusted on top of the Pilushan/Chulai Formation along F2 (Chinsui Fault).

D3: Erosional E-ward backfolding and backthrusting phase. The Yuli Belt appears as a large synformal structure with top-to-the-SE shear at the footwall of Shoufeng Fault (F3), in contact with the Tailuko Belt to the west as part of the hanging wall of the F3 (Fig. 5). The majority of the HP metamorphic material was eroded during this deformation stage with the exception of small relic blocks in the center of the synformal structure (e.g., cross section C-D; Fig. 2). Notably the trace of the F2 contact is poorly preserved and was only reported in the Xinwuliu Hsi area along the Yuli Belt (Stanley et al., 1981). A possible explanation for this might be that the Chulai Formation underwent essentially the same deformation history as the Yuli Belt (in D3-D4 phases), as indicated by sedimentary relationships and structural considerations (Ho, 1986; Fig. S4). Thus, the emplacement of the higher-grade metasedimentary Yuli Belt as a nappe on top of the lower-grade Chulai Formation was most likely a separate step prior to the D3 refolding and backthrusting (Figs. 3, 5). Future research should hence focus on kinematics and fault-related fabrics along the contact to test our model.

D4: Erosion phase. RSCM contours (Fig. 4), the continental margin, and the Luzon arc of the Philippine Sea plate are subparallel, nourishing an initial collision that was simultaneous along the NNE-strike. Apatite and zircon fission-track ages (Fuller et al., 2006; Resentini et al., 2020) and catchments studies (Dadson et al., 2003) both imply that erosion rates in the Backbone Slates were systematic higher towards the south (Fig. 4). F4 (Longitudinal Valley Fault) possibly overprinted the earlier structures in combination with later erosion.

5 CONCLUSIONS

We apply new RSCM temperature in from metasedimentary rocks of the Yuli Belt and the Chulai Formation. Peak metamorphic temperatures in the greenschist-facies metasediments, when compiled with published data, support systematic spatial variations across the eastern Taiwan Central Range. The Yuli Belt shows higher temperatures, at of c. 400–550 °C than adjacent units; close to inherited HP blocks metasediments of the Yuli Belt indicate maximum metamorphic temperatures > 500 °C; the temperature difference between the Yuli Belt and the Chulai Formation can exceed 100 °C. Therefore, it appears more likely that the contact between the Yuli Belt and the Chulai Formation is a fault contact (F2), suggesting a synformal structural position of the Yuli Belt, as result of backfolding of during the D3 phase of the Taiwan Central Range.

REFERENCES

Beyssac, O., Goffé, B., Chopin, C. and Rouzaud, J.N., 2002. Raman spectra of carbonaceous material in metasediments: a new geothermometer. *Journal of Metamorphic Geology*, **20**, 859–871. doi:10.1046/j.1525-1314.2002.00408.x

Beyssac, O., Simoes, M., Avouac, J. P., Farley, K. A., Chen, Y.G., Chan, Y.C. and Goffé, B., 2007. Late Cenozoic metamorphic evolution and exhumation of Taiwan. *Tectonics*, **26**, TC6001, doi:10.1029/2006TC002064

Beyssac, O., Negro, F., Simoes, M.Y., Chan, C. and Chen, Y. G., 2008. High-pressure metamorphism in Taiwan: from oceanic subduction to arc-continent collision. *Terra Nova*, **20**, 118-125, doi:10.1111/j.1365-3121.2008.00796.x

Chang, S.S. L. and W. R. Chi, 1983. Neogene Nannoplankton biostratigraphy in Taiwan and the tectonic implications. *Petroleum Geology of Taiwan*, **19**, 93–147

Chen, W. S., Chung, S. L. Chou, H. Y., Zugeerbai, Z., Shao, W. Y. and Lee, Y. H., 2017. A reinterpretation of the metamorphic Yuli belt: Evidence for a middle-late Miocene accretionary prism in eastern Taiwan. *Tectonics*, **36**, 188–206. https://doi.org/10.1002/2016TC004383

Chen, C. T., Chan, Y. C., Beyssac, O., Lu, C. Y., Chen, Y. G., Malavieille, J., Kidder, S. B. and Sun, H. C., 2019. Thermal history of the Northern Taiwanese slate belt and implications for wedge growth during the Neogene arc-continent collision. *Tectonics*, **38**, 3335–3350. https://doi.org/10.1029/2019TC005604

Chim, L. K., Yen, J. Y., Huang, S. Y., Liou, Y. S. and Tsai, L. L., 2018. Using Raman Spectroscopy of Carbonaceous Materials to track exhumation of an active orogenic

belt: An example from Eastern Taiwan. *Journal of Asian Earth Sciences*, **164**, 248–259. https://doi.org/10.1016/j.jseaes.2018.06.030

Chow, J.T. and Lin, C. C., 1974. Geology of Taiwan. Taiwan Provincial Documentary Committee, 450 p. (in Chinese)

Conand, C., Mouthereau, F., Ganne, J., Lin, A. T.-S., Lafhid, A., Daudet, M., Mesalles, L., Giletycz, S. and Bonzani, M., 2020. Strain partitioning and exhumation in oblique Taiwan collision: role of rift architecture and plate kinematics: *Tectonics*, **39**, p. e2019TC005798

Dadson, S.J., Hovius, N., Chen, H., Dade, W.B., Hsieh, M.L., Willett, S.D., Hu, J.D., Horng, M.J., Chen, M.C., Stark, C.P., Lague, D. and Lin, J.C., 2003. Links between erosion, runoff variability and seismicity in the Taiwan orogen. *Nature*, **426**, 648–651

Fuller, C.W., Willet, S.D., Fisher, D. and Lu, C.Y., 2006. A thermomechanical wedge model of Taiwan constrained by fission-track thermochronometry. *Tectonophysics*, **274**, 97–115

Henry D. G., Jarvis, I., Gillmore, G. and Stephenson, M., 2019. Raman spectroscopy as a tool to determine the thermal maturity of organic matter: Application to sedimentary, metamorphic and structural geology. *Earth-Science Reviews*, **198**, https://doi.org/10.1016/j.earscirev.2019.102936

Ho, C. S., 1986, A synthesis of the geologic evolution of Taiwan. *Tectonophysics*, **125**, 1-16. https://doi.org/10.1016/0040-1951(86)90004-1

Huang, C. Y., Yuan, P. B. and Tsao, S. J., 2006. Temporal and spatial records of active arc-continent collision in Taiwan: A synthesis. *Geological Society of America Bulletin*, **118**, 274-288, doi:10.1130/b25527.1

Kouketsu, Y., Tsai, C.H. and Enami, M., 2019. Discovery of unusual metamorphic temperatures in the Yuli belt, eastern Taiwan: New interpretation of data by Raman carbonaceous material geothermometry. *Geology*, **47**, 522–526. doi: https://doi.org/10.1130/G45934.1

Lahfid, A., Beyssac, O., Deville, E., Negro, F., Chopin, C. and Goffé, B., 2010. Evolution of the Raman spectrum of carbonaceous material in low-grade metasediments of the Glarus Alps (Switzerland). *Terra Nova*, **22**: 354–360. doi:10.1111/j.1365-3121.2010.00956.x

Liou, J. G., C. O. Ho and T. P. Yen, 1975. Petrology of some Glaucophane Schists and Related Rocks from Taiwan. *Journal of Petrology*, **16**, 80-109

293 Lin, C. W. and Chen, W. S., 2016. Geologic Map of Tawan. Published by Geological
294 Society of Taiwan
295 Mesalles, L., Y.-H. Lee, T.-C. Ma, W.-L. Tsai, X.-B. Tan and H.-Y. Lee, 2020. A
296 Late-Miocene Yuli Belt? New constraints on the eastern Central Range depositional
297 ages. *Terr. Atmos. Ocean. Sci.*, **31**, 1-12, doi: 10.3319/ TAO.2019.06.24.01
298 Resentini, A., Malusà, M. G. and Garzanti, E., 2020. Ongoing exhumation of the
299 Taiwan orogenic wedge revealed by detrital apatite thermochronology: The impact
300 of effective mineral fertility and zero-track grains. *Earth and Planetary Science*
301 *Letters*, **544**, 116374
302 Sandmann, S., Nagel, T. J., Froitzheim, N., Ustaszewski, K. and Münker, C., 2015.
303 Late Miocene to early Pliocene blueschist from Taiwan and its exhumation via
304 forearc extraction. *Terra Nova*, **27**, 285–291. https://doi.org/10.1111/ter.12158
305 Shyu, J. B. H., Sieh, K., Chen, Y. G. and Liu, C. S., 2005. Neotectonic architecture of
306 Taiwan and its implications for future large earthquakes. *J. Geophys. Res*., **110**,
307 B08402, doi:10.1029/2004JB003251
308 Sibuet, J. C., Hsu, S. K., Pichon, X. L., Formal, J. L., Reed, D., Moore, G. and Liu, C.
309 S., 2002. East Asia platetectonics since 15 Ma: constraints from the Taiwan region.
310 *Tectonophysics*, **344**, 103-134. https://doi.org/10.1016/S0040-1951(01)00202-5
311 Stanley, R. S., Hill, L. B., Chang, H. C. and Hu, H. N., 1981. A transect through the
312 metamorphic core of the central mountains, southern Taiwan, *Mem. Geol. Soc.*
313 *China*, **4**, 443–473
314 Suppe, J., 1984, Kinematics of arc-continent collision, flipping of subduction, and
315 back-arc spreading near Taiwan. *Geological Society of China Memoir*, **6**, 131-146
316 Syu, B.Y., 2009. Preliminary discussion on X-ray diffraction pattern and Raman
317 spectrum of carbonaceous materials in metamorphic complexes in Juisui and
318 WanJun, Taiwan. Master dissertation, National Taiwan Normal University, 59pp
319 Taylor, B. and Hayes, D. E., 1983. Origin and history of South China Sea Basin, In D.
320 E. Hayes (Ed.), The Tectonic and Geologic Evolution of Southeast Asian Seas and
321 Islands: Part 2, Am. Geophys. Union., Washington, DC, 23-56,
322 doi:10.1029/gm027p0023
323 Tsai, C. H., Lizuka, Y. and Ernst, W. G., 2013. Diverse mineral compositions,
324 textures, and metamorphic P-T conditions of the glaucophane bearing rocks in the
325 Tamayen mélange, Yuli belt, eastern Taiwan. *Journal of Asia Earth Sciences*, **63**,
326 218–233

Wopenka, B. and Pasteris, J.D., 1993. Structural characterization of kerogens to granulitefacies graphite: Applicability of Raman microprobe spectroscopy. *American Mineralogist*, **78**,533–577

Yang, C.-N. and Wang, Y., 1985. Petrotectonic study on the Yuli belt of the Tananao Schist in the Juisui area, eastern Taiwan. *Acta Geol. Taiwanica*, **23**, 153–180

Yen, T. P., 1963. The metamorphic belts within the Tananao schist terrane of Taiwan. *Proc. Geol. Soc. China*, **6**, 72–74

Yu, N.T., Teng, L.S., Chen, W.S., Yue, L.F. and Chen, M.M., 2013. Early post-rift sequence stratigraphy of a Mid-Tertiary rift basin in Taiwan: insights into a siliciclastic fill-up wedge. *Sediment. Geol.*, **286–287**, 39–57

Yui, T. F., Okamoto, K., Usuki, T., Lan, C. Y., Chu, H. T. and Liou, J. G., 2009. Late Triassic–Late Cretaceous accretion/subduction in the Taiwan region along the eastern margin of South China – evidence from zircon SHRIMP dating. *International Geology Review*, **51**, 304-328, DOI: 10.1080/00206810802636369

Yui, T.F., Huang, E. and Xu, J., 1996. Raman spectrum of carbonaceous material: a possible metamorphic grade indicator for low-grade metamorphic rocks. *J. metamorphic Geol.*, **14**, 115–124

Zhang, Y., Tsai, C.-T., Froitzheim, N., Ustaszewski, K., 2020. The Yuli Belt in Taiwan: part of the suture zone separating Eurasian and Philippine Sea plates. *Terr. Atmos. Ocean. Sci.*, accepted. DOI: 10.3319/TAO.2020.06.28.01

Figure captions

Fig. 1: (a) Tectonic map of Taiwan. Traditional nomenclature subdivides the Tananao Complex into the western Tailuko Belt (colored light gray) and the eastern Yuli Belt (colored dark gray) (e.g., Lin and Chen, 2016). (b) Map of peak temperatures in eastern Taiwan obtained from RSCM, compiling various sources. All RSCM were obtained using the calibration of Beyssac et al. (2002) for T>330°C and low temperatures (200°C < T < 330 °C) were obtained using Lahfid et al. (2010) marked with "*". (1): Data of Chim et al., (2018) are plotted as arithmetic means of a larger population of data at the localities shown. F2: Chinsui Fault (after Lin and Chen, 2016); F3: Shoufeng Fault (with different interpretations, e.g., Lin and Chen, 2016; Chen et al., 2017); F4: Longitudinal Valley Fault (LVF) (after Shyu et al., 2005).

Fig. 2: Geological map and cross sections (A-B and C-D) in the Lakulaku Hsi and Chinsui Hsi areas. See Fig. 1b for location. Parentheses enclosed letters indicate the locations of outcrops in Fig.S3, S4. The high-pressure metamorphosed units formed allochthonous nappe outliers of a former thrust sheet, emplacing on top of the lower-grade metasedimentary unit.

Fig. 3: Geological map and the cross section E-F of the Xinwuliu Hsi area. See Fig. 1b for location. (b): outcrop location in Fig.S3. The lower-grade metasedimentary unit of the Yuli Belt is interpreted to thrust on top of the Pilushan/Chulai Formation before the E-vergent refolding.

Fig. 4: RSCM temperature contours in the eastern Taiwan Central Range. Contours are processed by line smoothing (Gaussian Filtering, Sensitivity 3) within major morphotectonic units. Late Cretaceous granitoids intrusions are shown in the northern Tailuko Belt (Yui et al., 2009). Exposure of reset apatite and zircon fission-track ages (after Fuller et al., 2006 and Resentini et al., 2020) supports southward erosion rates are higher in the retro-side of the Taiwan orogen, as also suggested by catchments studies (after Dadson et al., 2003).

Fig. 5: Conceptual kinematic model to explain the Yuli Belt exhumation and structural position (modified after Zhang et al., 2020). D1 stage: high pressure metamorphic rock thrusted over the Yuli Belt metasedimentary unit along the F1 (HP thrust); D2 stage: W-ward thrusting of Yuli Belt onto Tailuko Belt along F2 (Chinsui Fault); D3 stage: E-ward backfolding and backthrusting along F3 (Shoufeng Fault), in combination with

later erosion; D4 stage: F4 (LVF, Longitudinal Valley Fault) possibly overprinted the earlier structures. See text for further discussion.

Figures

Fig. 1:

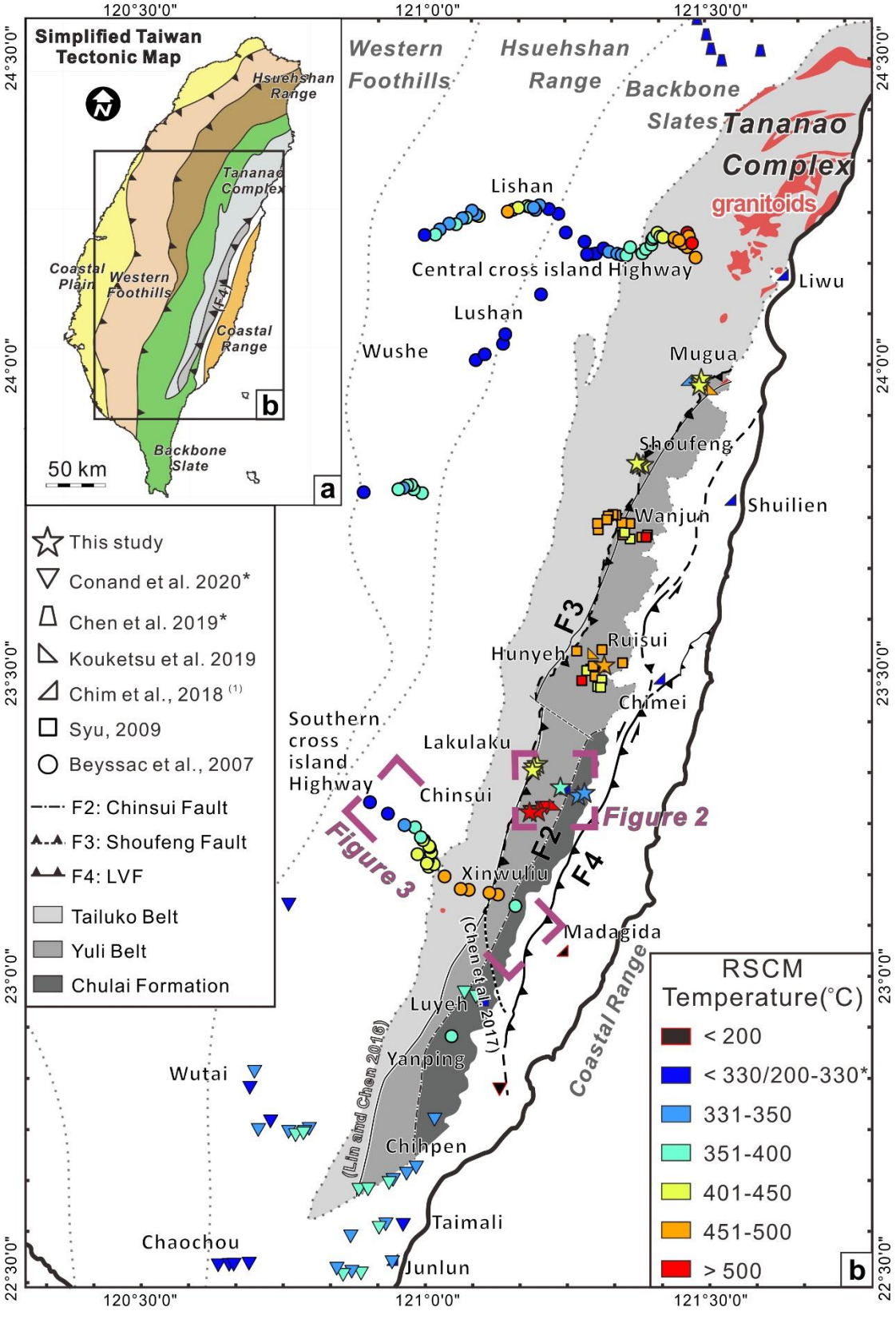

387 Fig. 2:

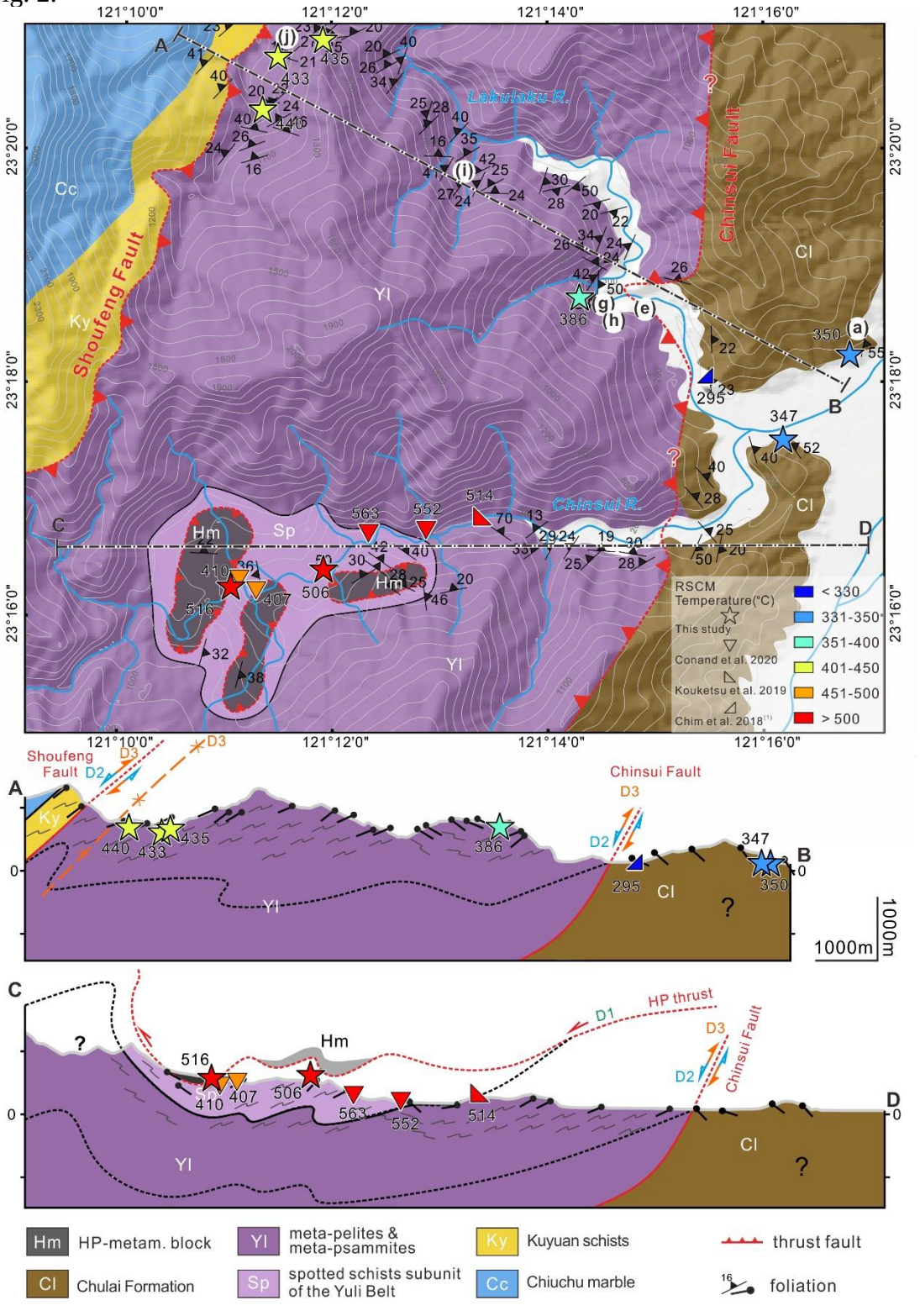

388
389

390 Fig. 3:

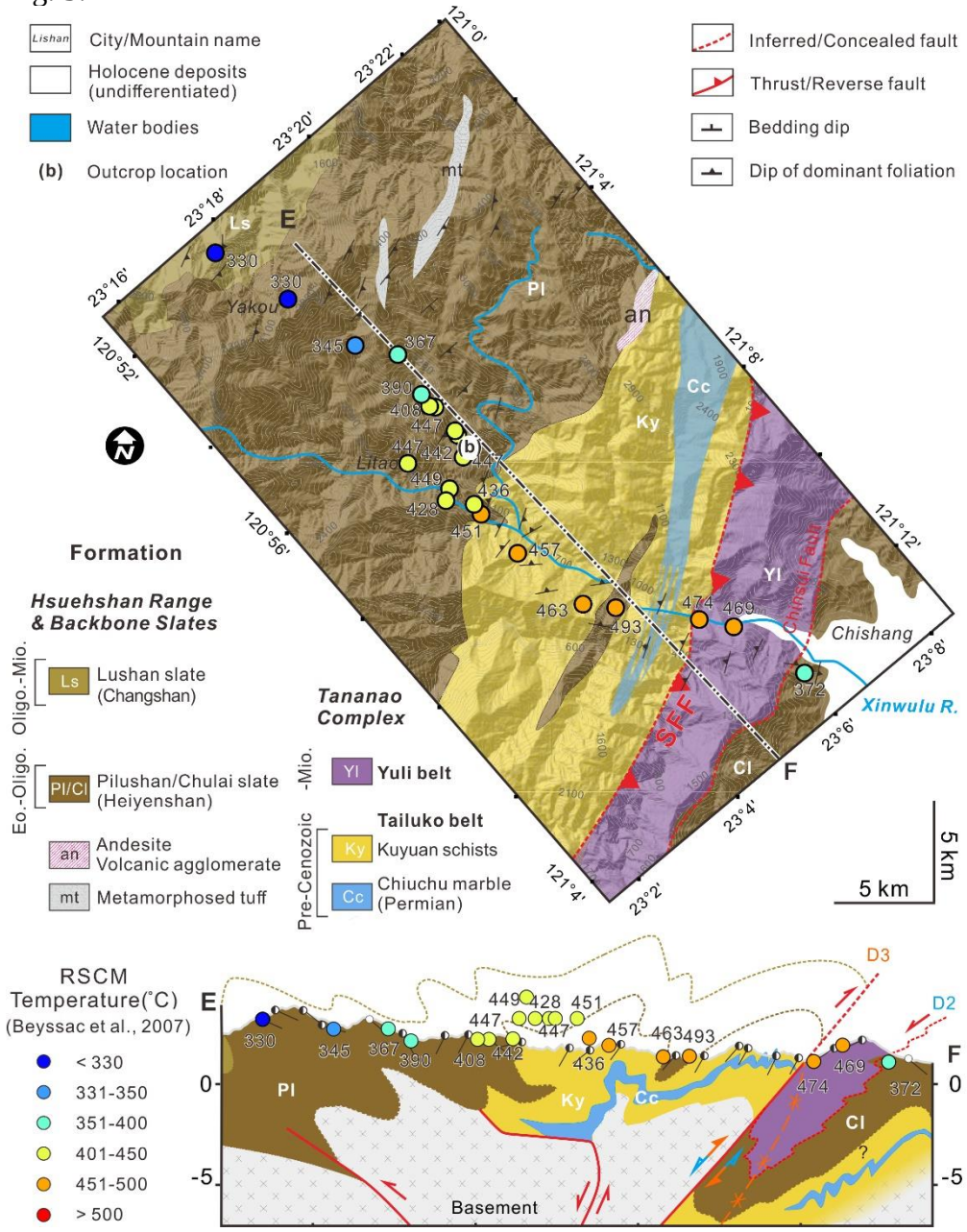

391
392

393 Fig. 4:

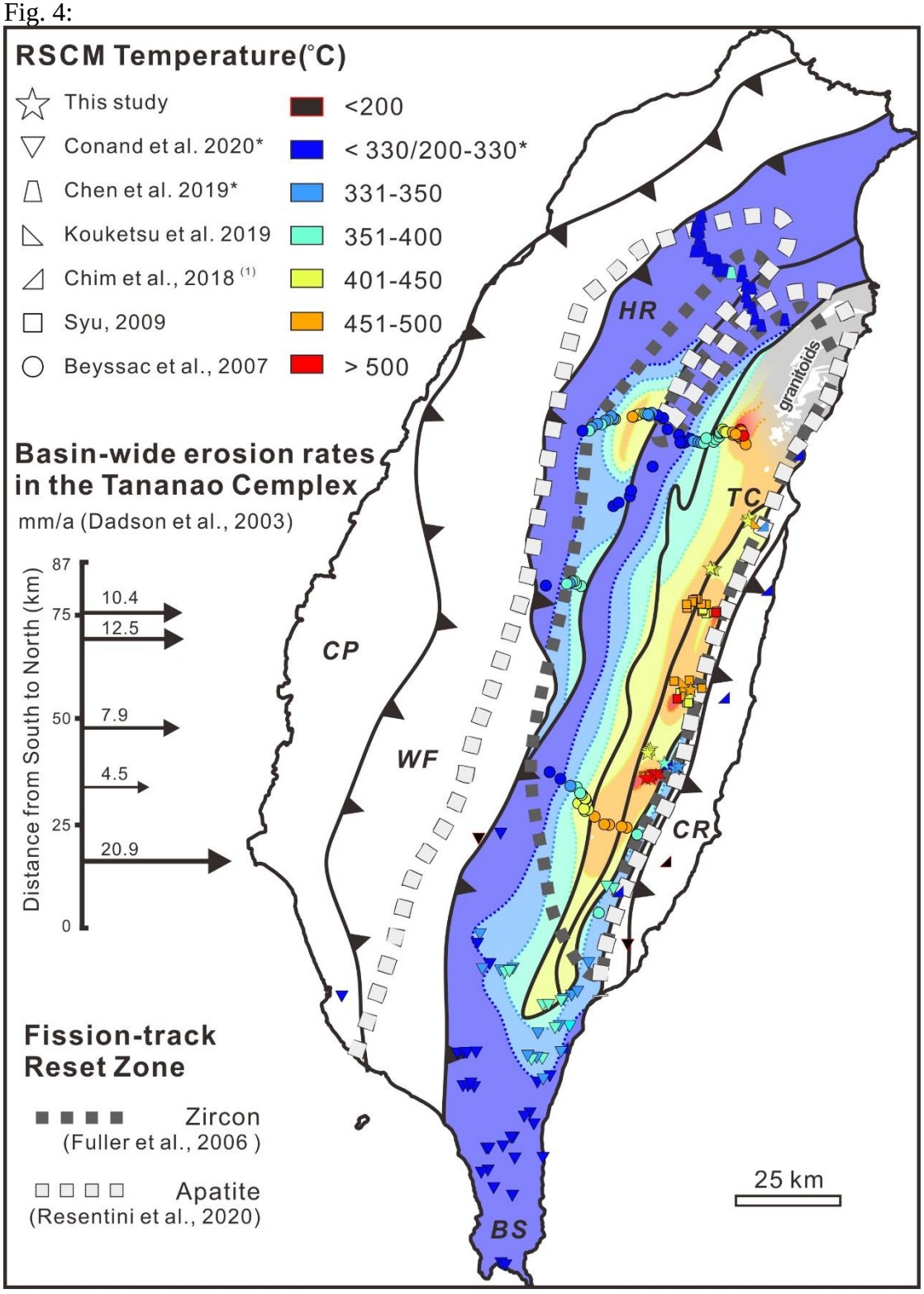

394
395

396 Fig. 5:

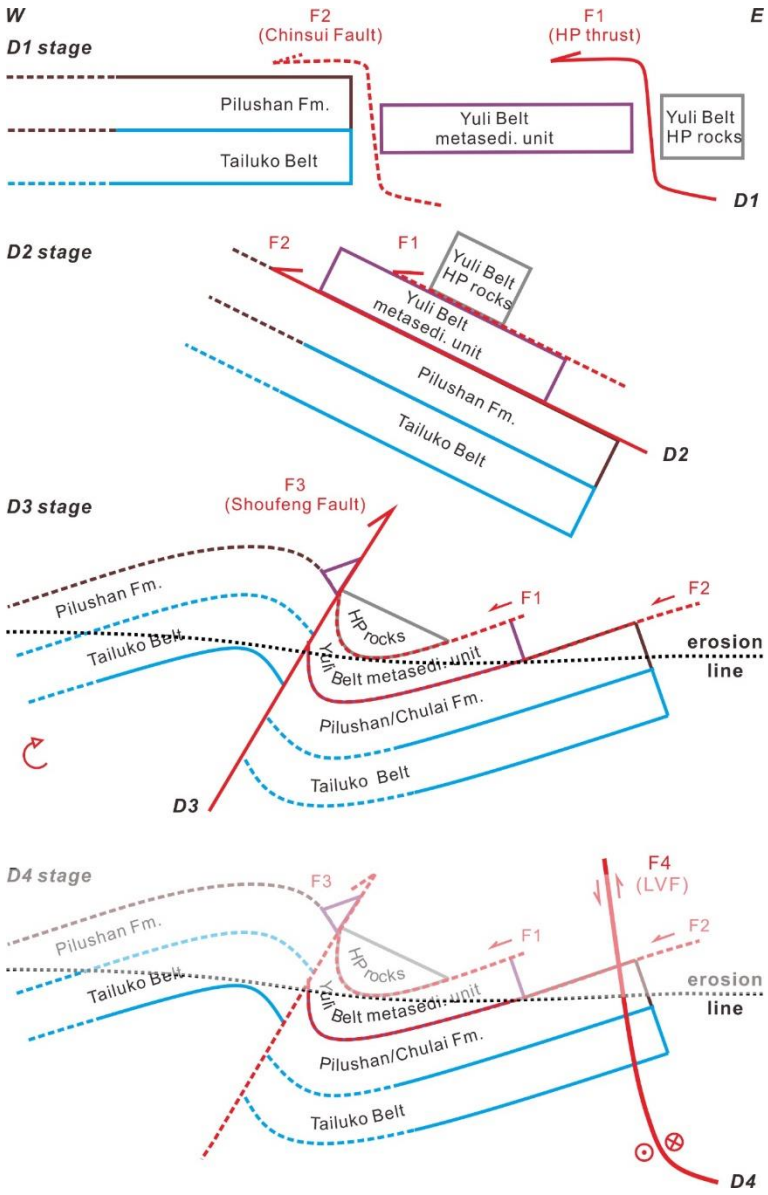
W
E
D1 stage
F2
(Chinsui Fault)
F1
(HP thrust)
Pilushan Fm.
Tailuko Belt
Yuli Belt
metasedi. unit
Yuli Belt
HP rocks
D1
D2 stage
F2
F1
Yuli Belt
HP rocks
Yuli Belt
metasedi. unit
Pilushan Fm.
Tailuko Belt
D2
D3 stage
F3
(Shoufeng Fault)
Pilushan Fm.
Tailuko Belt
HP rocks
F1
F2
Yuli Belt metasedi. unit
erosion
line
Pilushan/Chulai Fm.
Tailuko Belt
D3
D4 stage
F3
F4
(LVF)
Pilushan Fm.
Tailuko Belt
HP rocks
F1
F2
Yuli Belt metasedi. unit
erosion
line
Pilushan/Chulai Fm.
Tailuko Belt
D4

397

Tables

Table 1: RSCM data of the sixteen samples with point measurements. Details of each measurements see Appendix - Table S1.

Sample	Lithology	Longitude	Latitude	Spectra	R2 Ratio	sdv	T (°C)	1σ, °C
YQ17-3	albite mica quartz schist	282504	2600974	100	0.36	0.0482	**477**	22
YQ17-09	mica quartz schist	300000	2652623	107	0.53	0.0425	**401**	19
YQ17-10b	mica quartz schist	300090	2652897	69	0.46	0.0276	**432**	13
YQ17-12b	mica quartz schist	299713	2651633	81	0.50	0.0477	**415**	22
YQ17-15	mica quartz schist	277793	2576465	61	0.66	0.0077	**347**	3
YQ17-23a	talc schist	270475	2574522	62	0.30	0.0366	**506**	16
YQ17-28	albite quartz mica schist	268968	2574373	80	0.28	0.0379	**516**	17
YQ17-29	quartz mica schist	278916	2577907	62	0.64	0.0160	**350**	7
YQ18-01a	mica quartz schist	270366	2583101	31	0.45	0.0468	**435**	21
YQ18-02	mica quartz schist	269748	2582702	47	0.46	0.0400	**433**	18
YQ18-03	mica quartz schist	269505	2581975	47	0.44	0.0410	**440**	19
YQ18-05	quartz mica schist	274569	2578864	70	0.56	0.0483	**386**	22
YQ18-09	mica quartz schist	289548	2637285	61	0.45	0.0364	**436**	17
YQ18-11	mica quartz schist	288751	2637341	57	0.47	0.0574	**427**	26
YQ18-12	mica quartz schist	288435	2637562	61	0.41	0.0779	**455**	35
YQ18-13a	mica quartz schist	288401	2637603	66	0.47	0.0347	**426**	16

Supporting Information

Fig. S1: Representative microscopic features of black schists. Images on the left are in plane-polarized light, and on the right are in cross-polarized light. Abbreviations: Ab = albite; Bt = biotite; Cal = calcite; CM = carbonaceous material; Chl = chlorite; Ep = epidote; Qz = quartz; Tlc = =talc; Tin = titanite; Wm = white mica.

Fig. S2: Representative Raman spectra of the carbonaceous materials with estimated peaks in each sample.

Fig. S3: Outcrops and equal area, lower hemisphere ("Schmidt net") projections of Chulai and Pilushan Formation within the Backbone Slates considered representative for map-scale structures.

(a) and (c): Northeast-dipping low-grade metamorphic slates and thin intercalations of sandstones (S2) in the Chulai Formation. Location: west Lakulaku river, 23.301333°N, 121.290917°E.

(b) and (d): The east-facing metamorphic foliation (slaty cleavage, S2) of quartzite slate and dark phyllites in the Pilushan Formation. The refolded axial planar cleavage (S3) dips to the west. Location: east Litao, 23.191908°N, 121.018261°E.

Fig. S4: Field photos of the Chulai Formation and the Yuli Belt in the Lakulaku area, showing example of ductile shear zone. See Fig. 2 for outcrop locations. (e)-(h) are from the contact between the Chulai Formation and the Yuli Belt. (i) and (j) are from the Yuli Belt.

(e) and (f): Veined metapsammitic to metapelitic sediments are intensely deformed and affected by D3 refolding with gradational textural and metamorphic change in the contact zone. Fold axes gently plunge to the north. Location: 23.309016°N, 121.252120°E.

(g): Northwest-dipping low-grade metamorphic slates and thin intercalations of sandstones in the contact zone, showing deformation structures indicative of top-to-the SE shear and layer-parallel extension. Location: 23.309450°N, 121.248937°E.

(h): Structural planes with slickensides. Black arrows indicate the moving direction of the contrary side judged from steps. Northwest-dipping dominant foliation in the contact zone with top-to-the SSE shear sense of the hanging wall. Location: 23.309450°N, 121.248937°E.

(i): Simple shear deformed Yuli Belt schists with top-to-the-SE kinematic. Location: 23.337362°N, 121.217721°E

(j): Quartz veins crosscutting foliation planes in the Yuli Belt CM-rich schists, showing deformation structures indicative of top-to-the S shear. The plunge/trend of quartz stretching lineations in quartz layers is 012/09. Location: 23.345590°N, 121.198246°E.

Fig. S5: Lithosphere-scale kinematic model to explain the origin of the Yuli Belt of Taiwan (modified after Zhang et al., 2020). WF: Western Foothill; HR: Hsuehshan Range; BS: Backbone Slates; TC: Tananao Complex. See text and Fig. 5 for further discussion.

Table S1: RSCM data of the sixteen samples with point measurements. All peak metamorphic temperatures (T) were obtained using the calibration of Beyssac et al. (2002). Abbreviations: int = band intensity; FWHM = full width half maximum; R1 = (D1/G) (peak height ratio); R2 = D1/(G+D1+D2) area; T (TR2) = -445 × R2 + 641.

Fig. S1: Representative microscopic features of black schists. Images on the left are in plane-polarized light, and on the right are in cross-polarized light.

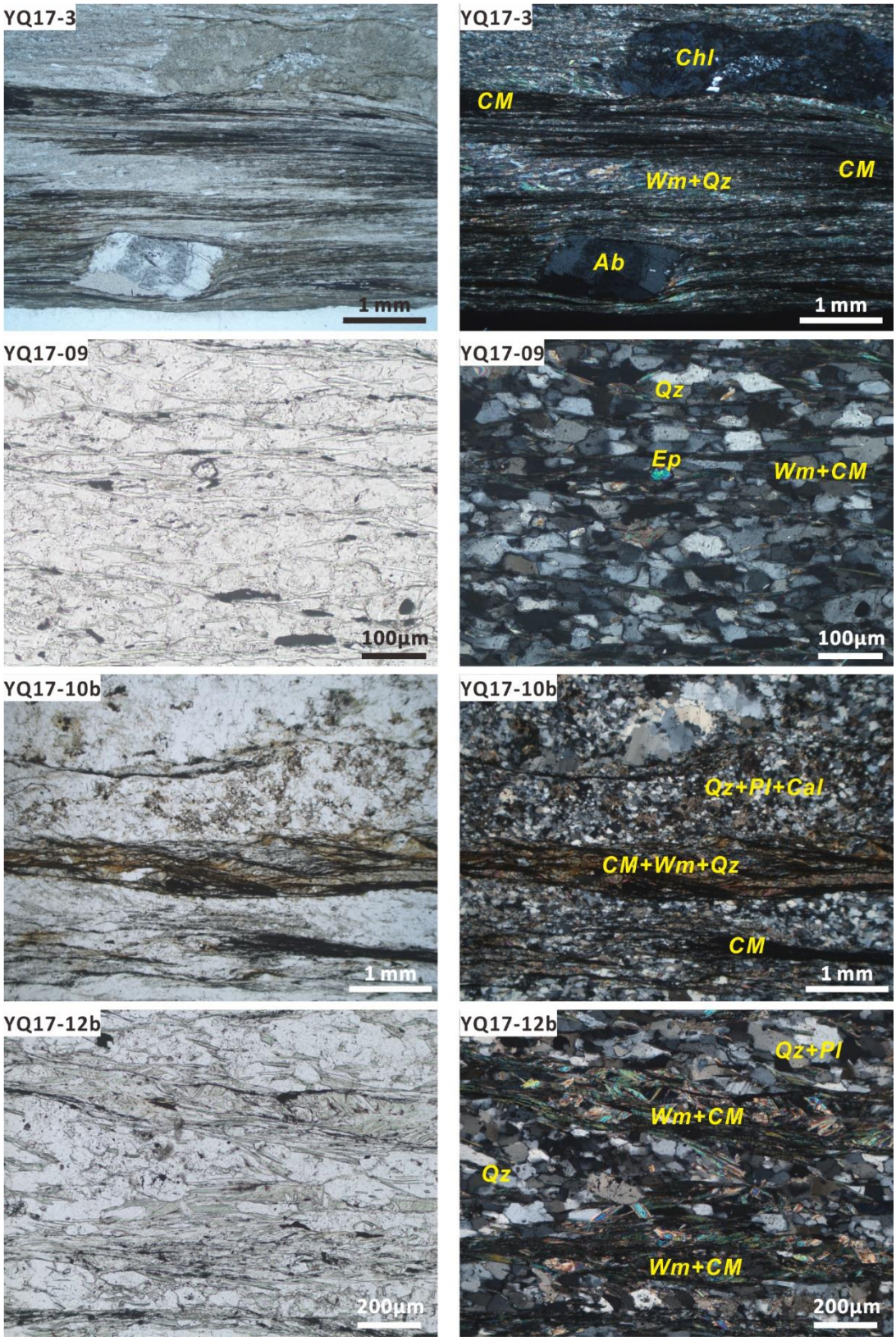

453

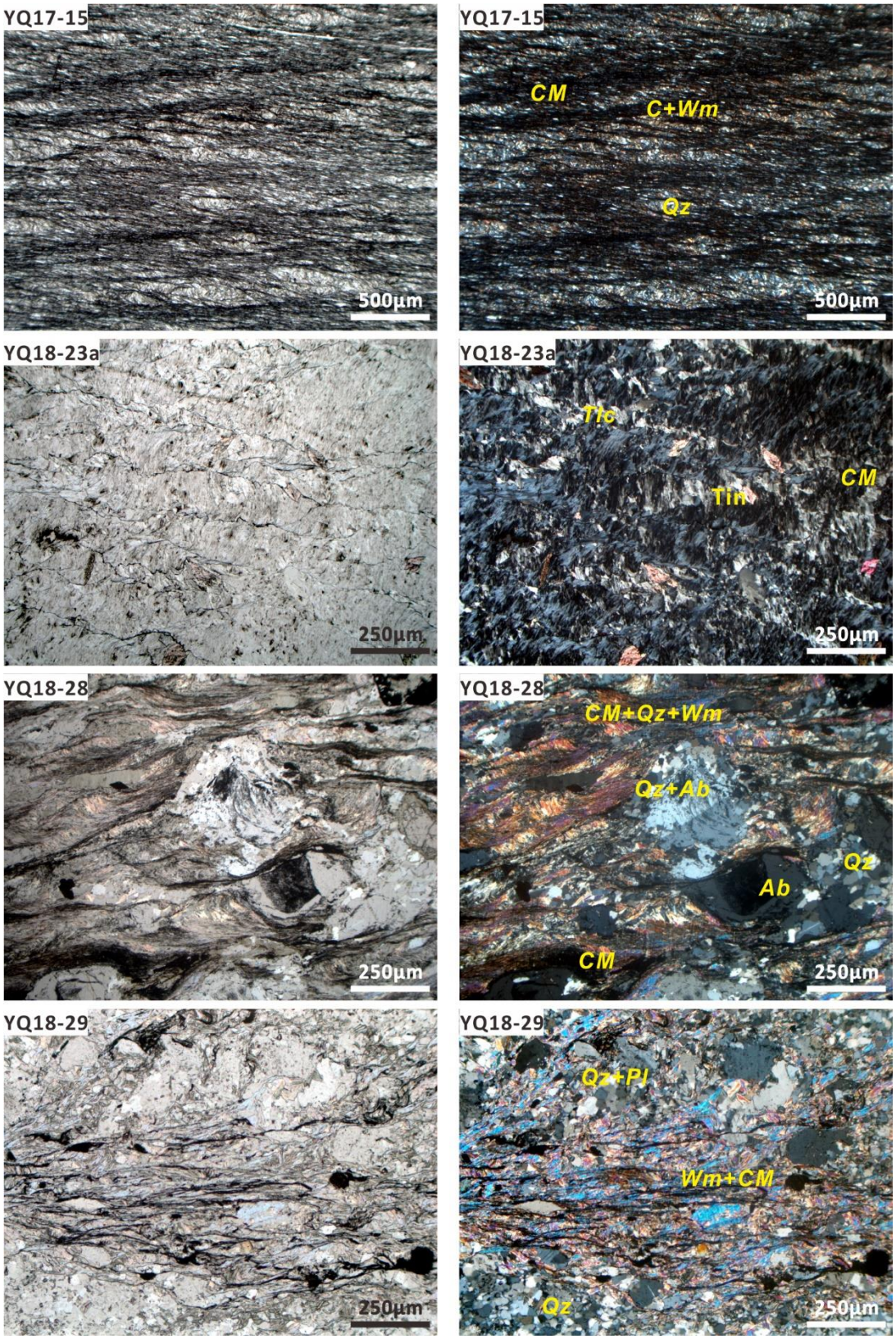

454
455
456

457

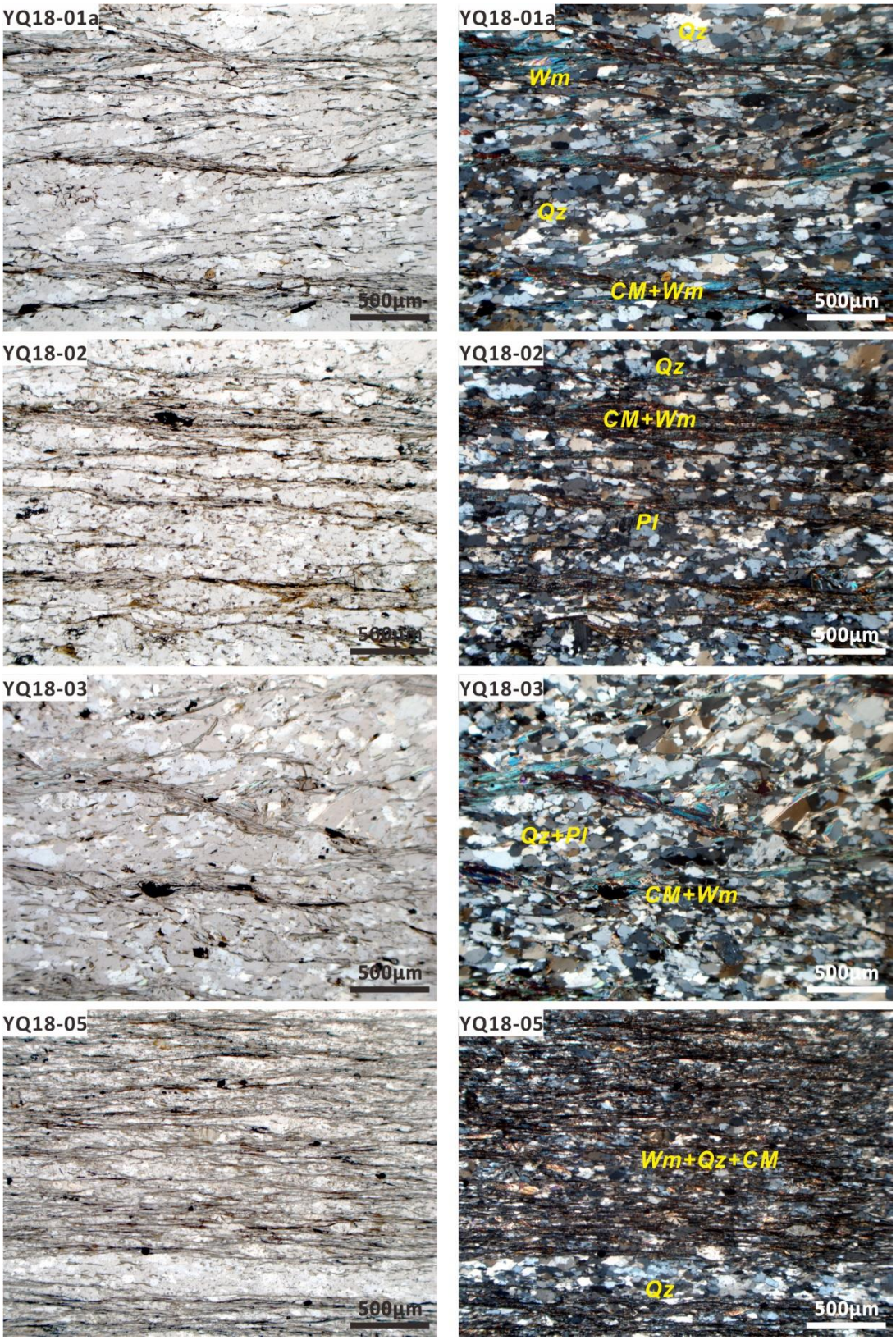
YQ18-01a
YQ18-01a
Qz
Wm
Qz
CM+Wm
500μm
500μm
YQ18-02
YQ18-02
Qz
CM+Wm
Pl
500μm
YQ18-03
YQ18-03
Qz+Pl
CM+Wm
500μm
YQ18-05
YQ18-05
Wm+Qz+CM
Qz
500μm
500μm

458
459

460

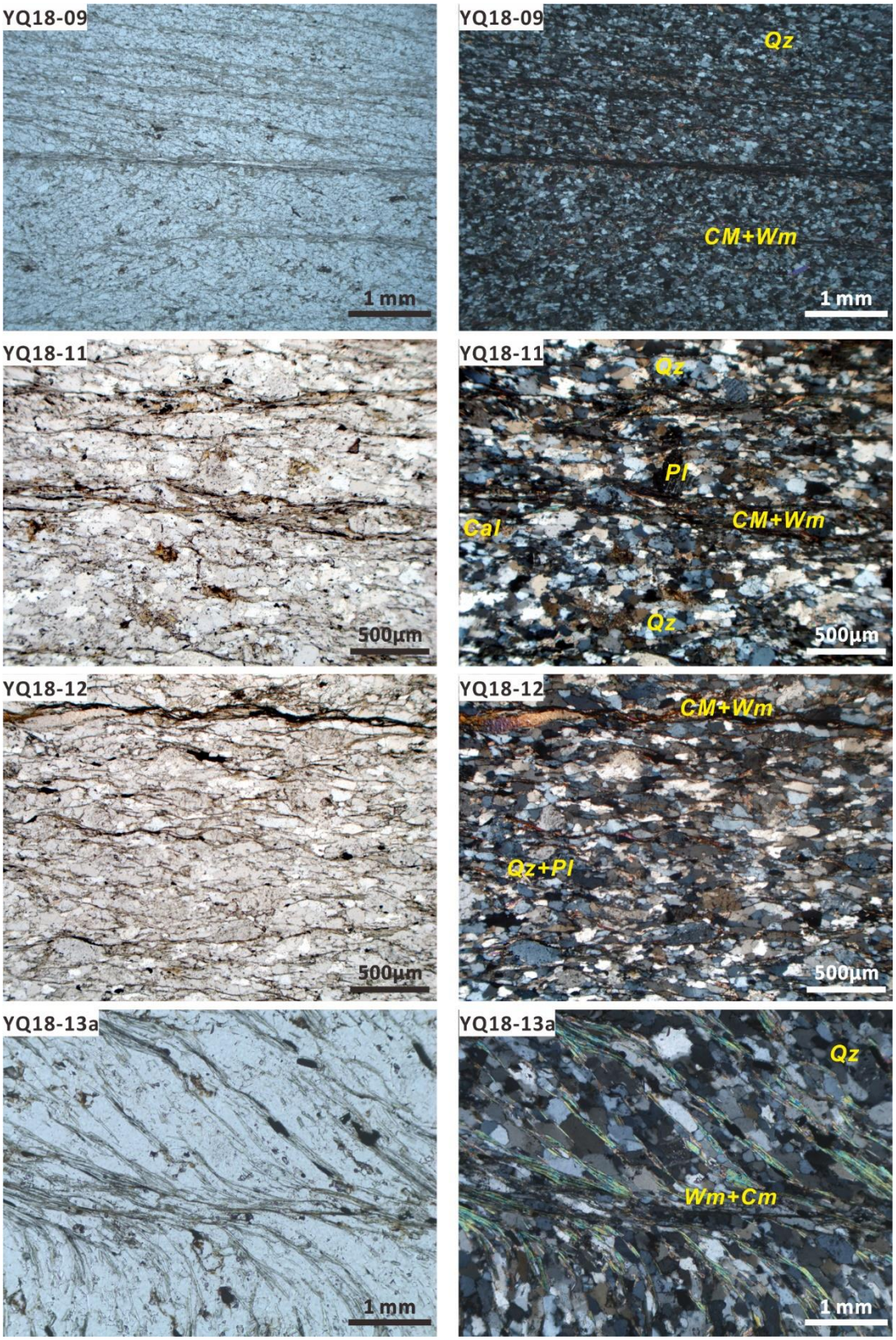
YQ18-09
1 mm
YQ18-09
Qz
CM+Wm
1 mm
YQ18-11
500μm
YQ18-11
Qz
Pl
Cal
CM+Wm
Qz
500μm
YQ18-12
500μm
YQ18-12
CM+Wm
Qz+Pl
500μm
YQ18-13a
1 mm
YQ18-13a
Qz
Wm+Cm
1 mm

461
462

Fig. S2: Representative Raman spectra of the carbonaceous materials in each sample.

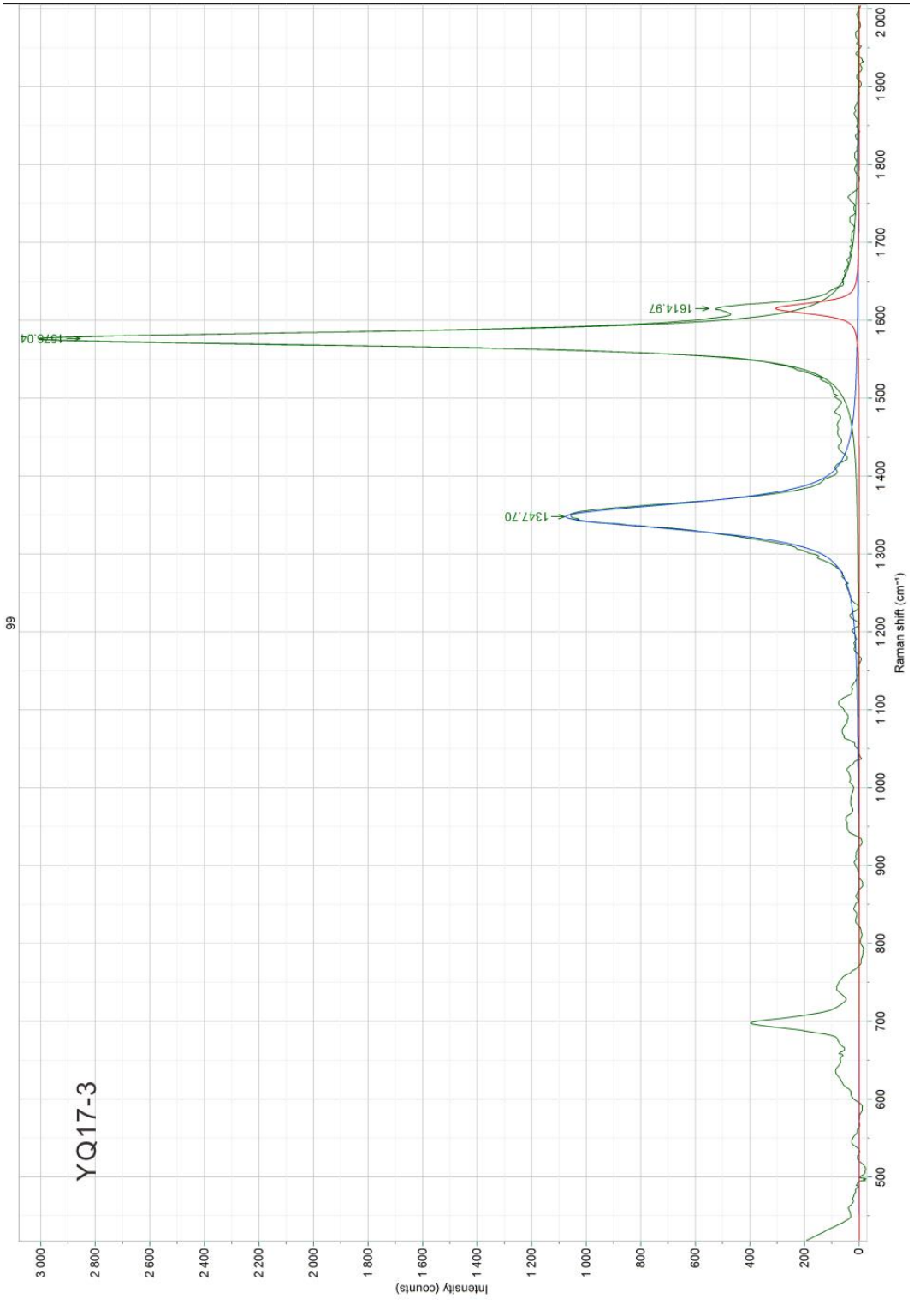

467

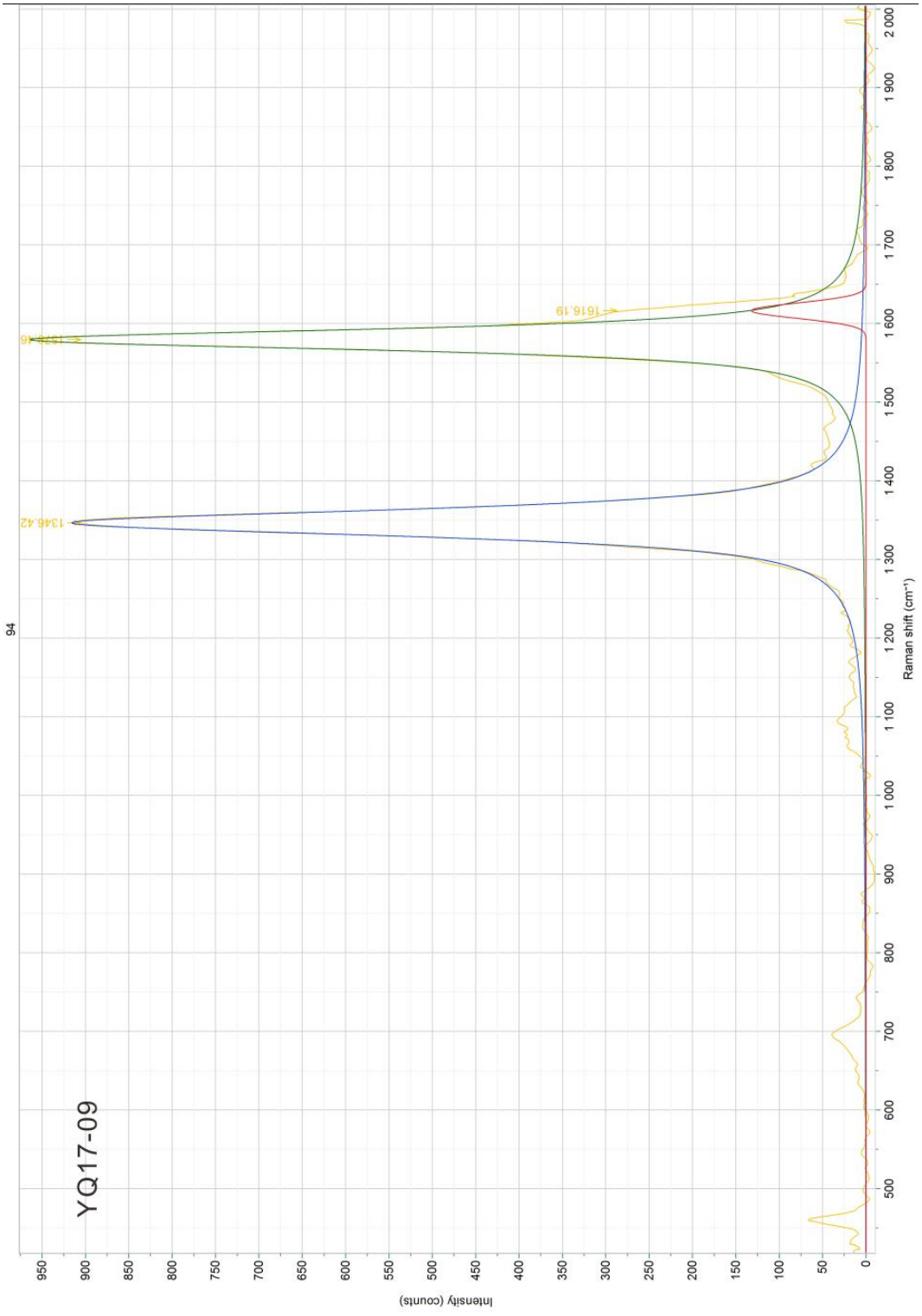

468
469

470

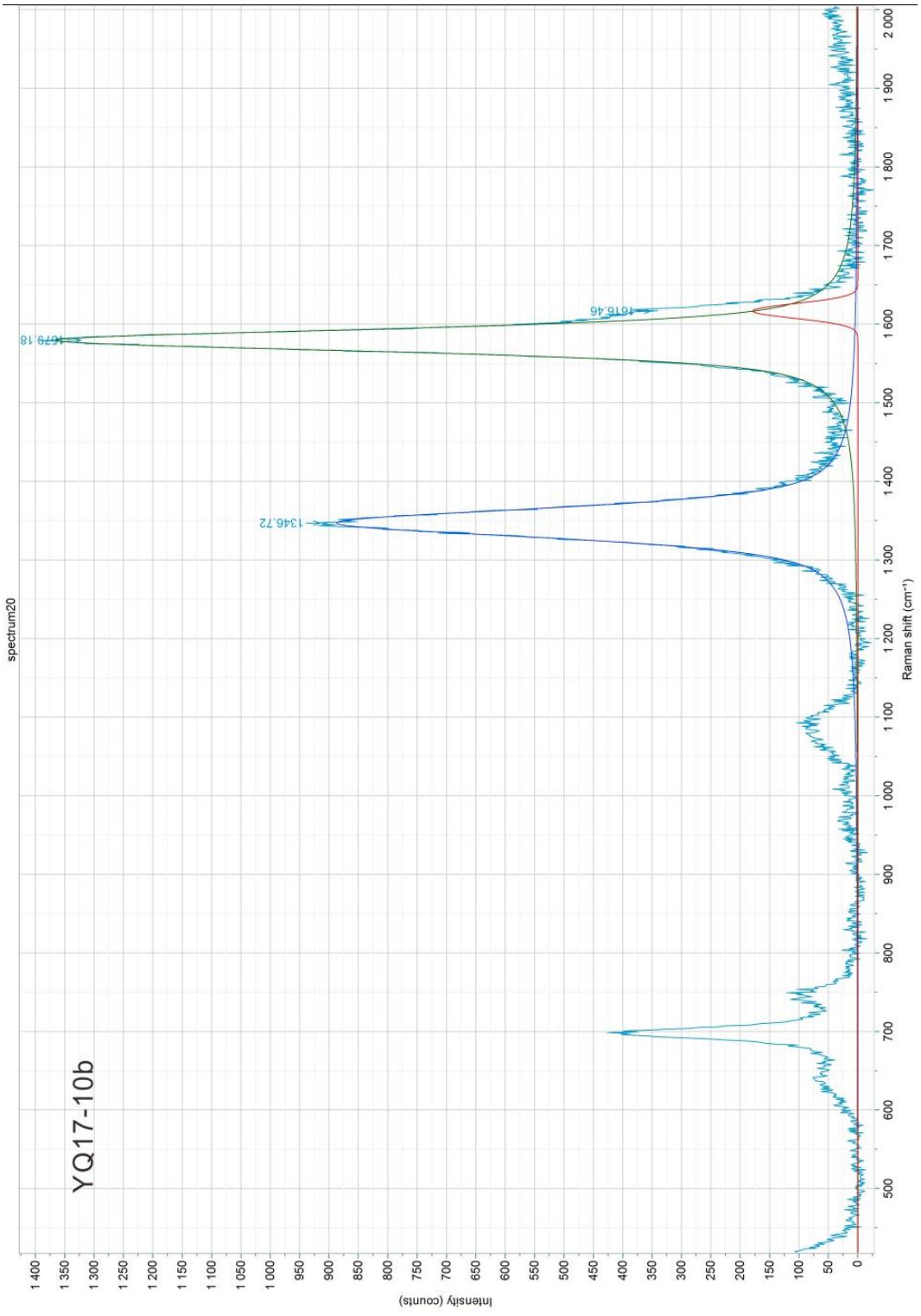
YQ17-10b
spectrum20
1679.18
1615.46
1346.72
Intensity (counts)
Raman shift (cm⁻¹)

471
472

473

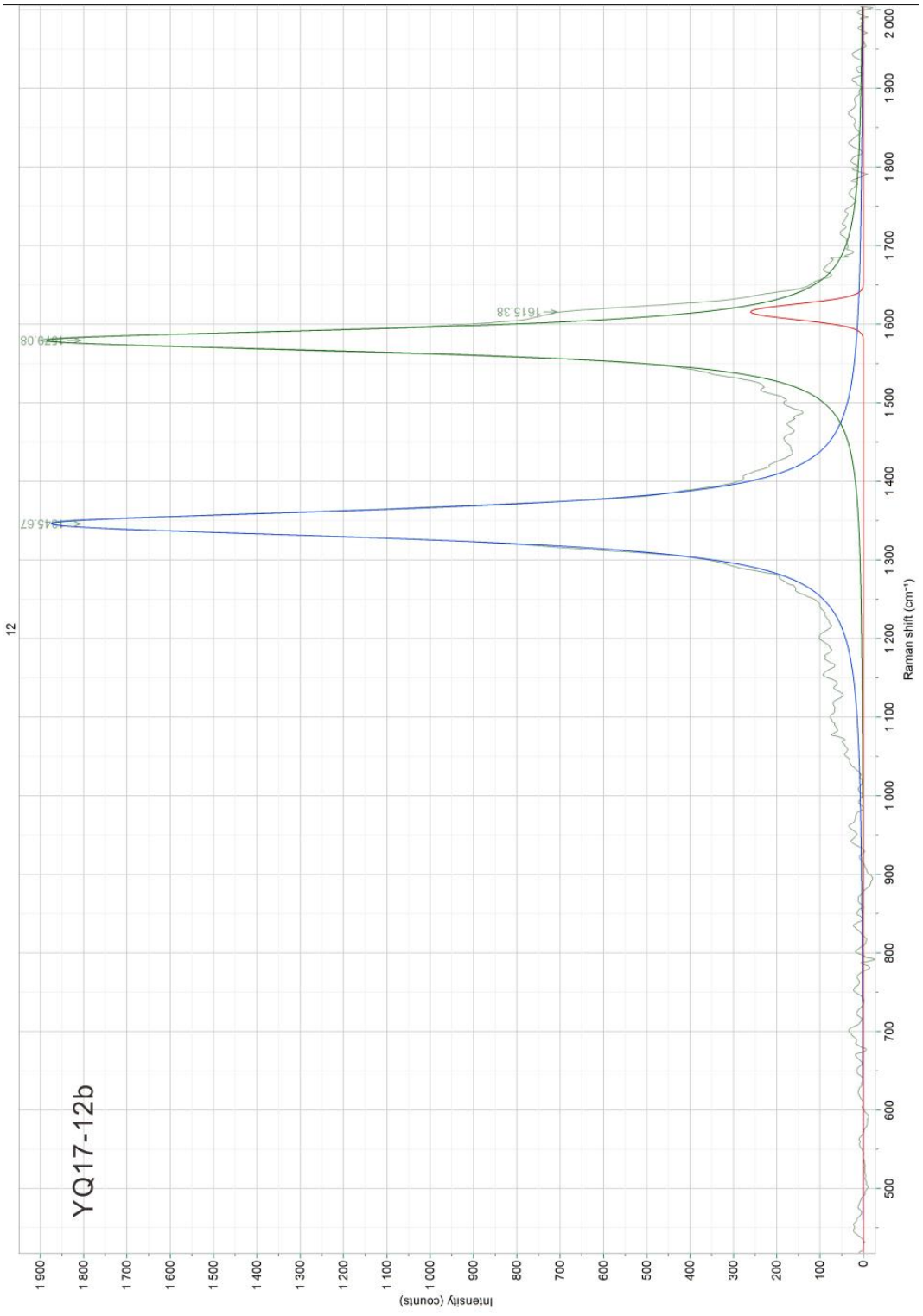
YQ17-12b
12
1615.38
1579.08
1345.67
Intensity (counts)
Raman shift (cm⁻¹)

474
475

476

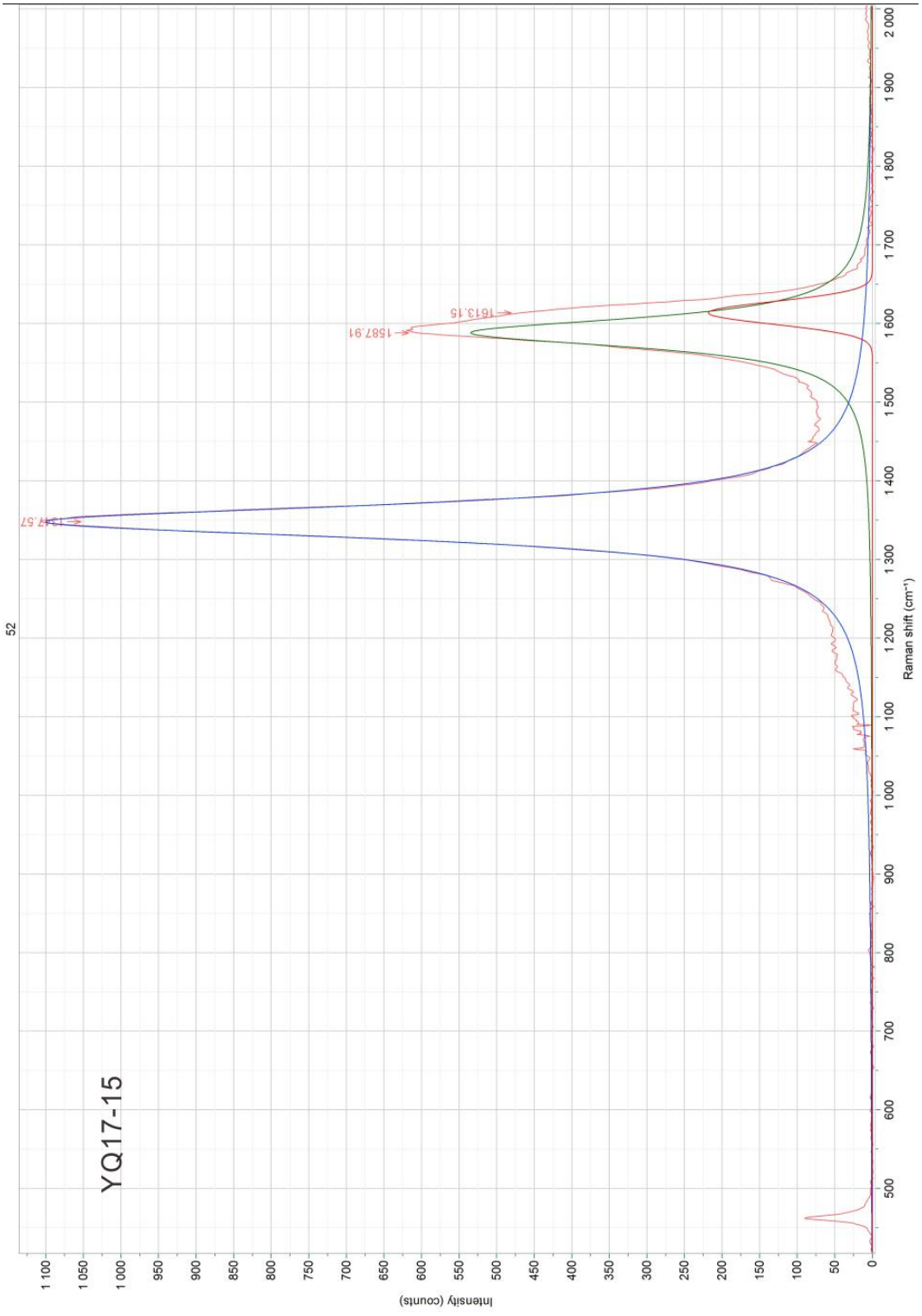
YQ17-15
52
1354.57
1587.91
1613.15
Raman shift (cm⁻¹)
Intensity (counts)

477
478

479

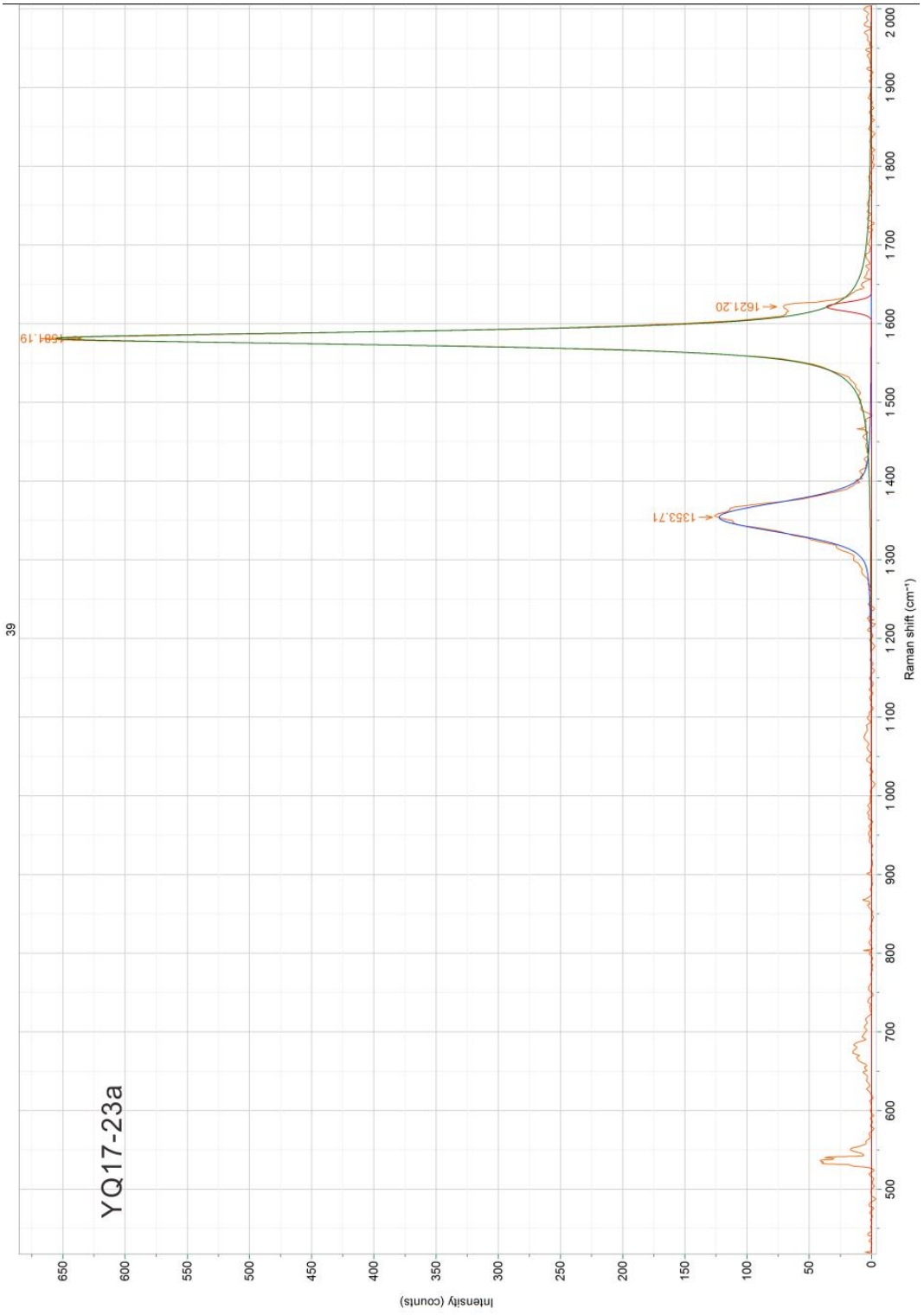
YQ17-23a
1581.19
1621.20
1353.71
Intensity (counts)
Raman shift (cm⁻¹)

480
481

482

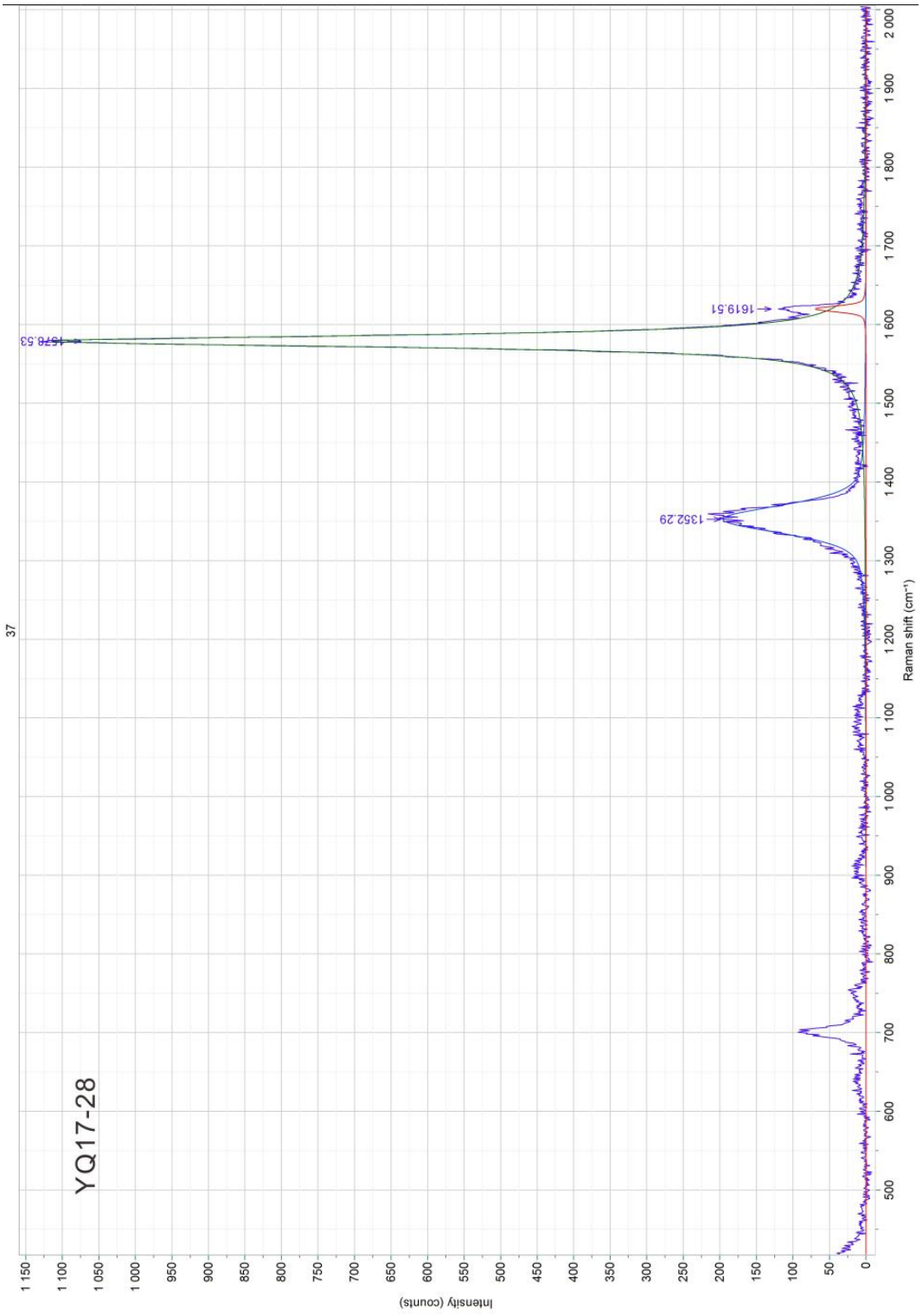
YQ17-28
37
1619.51
1578.53
1352.29
Raman shift (cm⁻¹)
Intensity (counts)

483
484

485

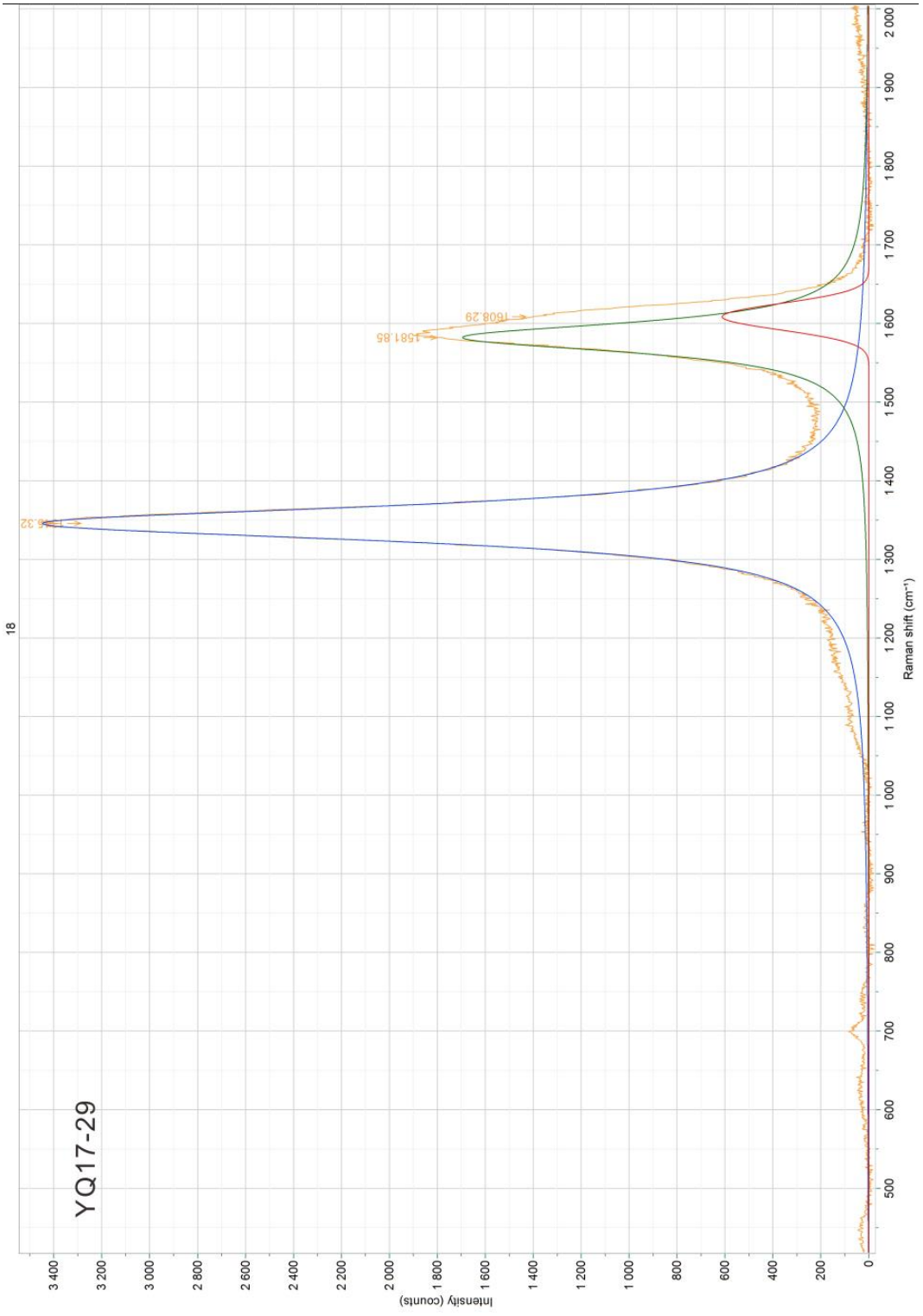

486
487

488

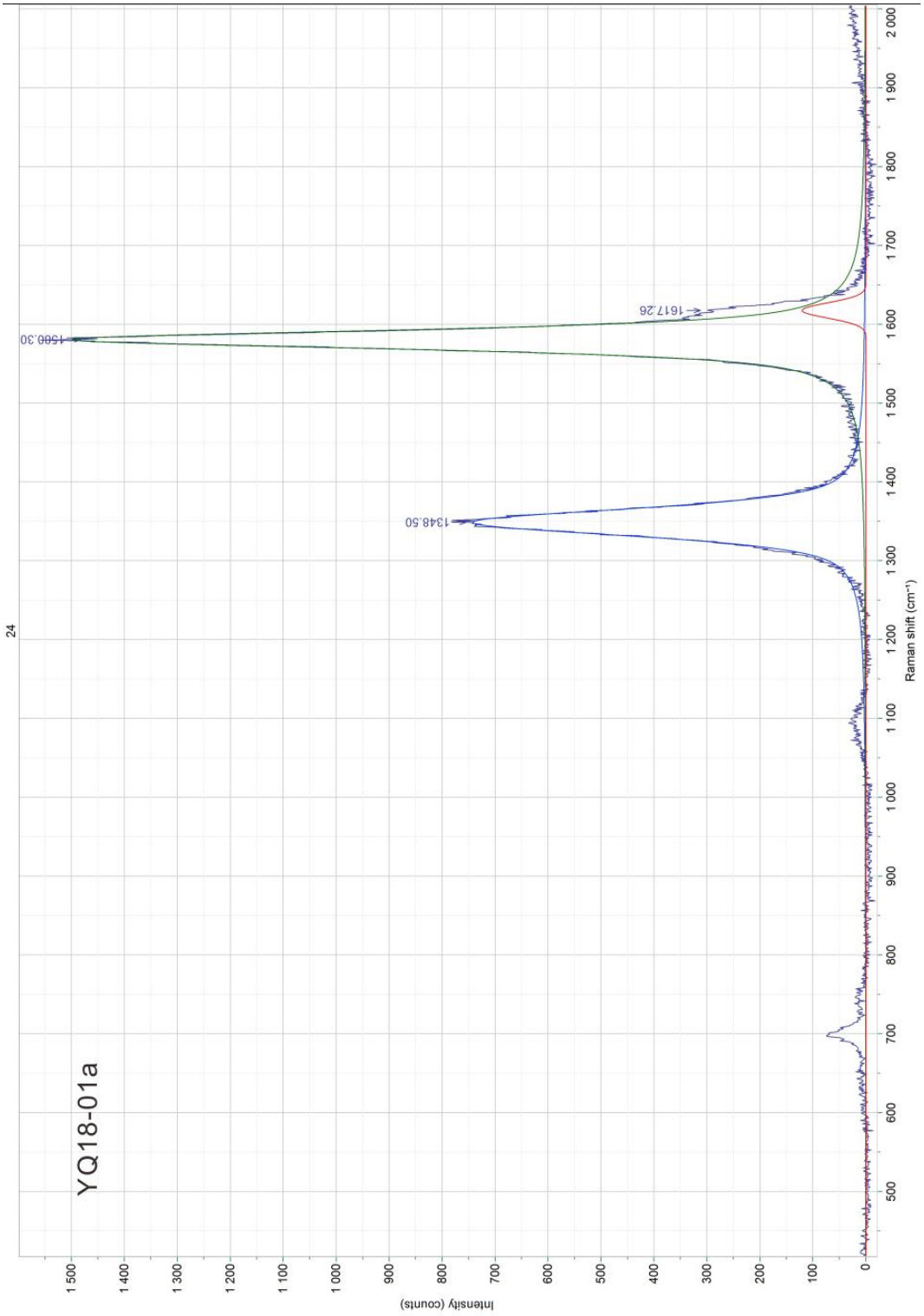
YQ18-01a
24
1617.26
1580.30
1348.50
Intensity (counts)
Raman shift (cm⁻¹)

489
490

491

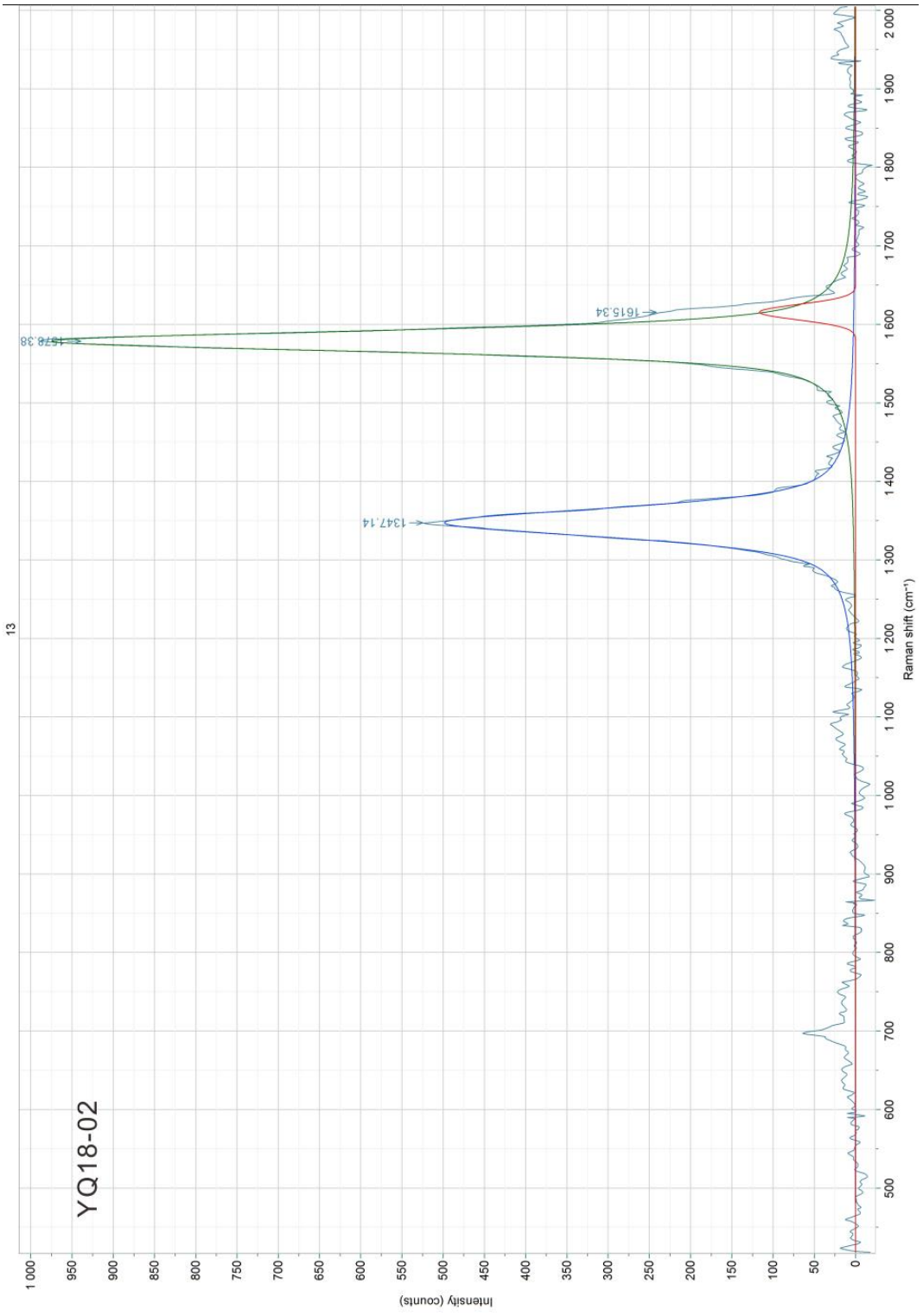
YQ18-02
13
1615.34
1578.38
1347.14
Intensity (counts)
Raman shift (cm⁻¹)

492
493

494

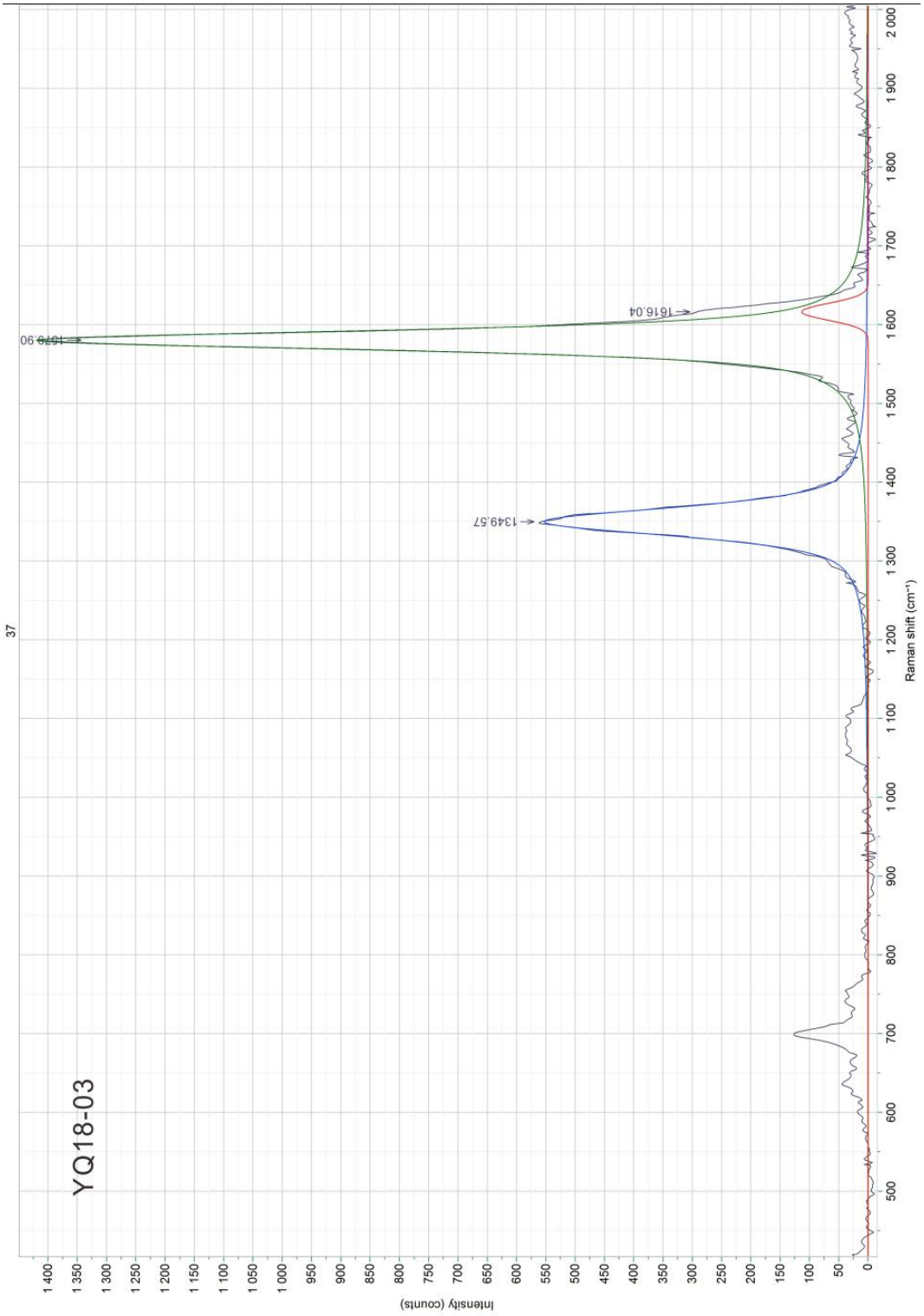
YQ18-03
37
1616.04
1579.90
1349.57
Intensity (counts)
Raman shift (cm⁻¹)

495
496

497

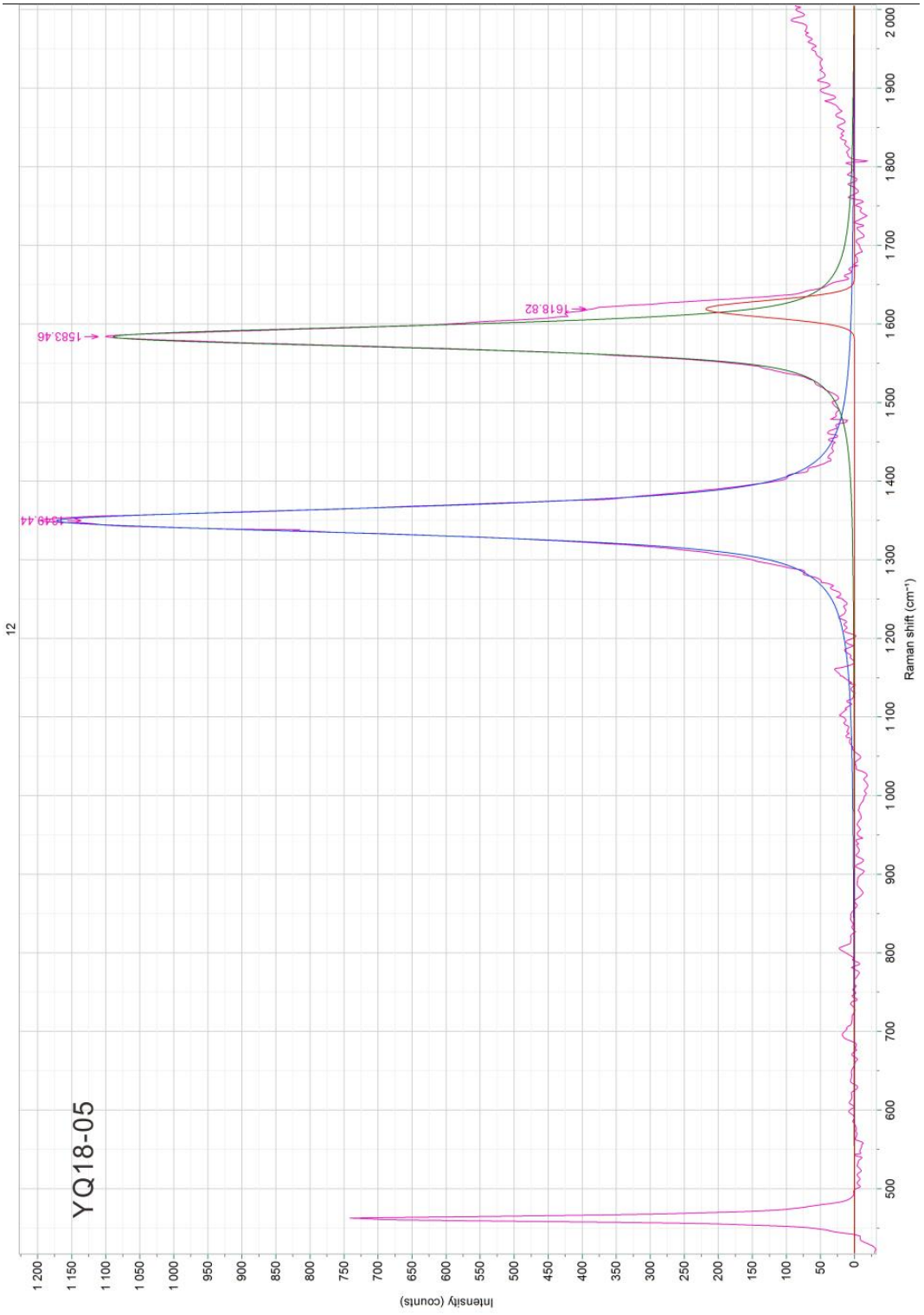
YQ18-05
12
1618.82
1583.46
1318.44
Intensity (counts)
Raman shift (cm⁻¹)

498
499

500

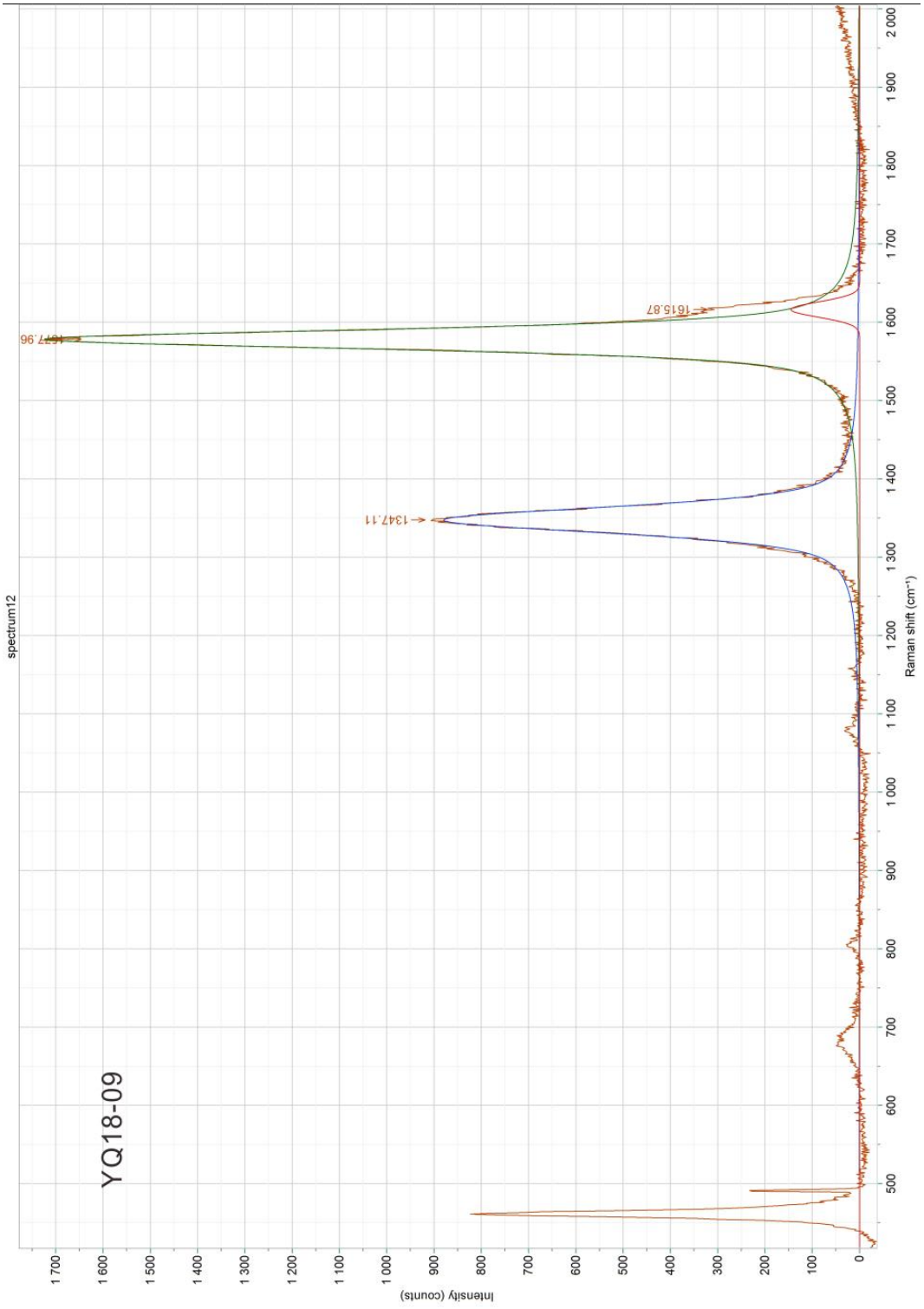
YQ18-09
spectrum12
1615.87
1627.96
1347.11
Intensity (counts)
Raman shift (cm⁻¹)

501
502

503

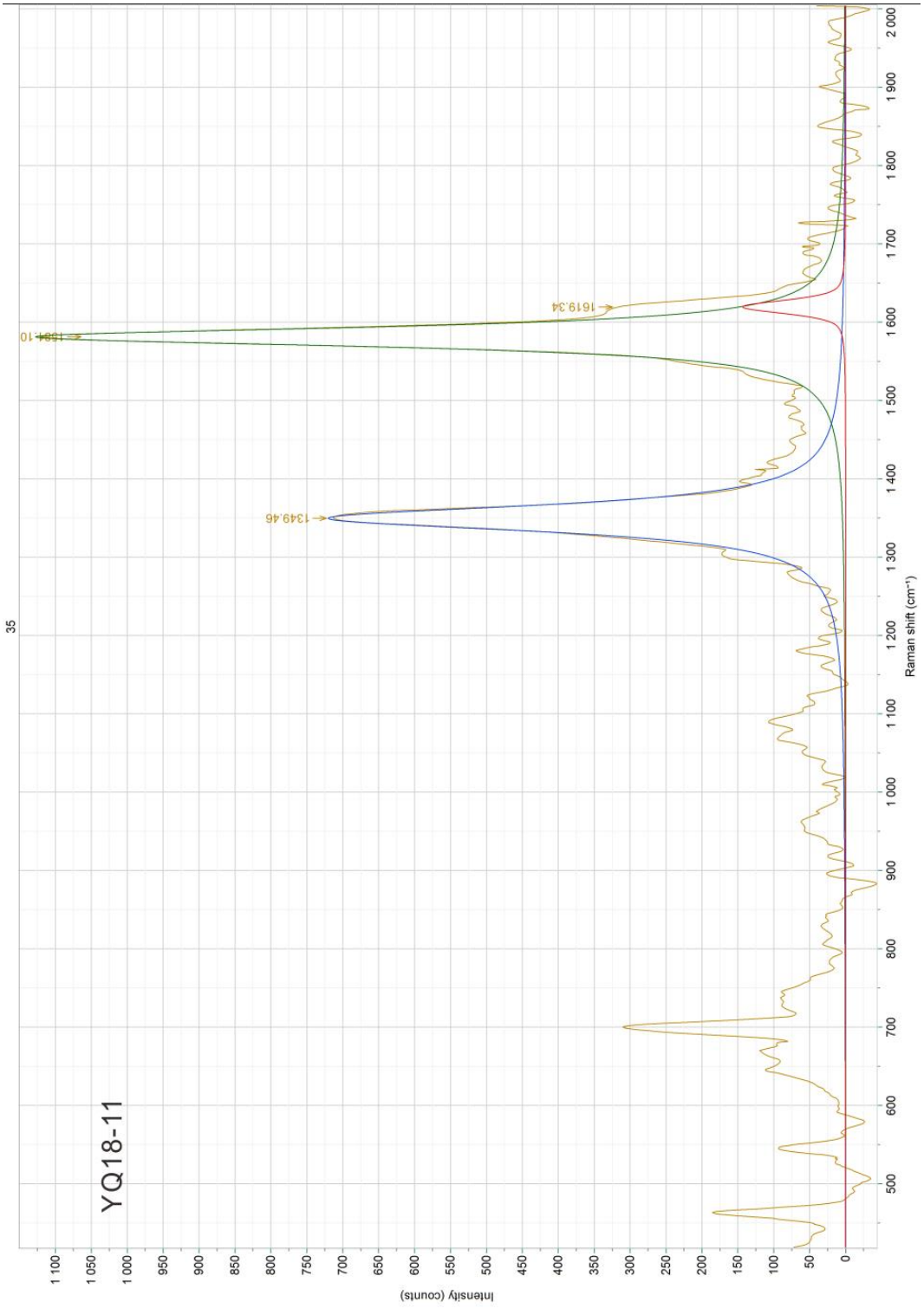
YQ18-11
35
1584.10
1619.34
1349.46
Intensity (counts)
Raman shift (cm⁻¹)

504

505

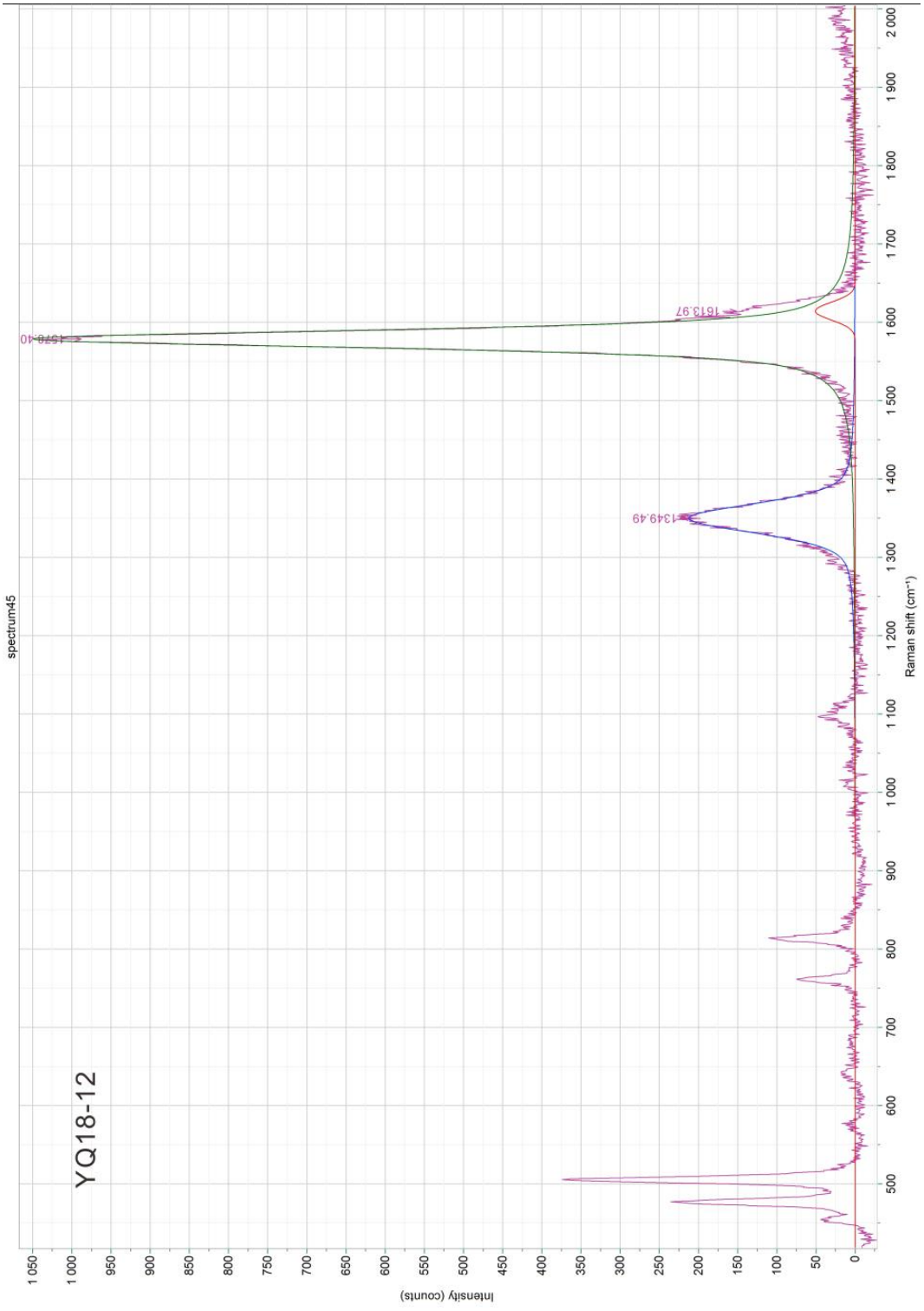
YQ18-12
spectrum45
1578.10
1613.97
1349.49
Intensity (counts)
Raman shift (cm⁻¹)

506

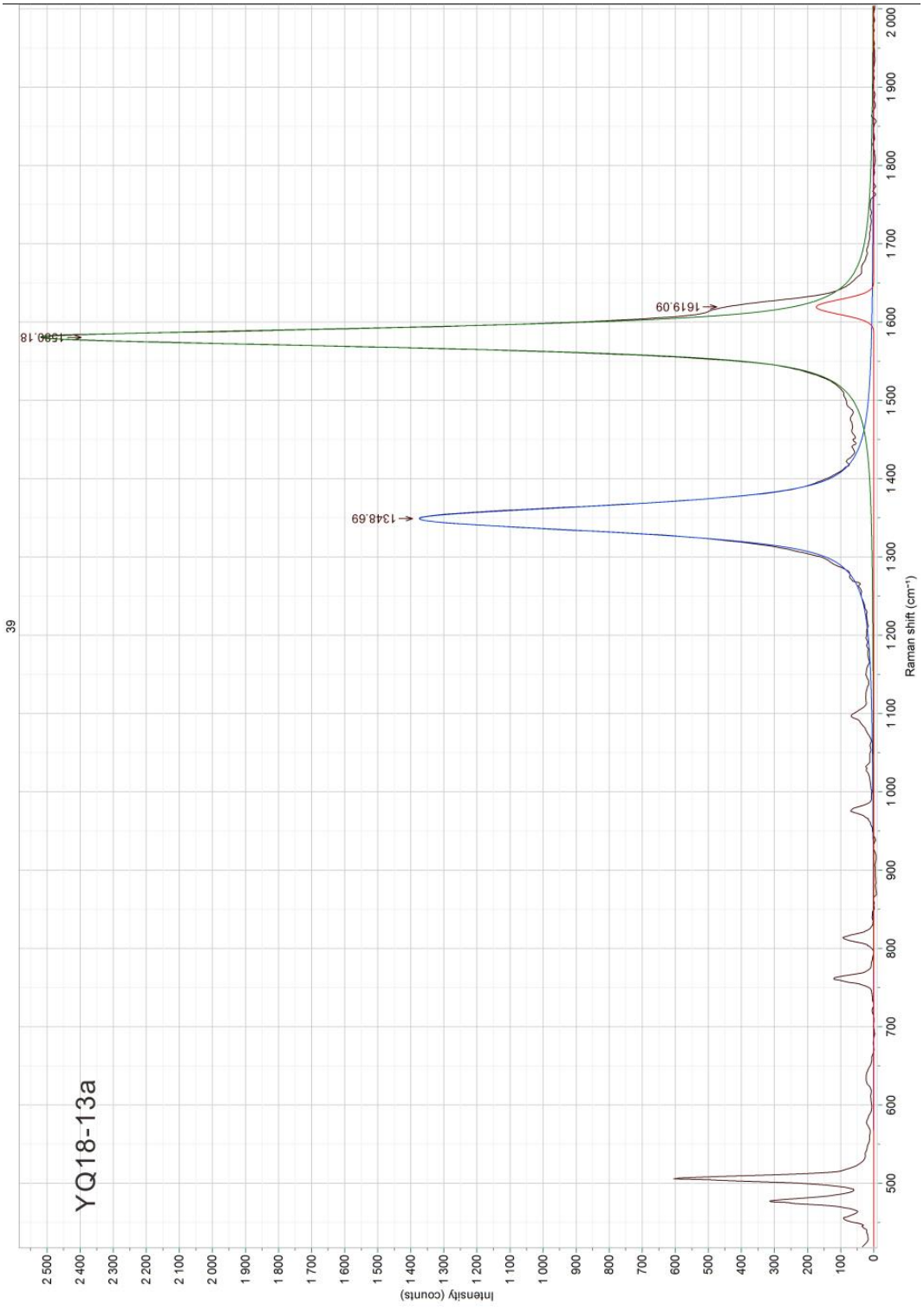
YQ18-13a
1619.09
1590.18
1348.69
Raman shift (cm⁻¹)
Intensity (counts)
39

507
508

Fig. S3: Outcrops and equal area, lower hemisphere ("Schmidt net") projections of Chulai and Pilushan Formation within the Backbone Slates considered representative for map-scale structures.

(a) and (c): Northeast-dipping low-grade metamorphic slates and thin intercalations of sandstones (S2) in the Chulai Formation. Location: west Lakulaku river in Fig. 2, 23.301333°N, 121.290917°E.

(b) and (d): The east-facing metamorphic foliation (slaty cleavage, S2) of quartzite slate and dark phyllites in the Pilushan Formation. The refolded axial planar cleavage (S3) dips to the west. Location: east Litao in Fig. 3, 23.191908°N, 121.018261°E.

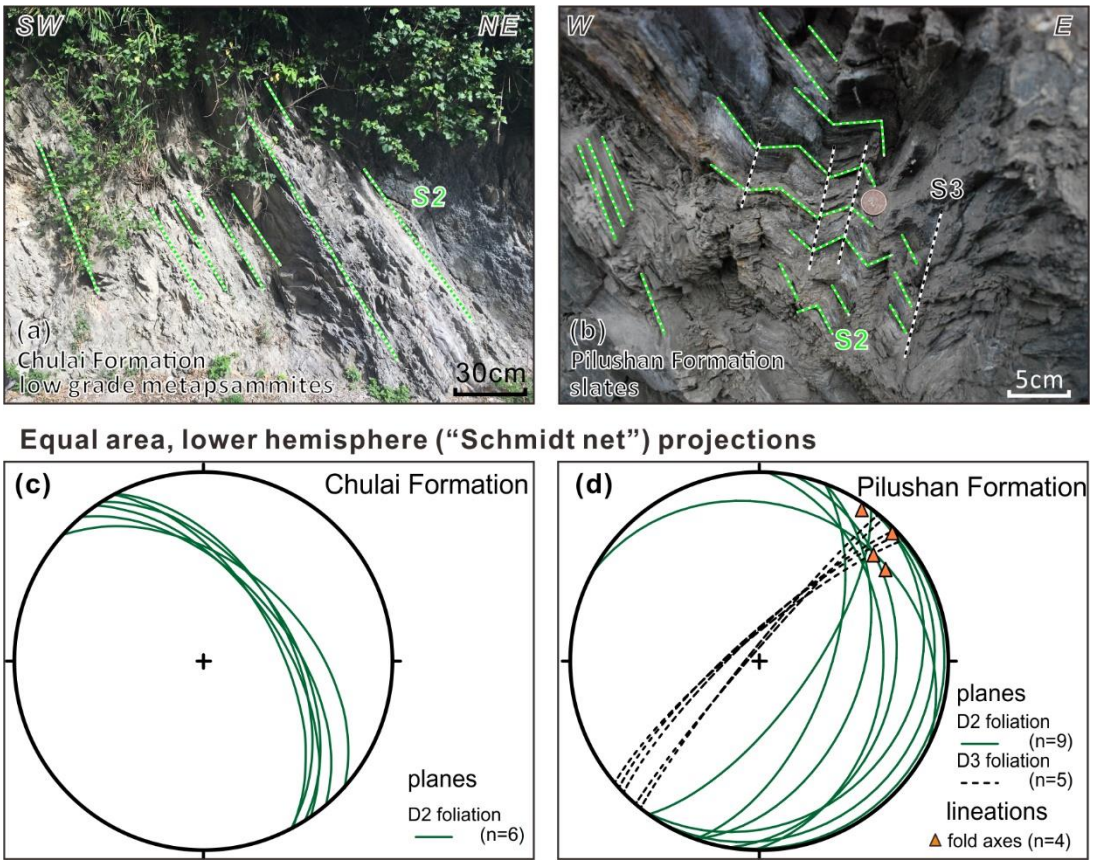

Fig. S4: Field photos of the Chulai Formation and the Yuli Belt in the Lakulaku area, showing example of ductile shear zone. See Fig. 2 for outcrop locations. (e)-(h) are from the contact between the Chulai Formation and the Yuli Belt. (i) and (j) are from the Yuli Belt.

(e) and (f): Veined metapsammitic to metapelitic sediments are intensely deformed affected by D3 refolding with gradational textural and metamorphic change in the contact zone. Fold axes gently plunge to the north. Location: 23.309016°N, 121.252120°E.

(g): Northwest-dipping low-grade metamorphic slates and thin intercalations of sandstones in the contact zone, showing deformation structures indicative of top-to-the SE shear and layer-parallel extension. Location: 23.309450°N, 121.248937°E.

(h): Structural planes with slickensides. Black arrows indicate the moving direction of the contrary side judged from steps. Northwest-dipping dominant foliation in the contact zone with top-to-the SSE shear sense of the hanging wall. Location: 23.309450°N, 121.248937°E.

(i): Simple shear deformed Yuli Belt schists with top-to-the-SE kinematic. Location: 23.337362°N, 121.217721°E

(j): Quartz veins crosscutting foliation planes in the Yuli Belt CM-rich schists, showing deformation structures indicative of top-to-the S shear. The plunge/trend of quartz stretching lineations in quartz layers is 012/09. Location: 23.345590°N, 121.198246°E.

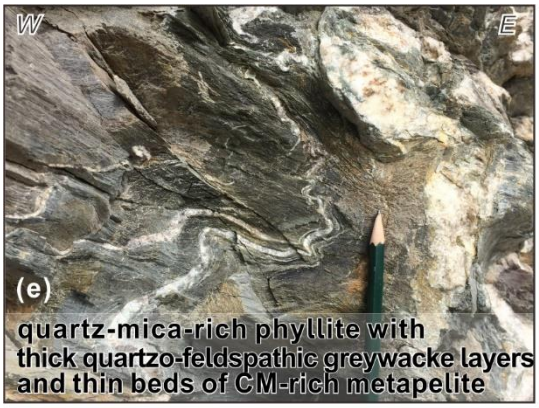
W
E
(e)
quartz-mica-rich phyllite with
thick quartzo-feldspathic greywacke layers
and thin beds of CM-rich metapelite

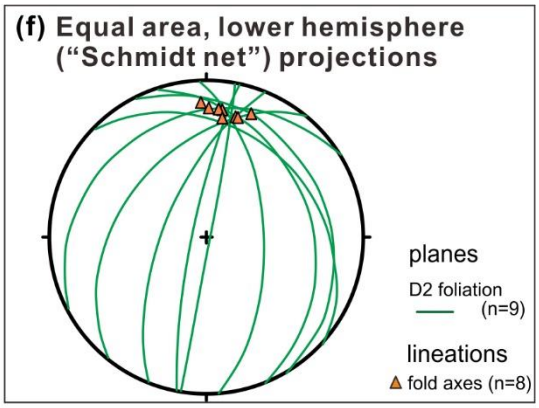
(f) Equal area, lower hemisphere
("Schmidt net") projections
planes
D2 foliation
(n=9)
lineations
fold axes (n=8)


SE
NW
(g)
10cm


SSE
NNW
Slickenfibres
(h)
2 cm


SE
NW
(i)
15cm

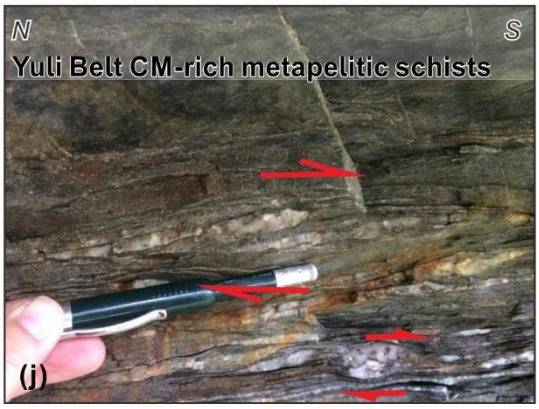
N
S
Yuli Belt CM-rich metapelitic schists
(j)

541

Fig. S5: Lithosphere-scale kinematic model to explain the origin of the Yuli Belt of Taiwan (modified after Zhang et al., 2020). WF: Western Foothill; HR: Hsuehshan Range; BS: Backbone Slates; TC: Tananao Complex. See text and Fig. 5 for further discussion.

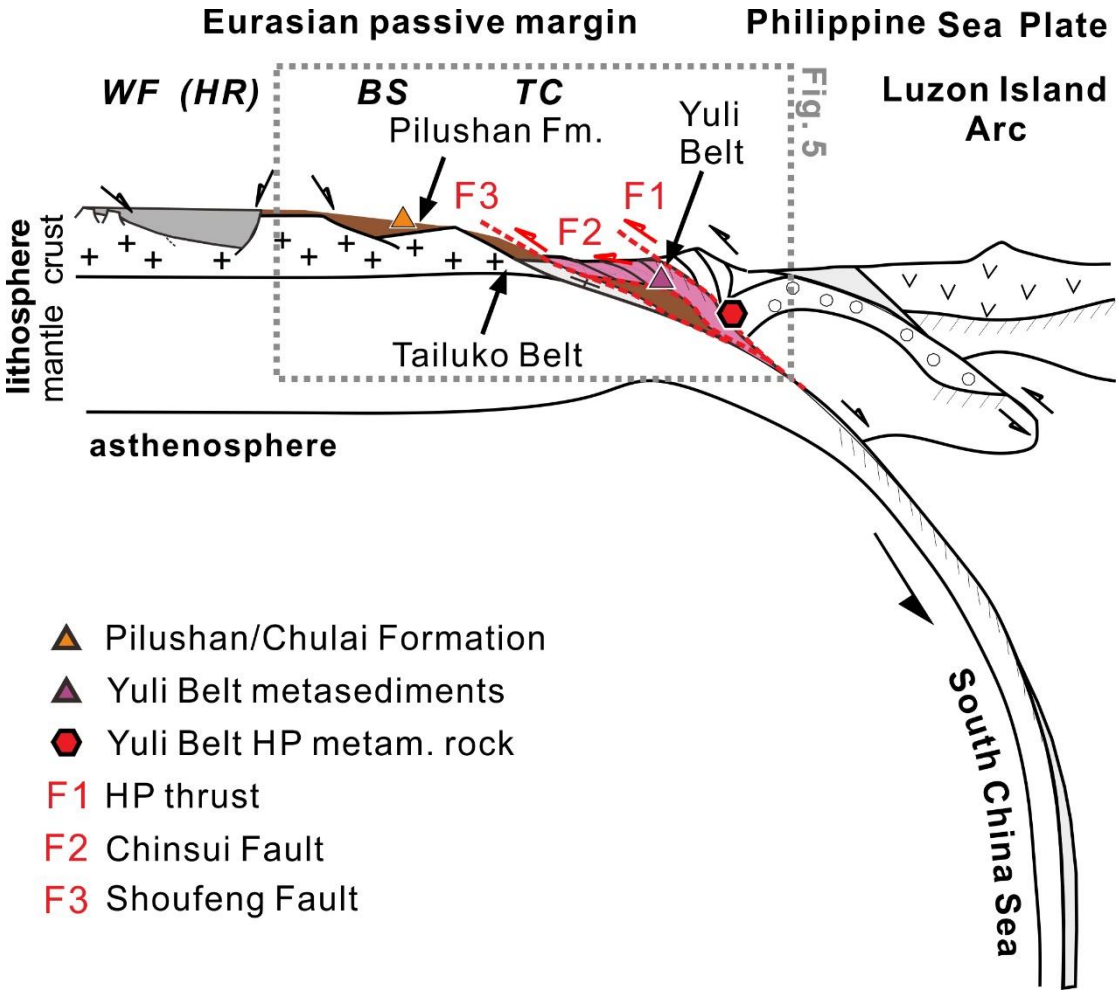

549 **Table S1**: RSCM data of the sixteen samples with point measurements. All peak
550 metamorphic temperatures (T) were obtained using the calibration of Beyssac et al.
551 (2002).

552 Abbreviations: int = band intensity; FWHM = full width half maximum; R1 = (D1/G)
553 $_{(peak\ height\ ratio)}$; R2 = D1/(G+D1+D2) $_{area}$; T $_{(TR2)}$ = -445 × R2 + 641.

554

Sample 1: YQ17-3

ID	D1_int	D1_FWHM	D1_area	G_int	G_FWHM	G_area	D2_int	D2_FWHM	D2_area	R1	R2	T
1	999	42	61508	3007	22	101733	291	15	6726	0.33	0.36	476
2	447	46	31407	1610	21	51961	145	14	3093	0.28	0.36	476
3	619	45	37532	2169	22	70960	219	14	3249	0.29	0.34	488
4	752	44	45229	2467	21	79076	221	14	3847	0.30	0.35	480
5	874	44	52360	2997	21	95259	288	12	4661	0.29	0.34	485
6	897	45	55343	2751	24	99746	259	15	4143	0.33	0.35	483
7	812	44	49054	3145	21	101260	261	12	5027	0.26	0.32	497
8	774	45	46091	2776	21	89314	227	16	4568	0.28	0.33	491
9	513	46	30879	1695	22	56519	174	15	3772	0.30	0.34	487
10	516	43	33966	1884	20	57501	207	26	5671	0.27	0.35	482
11	488	44	29478	1811	20	56430	191	11	2769	0.27	0.33	490
12	436	45	28266	1638	21	52855	177	11	2887	0.27	0.34	488
13	681	45	40256	2295	21	72372	227	13	3607	0.30	0.35	483
14	648	44	37493	2484	20	77092	207	13	2940	0.26	0.32	496
15	675	46	44216	2420	22	80765	223	15	5070	0.28	0.34	486
16	681	47	42915	2323	21	74090	200	14	3785	0.29	0.36	479
17	510	45	33531	1730	21	56413	156	12	2665	0.29	0.36	476
18	600	45	39388	1508	23	52335	158	16	2959	0.40	0.42	452
19	579	43	34966	1991	20	60285	182	15	4281	0.29	0.35	481
20	492	51	38711	1763	22	59652	141	25	5444	0.28	0.37	471
21	548	44	37581	1635	22	53979	172	19	3995	0.34	0.39	462
22	542	49	39445	1883	21	60793	163	20	3622	0.29	0.38	468
23	445	47	32092	1351	22	46477	125	14	2500	0.33	0.40	461
24	492	48	35606	1731	21	55081	195	13	3530	0.28	0.38	469
25	487	46	34555	2009	20	61520	214	12	3477	0.24	0.35	483
26	690	49	52237	2471	21	80644	246	16	5282	0.28	0.38	469
27	913	50	68404	3630	23	128812	279	15	5042	0.25	0.34	487
28	884	59	80209	2726	24	103112	287	32	14163	0.32	0.41	456
29	623	53	50540	1603	24	59429	282	22	9819	0.39	0.42	449
30	457	55	38732	1668	23	60482	135	14	2877	0.27	0.38	468
31	345	48	24337	2016	21	65847	101	11	1227	0.17	0.27	520
32	569	50	44120	1893	24	69669	155	14	3157	0.30	0.38	469
33	386	47	28181	1440	21	47171	106	27	4510	0.27	0.35	480

34	606	44	40877	2133	22	69929	187	21	4548	0.28	0.35	480
35	595	47	41332	2231	22	76287	176	17	3384	0.27	0.34	486
36	748	48	46693	3038	23	104628	189	18	3585	0.25	0.30	504
37	937	44	56824	3007	22	97657	282	16	5553	0.31	0.36	479
38	736	40	42594	2022	21	64741	215	14	3239	0.36	0.39	466
39	440	48	32549	1814	23	64151	164	20	5205	0.24	0.32	496
40	719	42	42613	2038	22	68614	200	21	4512	0.35	0.37	473
41	590	47	42863	2118	21	68912	255	13	5123	0.28	0.37	474
42	633	47	45316	1349	25	52259	217	31	10523	0.47	0.42	450
43	409	46	28866	2518	21	82204	137	16	2299	0.16	0.25	525
44	449	54	36928	1252	23	43825	112	13	1598	0.36	0.45	437
45	759	46	45455	2700	22	89962	271	16	5818	0.28	0.32	495
46	759	45	46307	2589	21	83421	233	12	3522	0.29	0.35	483
47	519	44	32727	1767	21	57419	160	13	2595	0.29	0.35	480
48	385	56	33251	1092	22	37904	109	17	2946	0.35	0.45	437
49	433	52	34351	1410	21	46588	125	14	2769	0.31	0.41	454
50	718	49	54112	2446	21	78512	209	14	4680	0.29	0.39	462
51	603	47	43723	1926	22	60844	175	21	5636	0.31	0.40	460
52	342	44	21091	1402	20	42910	116	20	2470	0.24	0.32	497
53	412	47	30123	2037	22	68182	148	11	2506	0.20	0.30	505
54	641	56	54696	2003	22	68496	251	15	5828	0.32	0.42	448
55	825	53	67046	2695	22	92114	271	14	5942	0.31	0.41	456
56	734	46	47340	3501	23	120776	169	19	3590	0.21	0.28	516
57	752	45	45794	2847	21	92583	246	13	3452	0.26	0.32	494
58	723	51	56150	2166	23	75986	187	22	6308	0.33	0.41	456
59	586	48	40928	2088	22	71213	170	14	2565	0.28	0.36	479
60	447	43	27286	1672	19	50083	126	16	2889	0.27	0.34	486
61	1212	62	114596	3781	22	131232	304	19	8795	0.32	0.45	436
62	386	46	23182	1488	21	48120	90	18	1719	0.26	0.32	497
63	665	47	47197	2156	22	72413	205	18	5339	0.31	0.38	469
64	348	43	23079	1546	21	50827	142	12	2509	0.23	0.30	504
65	433	60	40065	2119	22	71643	133	32	6543	0.20	0.34	487
66	465	45	30073	1735	20	54077	155	16	2590	0.27	0.35	483
67	565	46	37123	1964	21	65446	156	15	2510	0.29	0.35	480
68	756	58	67304	2324	22	79317	240	17	6165	0.33	0.44	441
69	639	44	42651	2403	20	70492	237	28	6941	0.27	0.36	479
70	741	46	47256	2747	21	87849	226	14	3990	0.27	0.34	486
71	810	52	64880	1776	23	64569	223	15	4984	0.46	0.48	421
72	870	89	117454	1910	26	78214	260	27	10712	0.46	0.57	382
73	1044	44	63484	3952	21	127022	368	15	7698	0.26	0.32	495
74	676	44	45469	2475	21	79466	262	13	4379	0.27	0.35	481
75	760	47	48841	3088	21	98808	248	17	5375	0.25	0.32	496

76	454	45	28288	2166	21	68537	166	14	2548	0.21	0.28	511
77	650	46	41101	2249	21	72067	161	18	3406	0.29	0.35	481
78	470	47	34267	1775	23	63411	183	15	4384	0.26	0.34	488
79	461	52	36787	1195	22	40813	99	16	1674	0.39	0.46	430
80	438	45	30459	1397	22	43866	153	22	3648	0.31	0.39	463
81	704	42	43072	2413	21	76810	217	20	4563	0.29	0.35	484
82	658	43	43223	2704	20	84882	207	15	4958	0.24	0.32	493
83	558	55	47285	2001	22	69110	195	11	2893	0.28	0.40	461
84	719	46	44166	2499	22	80775	201	19	3982	0.29	0.34	485
85	567	44	38476	2155	21	69068	170	24	4424	0.26	0.34	485
86	728	42	46565	1905	24	64132	263	33	9243	0.38	0.39	464
87	478	46	32868	1628	20	51035	166	16	4236	0.29	0.37	471
88	679	47	45733	2236	22	76677	254	15	5109	0.30	0.36	478
89	801	63	76873	2333	25	90131	253	16	4544	0.34	0.45	437
90	629	46	36490	2897	20	87726	248	11	3450	0.22	0.29	511
91	543	54	45167	1658	23	60243	217	17	5699	0.33	0.41	456
92	1046	67	107029	3086	24	117030	367	32	17942	0.34	0.44	440
93	849	43	50388	2407	21	74922	261	14	4866	0.35	0.39	465
94	974	40	54350	2494	22	81694	281	11	4632	0.39	0.39	465
95	770	43	46074	2688	21	85185	262	14	5400	0.29	0.34	488
96	553	46	39206	1819	20	57574	202	17	5403	0.30	0.38	466
97	602	46	41613	1978	22	67454	200	13	4084	0.30	0.37	474
98	607	47	36646	2451	20	76182	183	18	4108	0.25	0.31	498
99	1075	42	64215	3010	22	101459	306	16	7045	0.36	0.37	472
100	912	45	59001	3792	21	121640	268	15	4549	0.24	0.32	496

555

556

Sample 2: YQ17-09

ID	D1_int	D1_FWHM	D1_area	G_int	G_FWHM	G_area	D2_int	D2_FWHM	D2_area	R1	R2	T
1	715	41	45592	726	32	35642	107	29	3348	0.98	0.54	396
2	1173	45	81172	1722	34	88865	214	23	5312	0.68	0.46	430
3	819	41	52121	1011	34	50153	137	25	3660	0.81	0.49	417
4	1306	43	86719	1353	36	74563	214	22	5002	0.97	0.52	404
5	336	42	21789	416	34	20431	36	32	1243	0.81	0.50	413
6	535	42	32615	351	37	18851	59	24	1500	1.52	0.62	361
7	993	46	69653	1410	34	73592	157	21	3488	0.70	0.47	425
8	652	44	44012	778	31	36726	152	28	5186	0.84	0.51	408
9	823	44	56412	695	37	39423	122	25	3806	1.18	0.57	383
10	540	43	35718	536	35	28644	67	25	1798	1.01	0.54	395
11	403	45	27668	296	36	15802	53	26	1463	1.36	0.62	361
12	475	41	30052	425	29	19196	107	35	4752	1.12	0.56	388
13	409	38	24153	403	34	20187	27	27	775	1.02	0.54	397
14	710	43	46348	729	34	37737	114	28	3364	0.97	0.53	400
15	1306	44	86086	2763	32	124139	265	25	6903	0.47	0.40	461
16	2223	43	142839	2261	34	116623	319	24	8187	0.98	0.53	398
17	1031	42	66928	1015	33	51737	175	27	5103	1.02	0.54	395
18	1459	40	91111	1230	34	64433	192	25	5020	1.19	0.57	383
19	898	42	56966	1267	32	58695	162	25	4321	0.71	0.47	425
20	807	41	51495	700	33	35029	149	25	3971	1.15	0.57	382
21	924	46	65591	799	41	50037	136	20	2964	1.16	0.55	389
22	299	40	18375	375	32	17418	52	25	1378	0.80	0.49	416
23	419	40	25877	371	33	18740	86	31	3570	1.13	0.54	397
24	1945	49	148003	2149	41	135359	206	22	4854	0.90	0.51	407
25	908	42	58259	769	33	39088	163	33	6536	1.18	0.56	386
26	1265	41	80809	1030	33	51122	235	26	6415	1.23	0.58	375
27	494	43	31157	578	34	29389	76	22	1767	0.85	0.50	413
28	728	41	44791	1029	31	45895	176	26	4802	0.71	0.47	428
29	600	40	36617	617	31	28441	153	23	4947	0.97	0.52	403
30	2094	44	141743	2566	37	144328	239	25	9137	0.82	0.48	423
31	369	43	24514	437	30	20490	88	28	2876	0.84	0.51	408
32	1483	43	93068	1271	36	65848	220	23	5437	1.17	0.57	383
33	891	43	54129	1036	35	50772	142	25	3813	0.86	0.50	414
34	1478	43	95254	1591	34	79053	228	26	6320	0.93	0.53	401
35	720	40	44476	881	32	41163	134	22	3114	0.82	0.50	413
36	3048	58	270362	5430	42	351864	504	29	20842	0.56	0.42	450
37	1797	43	111340	1854	34	91086	289	23	7066	0.97	0.53	399
38	1272	43	81776	1175	36	61863	174	27	4926	1.08	0.55	391
39	524	37	29343	474	31	21556	85	20	1834	1.11	0.56	388

40	1248	42	71856	1148	33	55346	205	23	5123	1.09	0.54	394
41	1020	37	55564	909	33	41926	149	21	3370	1.12	0.55	390
42	2001	45	126219	3138	34	153121	343	23	8380	0.64	0.44	441
43	1975	41	126428	1815	36	99784	101	34	4530	1.09	0.55	392
44	960	42	62546	809	34	42240	176	23	4555	1.19	0.57	381
45	968	41	61460	1148	34	57670	123	26	3353	0.84	0.50	413
46	460	43	29190	556	32	26888	69	29	2125	0.83	0.50	413
47	1590	41	98594	1301	37	69944	228	24	5845	1.22	0.57	384
48	813	43	53416	1140	35	58039	89	21	1968	0.71	0.47	427
49	1033	41	64349	1112	31	50348	199	30	6318	0.93	0.53	399
50	1319	41	83228	1196	31	56635	283	26	7869	1.10	0.56	385
51	551	42	35317	388	37	20553	110	26	2995	1.42	0.60	368
52	639	44	43581	575	33	29019	166	35	6213	1.11	0.55	389
53	344	41	21550	349	34	17050	70	35	2643	0.98	0.52	403
54	477	46	33345	484	39	26661	83	24	2102	0.99	0.54	397
55	585	42	37902	512	34	25768	105	32	3574	1.14	0.56	385
56	672	43	44316	589	32	28858	157	30	5030	1.14	0.57	383
57	700	43	45831	733	34	37490	121	29	4231	0.96	0.52	403
58	432	42	26707	805	31	36027	99	23	2394	0.54	0.41	454
59	714	42	45857	926	33	47169	113	23	2716	0.77	0.48	423
60	737	42	47616	771	35	38279	144	22	3382	0.96	0.53	398
61	321	42	20891	488	31	22785	64	24	1678	0.66	0.46	431
62	961	46	64363	1003	36	53095	133	30	4296	0.96	0.53	400
63	547	43	36537	627	32	29631	102	29	3171	0.87	0.53	401
64	287	41	18332	325	34	15794	39	25	1065	0.88	0.52	404
65	538	45	36290	540	34	27391	87	27	2549	1.00	0.55	392
66	966	45	65911	886	36	48202	146	25	3938	1.09	0.56	387
67	638	39	38212	677	32	32639	104	21	2368	0.94	0.52	404
68	925	44	60483	890	35	45097	156	25	4211	1.04	0.55	390
69	812	43	53639	936	32	45385	150	25	3957	0.87	0.52	404
70	736	46	49886	599	36	32773	104	28	3145	1.23	0.58	376
71	644	44	41251	624	37	33554	73	21	1616	1.03	0.54	395
72	559	43	36169	564	31	26334	97	33	3438	0.99	0.55	391
73	172	38	10086	158	34	7047	24	24	600	1.09	0.57	382
74	221	46	14311	205	36	9935	40	21	916	1.08	0.57	382
75	212	45	13277	251	30	10944	40	20	870	0.84	0.53	400
76	226	42	13641	252	34	13124	33	18	615	0.90	0.50	414
77	372	45	25963	391	35	19965	66	25	1739	0.95	0.54	393
78	1895	45	124009	2242	36	119117	287	27	8267	0.85	0.49	417
79	758	40	45677	721	35	35482	105	26	2888	1.05	0.54	394
80	290	39	17123	307	32	14788	51	25	1344	0.94	0.51	407
81	428	43	28047	463	36	24012	76	23	1876	0.92	0.52	404

82	382	42	24955	319	37	16576	73	26	2027	1.20	0.57	380
83	1046	43	68055	971	35	50210	159	27	4621	1.08	0.55	389
84	431	42	28252	462	32	22493	76	29	2391	0.93	0.53	399
85	501	42	32708	618	32	29476	102	28	3000	0.81	0.50	413
86	480	44	32724	733	31	32790	117	33	4040	0.66	0.47	427
87	1416	41	87816	1170	36	61835	234	25	6184	1.21	0.56	385
88	471	42	29820	423	33	20846	74	28	2187	1.11	0.56	384
89	588	40	35653	509	33	24830	97	30	3138	1.16	0.56	386
90	510	38	29941	550	32	25777	75	25	1992	0.93	0.52	405
91	408	37	22151	457	29	19296	58	21	1262	0.89	0.52	405
92	589	40	35272	457	36	22532	87	25	2336	1.29	0.59	374
93	1086	43	68528	1051	33	52100	172	23	4192	1.03	0.55	391
94	916	40	53477	964	32	45386	132	23	3207	0.95	0.52	403
95	369	38	21067	486	30	21378	58	25	1536	0.76	0.48	423
96	554	38	32230	720	31	33051	73	21	1651	0.77	0.48	422
97	366	38	19702	442	31	19189	63	24	1589	0.83	0.49	420
98	266	38	15427	301	31	13866	38	22	863	0.88	0.51	408
99	201	45	13898	404	32	20160	34	13	687	0.50	0.40	459
100	816	43	51774	977	34	47995	159	20	3456	0.84	0.50	413
101	413	41	25756	598	32	27504	80	21	1827	0.69	0.47	428
102	1009	41	62830	840	31	38704	204	27	5926	1.20	0.58	375
103	669	41	42368	600	35	30874	120	25	3241	1.12	0.55	389
104	521	42	33806	535	32	25285	142	26	3861	0.97	0.54	397
105	805	43	50958	722	36	37558	121	26	3307	1.12	0.55	388
106	655	46	46342	568	39	32697	99	22	2367	1.15	0.57	382
107	659	41	42203	501	34	25322	115	32	3862	1.32	0.59	372

Sample 3: YQ17-10b

ID	D1_int	D1_FWHM	D1_area	G_int	G_FWHM	G_area	D2_int	D2_FWHM	D2_area	R1	R2	T
1	1243	40	77128	1839	30	84712	326	18	6263	0.68	0.46	432
2	1623	46	115557	2716	33	139378	245	16	4227	0.60	0.45	438
3	2786	44	189554	3973	36	223022	261	25	6814	0.70	0.45	435
4	994	40	59396	1604	30	70792	225	22	5289	0.62	0.44	442
5	1062	52	84267	2140	36	118093	208	25	5556	0.50	0.41	457
6	987	39	59105	1567	30	69374	237	19	4699	0.63	0.44	439
7	1423	40	85233	1753	31	78854	317	22	7384	0.81	0.50	415
8	666	40	39185	933	32	42348	141	21	3084	0.71	0.46	430
9	857	45	59073	1244	36	69103	122	17	2177	0.69	0.45	435
10	1209	41	69598	1623	33	74865	194	23	4703	0.74	0.47	429
11	773	43	48906	1364	30	60054	150	24	3833	0.57	0.43	444
12	587	38	34300	1026	30	45471	127	22	2956	0.57	0.41	452
13	865	39	49444	1470	31	65044	202	21	4533	0.59	0.42	452
14	695	41	41463	972	33	45052	122	26	3321	0.71	0.46	431
15	1590	44	95387	2225	34	106216	228	26	6325	0.71	0.46	432
16	909	43	60606	1494	34	75608	148	21	3363	0.61	0.43	443
17	663	41	39631	969	33	44989	135	20	2855	0.68	0.45	435
18	634	43	38261	1121	32	50624	124	22	2981	0.57	0.42	451
19	1421	45	98701	2312	33	118746	194	19	3953	0.61	0.45	438
20	576	41	35847	916	32	43162	110	20	2356	0.63	0.44	441
21	1556	44	95271	2239	34	106838	271	22	6398	0.70	0.46	433
22	473	42	28938	678	33	31622	94	21	2154	0.70	0.46	431
23	959	44	61527	1411	34	68098	163	23	3930	0.68	0.46	431
24	2128	51	165894	2767	40	170035	126	22	2990	0.77	0.49	418
25	1341	46	94996	2191	34	115834	224	21	5017	0.61	0.44	441
26	466	41	27596	656	30	28888	106	22	2507	0.71	0.47	428
27	1208	45	83100	1796	33	92342	170	19	3454	0.67	0.46	430
28	766	41	47986	1272	29	55608	183	18	3516	0.60	0.45	437
29	837	44	56154	1256	33	63634	130	17	2412	0.67	0.46	432
30	1589	62	151048	2470	41	157412	160	5	873	0.64	0.49	419
31	1428	42	83185	2005	33	93867	231	24	5785	0.71	0.45	434
32	2261	40	138418	4006	30	176576	540	19	11186	0.56	0.42	448
33	623	44	42658	896	35	47711	112	17	2031	0.70	0.46	431
34	1356	42	87866	2499	30	115307	251	21	5730	0.54	0.42	450
35	1796	46	128589	2860	35	154504	224	19	4610	0.63	0.45	438
36	1113	41	64747	1595	33	74028	192	25	5037	0.70	0.45	436
37	618	39	36068	1005	31	44207	116	23	2864	0.62	0.43	444
38	1223	40	74352	1992	32	91222	263	23	6356	0.61	0.43	444
39	843	45	58163	1335	35	67409	134	24	3381	0.63	0.45	436

40	577	41	35252	1128	30	49898	140	19	2789	0.51	0.40	459
41	1413	41	81667	1882	34	88619	252	23	6083	0.75	0.46	430
42	652	43	39226	1002	33	45715	140	21	3203	0.65	0.45	439
43	828	41	49183	1393	32	62992	162	21	3553	0.59	0.42	448
44	933	40	54738	1507	30	65993	209	21	4566	0.62	0.44	442
45	888	45	58955	949	34	47287	166	21	3774	0.94	0.54	397
46	696	45	48643	1039	32	50273	118	24	3010	0.67	0.48	424
47	1246	50	96086	1571	41	98161	159	26	4374	0.79	0.48	421
48	676	42	39009	912	33	41858	144	21	3174	0.74	0.46	430
49	1156	46	75099	1303	38	70776	169	24	4271	0.89	0.50	413
50	873	45	59040	1189	34	59571	145	26	3961	0.73	0.48	422
51	515	44	35006	698	34	35223	81	23	1949	0.74	0.48	420
52	864	45	59273	1108	35	56450	132	25	3464	0.78	0.50	415
53	702	44	47105	838	33	41767	117	22	2796	0.84	0.51	407
54	840	45	52622	1242	34	58852	173	23	4180	0.68	0.45	434
55	760	42	47035	936	34	45776	133	21	2958	0.81	0.49	418
56	714	43	47799	1046	34	52956	120	24	3027	0.68	0.46	431
57	665	45	45133	825	35	42226	109	24	2732	0.81	0.50	413
58	589	44	39553	795	34	39724	101	21	2234	0.74	0.49	420
59	639	45	43926	864	34	42870	109	23	2614	0.74	0.49	417
60	524	44	34485	765	33	37725	85	23	2124	0.68	0.46	430
61	564	45	38467	837	34	41592	93	26	2582	0.67	0.47	429
62	1209	46	74203	1790	34	83933	225	23	5459	0.68	0.45	435
63	630	45	41983	913	35	45613	123	21	2793	0.69	0.46	430
64	887	45	55431	1365	34	64741	179	22	4168	0.65	0.45	438
65	720	45	49420	1467	32	66915	132	24	3337	0.49	0.41	453
66	585	44	37232	770	36	40809	108	19	2198	0.76	0.46	430
67	1091	42	66007	1439	34	67560	194	23	4761	0.76	0.48	424
68	804	45	49096	1109	35	53094	159	24	4048	0.72	0.46	431
69	891	45	59800	962	34	48813	156	22	3727	0.93	0.53	399

559

560

Sample 4: YQ17-12b

ID	D1_int	D1_FWHM	D1_area	G_int	G_FWHM	G_area	D2_int	D2_FWHM	D2_area	R1	R2	T
1	870	43	54928	1150	33	54440	161	22	3699	0.76	0.49	420
2	686	42	39076	1074	32	48642	133	22	3045	0.64	0.43	445
3	343	41	20667	539	31	23944	57	23	1388	0.64	0.45	437
4	1495	44	101423	1780	35	96829	228	23	5692	0.84	0.50	415
5	845	41	50987	1040	33	50393	119	22	2837	0.81	0.49	418
6	1142	42	74438	806	37	45945	188	21	4798	1.42	0.59	370
7	793	39	48391	758	33	37554	142	23	3506	1.05	0.54	395
8	593	41	35694	716	34	37371	78	20	1647	0.83	0.48	424
9	1900	49	142539	2063	43	135704	211	18	3999	0.92	0.51	411
10	259	40	15609	389	30	17698	27	24	677	0.67	0.46	432
11	710	41	43917	621	32	30238	124	28	3676	1.14	0.56	384
12	1876	44	126624	1886	36	104372	260	23	6369	0.99	0.53	398
13	584	44	40077	466	39	28086	79	25	2085	1.25	0.57	381
14	1781	44	121993	1090	45	74898	202	55	16934	1.63	0.57	381
15	1603	42	103840	1463	35	77891	228	22	5401	1.10	0.55	389
16	1156	39	69150	1761	32	82105	192	21	4273	0.66	0.44	439
17	257	44	16802	354	33	17328	34	23	825	0.73	0.48	422
18	359	41	22546	377	36	19507	55	25	1451	0.95	0.52	405
19	825	42	49480	846	33	41034	132	20	2800	0.98	0.53	400
20	1151	44	74276	1380	34	68453	183	24	4688	0.83	0.50	412
21	2865	42	187177	2749	37	155314	338	24	8703	1.04	0.53	398
22	569	41	34657	754	30	34353	87	21	1943	0.75	0.49	419
23	363	42	20662	461	31	20841	54	24	1344	0.79	0.48	422
24	239	41	15167	301	33	14333	37	20	775	0.80	0.50	413
25	740	41	43796	834	33	40091	105	27	3001	0.89	0.50	412
26	1775	42	115190	2264	34	118822	249	18	5645	0.78	0.48	422
27	652	43	42551	770	34	40767	94	26	2567	0.85	0.50	416
28	259	44	16154	296	35	15370	50	20	1070	0.88	0.50	415
29	807	42	47243	915	34	44352	126	22	2888	0.88	0.50	413
30	416	43	25608	484	35	25643	41	21	900	0.86	0.49	418
31	447	41	25636	282	35	14179	80	22	1829	1.58	0.62	361
32	1365	45	91690	1378	35	73466	212	24	5340	0.99	0.54	396
33	509	43	30803	714	33	34369	87	21	1934	0.71	0.46	432
34	1839	35	97411	1055	32	50956	283	21	6323	1.74	0.63	354
35	440	41	26708	627	33	29806	62	18	1196	0.70	0.46	430
36	1471	42	91330	1749	33	86968	195	23	4709	0.84	0.50	414
37	331	40	19529	440	34	21404	51	21	1121	0.75	0.46	430
38	765	44	50993	1054	33	51965	144	22	3429	0.73	0.48	423
39	594	41	35127	915	34	42756	93	25	2516	0.65	0.44	442

40	944	40	55628	1297	32	60407	143	20	3096	0.73	0.47	429
41	1611	42	98782	2412	31	109944	245	21	5488	0.67	0.46	431
42	862	42	52345	1473	32	66594	152	20	3177	0.59	0.43	446
43	578	44	37213	717	34	34834	102	23	2572	0.81	0.50	414
44	304	41	17950	375	32	17458	59	23	1457	0.81	0.49	419
45	253	40	14994	312	33	14766	44	20	925	0.81	0.49	419
46	451	46	30780	622	33	31799	59	18	1106	0.73	0.48	421
47	830	43	52999	1153	34	56504	136	25	3654	0.72	0.47	428
48	614	40	38226	758	33	37538	87	20	1861	0.81	0.49	417
49	874	42	53978	1078	34	52984	140	23	3372	0.81	0.49	418
50	578	39	33631	729	32	34226	70	25	1870	0.79	0.48	422
51	1328	39	79457	1034	35	53418	220	22	5252	1.28	0.58	379
52	448	39	26681	663	32	30396	87	22	2041	0.68	0.45	436
53	701	43	41252	1359	31	58926	142	22	3353	0.52	0.40	460
54	1852	42	119003	2289	35	115084	282	23	6960	0.81	0.49	416
55	950	39	55704	946	32	44061	181	21	4088	1.00	0.54	397
56	1200	39	70719	1018	34	51597	167	24	4221	1.18	0.56	387
57	332	40	20374	388	32	18610	61	19	1389	0.86	0.50	411
58	418	41	26274	389	34	19882	66	22	1908	1.07	0.55	392
59	751	40	44003	987	35	49394	103	26	2822	0.76	0.46	433
60	742	41	45313	698	35	36617	95	23	2286	1.06	0.54	396
61	1292	53	104854	1525	43	100695	141	19	2826	0.85	0.50	412
62	966	42	60004	864	34	41860	182	22	4305	1.12	0.57	384
63	369	40	21959	450	33	20974	60	26	1668	0.82	0.49	417
64	1332	51	103926	1698	38	100091	330	28	14458	0.78	0.48	425
65	647	43	41343	1042	32	48911	113	22	2631	0.62	0.45	438
66	1081	45	71912	1633	34	80045	191	24	4945	0.66	0.46	432
67	632	48	44764	931	35	46737	126	23	3116	0.68	0.47	426
68	465	44	29078	720	32	33512	92	21	2095	0.65	0.45	436
69	796	42	48755	1112	31	50691	135	25	3540	0.72	0.47	426
70	1671	46	118955	2200	37	125376	228	19	5120	0.76	0.48	424
71	1013	40	60791	1415	32	66950	151	21	3315	0.72	0.46	430
72	1019	41	60678	959	32	46239	182	22	4245	1.06	0.55	393
73	903	43	57008	933	34	45456	179	24	4587	0.97	0.53	399
74	1466	41	91102	1227	35	64226	213	22	4991	1.20	0.57	382
75	414	46	26585	843	30	37717	74	27	2116	0.49	0.40	459
76	518	45	34358	871	31	39477	114	24	2914	0.60	0.45	437
77	457	41	27566	609	32	29598	67	21	1514	0.75	0.47	427
78	1046	44	70617	1389	33	70155	204	23	5181	0.75	0.48	421
79	877	43	57950	618	35	33136	123	25	3218	1.42	0.61	361
80	505	42	32619	471	33	24060	70	23	1686	1.07	0.56	387
81	800	46	56584	759	36	41977	102	20	2115	1.05	0.56	385

561

Sample 5: YQ17-15

ID	D1_int	D1_FWHM	D1_area	G_int	G_FWHM	G_area	D2_int	D2_FWHM	D2_area	R1	R2	T
1	295	52	23408	160	45	10870	54	28	1619	1.84	0.65	344
2	615	50	47337	338	44	22684	114	35	4246	1.82	0.64	351
3	797	52	63583	412	47	29100	172	36	6617	1.93	0.64	350
4	641	53	51991	295	48	21499	156	39	6408	2.17	0.65	345
5	585	52	46313	279	45	19096	137	37	5402	2.10	0.65	343
6	326	52	26179	161	46	11399	69	37	2765	2.02	0.65	346
7	435	51	32986	234	44	15759	85	34	3081	1.86	0.64	351
8	390	50	29111	209	44	13776	73	32	2471	1.87	0.64	349
9	414	54	33930	199	47	14258	103	39	4238	2.08	0.65	347
10	795	54	66317	329	56	28109	192	45	9213	2.41	0.64	350
11	599	51	46219	308	44	20487	127	32	4346	1.94	0.65	345
12	666	53	54292	305	47	21849	159	38	6512	2.18	0.66	342
13	902	58	79788	398	52	31353	250	40	10568	2.27	0.66	343
14	730	50	55508	349	45	23412	154	35	5788	2.09	0.66	343
15	730	50	55440	357	45	24391	148	39	6095	2.04	0.65	347
16	796	53	64378	370	48	27348	176	39	7364	2.15	0.65	345
17	1185	49	89030	674	44	45580	195	27	5605	1.76	0.63	352
18	539	50	40761	285	43	18305	107	31	3541	1.89	0.65	345
19	494	53	39222	241	48	17775	107	39	4390	2.05	0.64	350
20	389	51	29798	216	44	14429	76	30	2465	1.80	0.64	351
21	830	52	66454	427	45	29458	174	32	5846	1.94	0.65	344
22	763	52	60606	335	47	23723	184	39	7662	2.28	0.66	341
23	563	54	46189	275	46	19225	139	35	5222	2.05	0.65	343
24	460	54	38281	218	51	17129	107	40	4591	2.11	0.64	351
25	808	53	65339	443	46	31316	140	35	5165	1.82	0.64	349
26	936	51	72822	476	45	32542	191	36	7404	1.97	0.65	347
27	557	52	42618	310	47	20341	108	30	3456	1.80	0.64	349
28	643	49	46812	348	40	21352	140	32	4819	1.85	0.64	349
29	539	50	41753	270	46	18920	114	38	4661	2.00	0.64	350
30	620	53	49630	292	48	21319	137	40	5852	2.12	0.65	347
31	617	53	49409	259	55	21784	135	43	6152	2.38	0.64	350
32	529	51	41375	281	44	18858	96	31	3139	1.88	0.65	344
33	729	50	56168	380	45	26019	150	37	5947	1.92	0.64	351
34	815	52	65255	391	45	26931	187	36	7128	2.08	0.66	342
35	705	59	63320	286	56	24289	216	42	9625	2.46	0.65	345
36	791	52	62844	398	45	27154	166	32	5632	1.99	0.66	342
37	761	54	62783	348	53	28287	187	45	8870	2.19	0.63	355
38	768	53	62195	313	52	24790	195	43	8883	2.45	0.65	346
39	656	51	50938	310	45	21396	150	37	5858	2.11	0.65	345

40	726	51	56444	354	44	24159	163	37	6417	2.05	0.65	346
41	874	54	71965	435	46	30662	204	35	7652	2.01	0.65	344
42	474	51	37239	229	45	15727	99	38	3980	2.07	0.65	343
43	844	51	65351	411	45	27937	192	35	7108	2.05	0.65	345
44	701	52	54024	390	42	24962	128	33	4523	1.80	0.65	347
45	764	51	60382	422	43	28003	157	31	5217	1.81	0.65	347
46	689	53	55918	354	44	24001	166	37	6452	1.95	0.65	346
47	777	50	60157	373	47	26957	185	40	7949	2.08	0.63	353
48	664	52	53347	386	51	27427	76	31	2490	1.72	0.64	349
49	899	51	70973	421	49	31507	197	41	8541	2.14	0.64	350
50	799	52	61905	391	44	26433	191	36	7249	2.04	0.65	346
51	645	55	54038	311	48	22934	166	39	6890	2.07	0.64	348
52	1101	52	88253	534	45	36994	218	34	7877	2.06	0.66	339
53	632	49	47355	352	43	23241	112	32	3839	1.80	0.64	352
54	1087	51	85862	576	45	40006	228	33	8022	1.89	0.64	349
55	1056	51	81226	600	46	41248	165	29	5108	1.76	0.64	351
56	702	55	59247	336	47	24356	163	36	6143	2.09	0.66	341
57	824	54	68094	393	49	29237	211	39	8797	2.10	0.64	349
58	784	49	58873	424	43	27587	158	31	5221	1.85	0.64	349
59	779	52	61666	398	45	27560	186	39	7758	1.96	0.64	352
60	1022	50	78767	517	45	35516	234	38	9433	1.97	0.64	351
61	611	53	49167	327	44	22284	118	34	4249	1.87	0.65	345

562

Sample 6: YQ17-23a

ID	D1_int	D1_FWHM	D1_area	G_int	G_FWHM	G_area	D2_int	D2_FWHM	D2_area	R1	R2	T
1	38	44	2387	136	22	4272	12	27	340	0.28	0.34	486
2	54	47	2930	266	21	8204	15	19	291	0.20	0.26	524
3	34	47	2105	150	21	4819	10	14	190	0.23	0.30	506
4	108	45	5856	446	21	14027	38	11	537	0.24	0.29	511
5	34	46	1966	138	22	4606	9	20	194	0.25	0.29	509
6	64	47	3809	335	24	11531	18	22	412	0.19	0.24	531
7	46	46	3309	194	21	6015	17	29	527	0.24	0.34	488
8	76	45	4124	325	21	10142	26	11	391	0.23	0.28	513
9	49	45	2903	236	21	7211	10	30	302	0.21	0.28	514
10	95	46	5278	352	21	11145	28	15	452	0.27	0.31	499
11	101	47	5677	508	22	17099	29	13	400	0.20	0.24	530
12	89	45	4722	493	21	15111	24	15	388	0.18	0.23	535
13	104	46	5832	400	22	12742	30	16	523	0.26	0.31	502
14	64	46	3576	284	20	8603	19	13	263	0.22	0.29	510
15	88	45	4811	372	20	11028	28	11	473	0.24	0.29	507
16	64	46	3671	259	22	8422	17	16	291	0.25	0.30	506
17	56	45	3427	246	21	7729	19	17	369	0.23	0.30	506
18	65	45	3735	234	21	7220	18	18	339	0.28	0.33	491
19	42	47	2967	192	21	6121	14	12	232	0.22	0.32	496
20	88	46	4962	428	20	13161	26	15	421	0.21	0.27	519
21	58	46	3328	216	21	6653	14	13	276	0.27	0.32	493
22	71	46	3909	253	22	7975	17	24	427	0.28	0.32	497
23	115	45	6359	492	20	14768	41	12	684	0.23	0.29	508
24	109	45	5924	653	20	19949	33	12	434	0.17	0.23	539
25	96	45	5439	420	20	12952	26	16	455	0.23	0.29	510
26	124	46	6810	685	20	21104	41	11	538	0.18	0.24	532
27	103	46	5684	442	20	13505	34	10	380	0.23	0.29	509
28	79	50	5685	352	22	11758	28	25	773	0.22	0.31	499
29	82	49	6080	320	21	10018	22	16	366	0.26	0.37	473
30	61	47	3562	344	19	10382	19	10	195	0.18	0.25	526
31	101	44	5575	380	22	12370	30	11	475	0.26	0.30	503
32	41	48	2267	134	21	4234	11	21	257	0.31	0.34	488
33	65	46	3492	251	21	7868	24	8	300	0.26	0.30	505
34	42	47	2417	162	23	5433	12	10	186	0.26	0.30	504
35	87	46	4871	375	22	12141	28	13	467	0.23	0.28	514
36	103	45	5974	274	21	8848	25	20	529	0.38	0.39	464
37	121	46	6680	622	21	19598	47	11	688	0.19	0.25	528
38	122	45	6718	479	21	15016	43	11	695	0.25	0.30	505
39	123	45	6671	656	20	20051	36	13	494	0.19	0.25	529

40	83	47	4648	448	22	14650	15	24	393	0.18	0.24	534
41	103	45	5882	390	21	12467	27	19	531	0.26	0.31	499
42	154	47	9153	571	22	19050	42	18	818	0.27	0.32	497
43	65	46	3644	167	23	5618	15	21	334	0.39	0.38	468
44	114	45	6651	408	22	13162	25	30	792	0.28	0.32	494
45	25	47	1678	182	21	5477	7	27	215	0.14	0.23	537
46	44	46	2389	180	21	5748	12	17	216	0.24	0.29	511
47	34	47	2187	165	23	5553	10	22	227	0.21	0.27	516
48	54	46	3179	191	22	6194	14	20	284	0.28	0.33	491
49	99	46	5455	386	22	12257	27	20	569	0.26	0.30	505
50	105	45	5975	467	21	14552	26	18	495	0.23	0.28	512
51	51	46	3235	207	21	6511	14	24	352	0.25	0.32	495
52	62	45	3844	226	22	7180	16	24	395	0.27	0.34	488
53	57	46	3310	222	23	7519	15	20	314	0.26	0.30	506
54	119	44	6647	367	22	12176	32	15	513	0.32	0.34	485
55	61	47	3439	245	22	7885	15	19	291	0.25	0.30	506
56	38	46	2300	119	22	3884	11	23	270	0.32	0.36	479
57	44	44	2740	147	23	4807	13	33	465	0.30	0.34	485
58	81	46	4609	290	22	9242	24	17	432	0.28	0.32	494
59	110	45	6062	528	21	16394	35	12	509	0.21	0.26	521
60	87	46	4976	327	21	10432	28	12	451	0.27	0.31	498
61	123	46	6871	522	20	16104	37	13	601	0.24	0.29	508
62	38	46	2250	180	19	5454	11	16	190	0.21	0.29	511

563

Sample 7: YQ17-28

ID	D1_int	D1_FWHM	D1_area	G_int	G_FWHM	G_area	D2_int	D2_FWHM	D2_area	R1	R2	T
1	164	42	9360	874	18	24485	37	12	479	0.19	0.27	517
2	165	44	10857	793	19	23818	55	11	623	0.21	0.31	501
3	162	46	11563	830	19	23871	80	26	2241	0.20	0.31	501
4	168	42	10759	836	19	24321	72	29	2205	0.20	0.29	510
5	193	44	10855	928	21	29103	30	20	626	0.21	0.27	519
6	264	42	15387	1288	19	37055	92	12	1364	0.20	0.29	511
7	86	45	5959	338	20	10019	38	25	1023	0.25	0.35	482
8	190	44	9836	882	19	25338	41	12	523	0.22	0.28	516
9	178	46	11872	661	20	20081	47	21	1031	0.27	0.36	477
10	114	45	7867	677	18	19058	63	25	1645	0.17	0.28	516
11	152	46	9737	774	20	22687	47	10	486	0.20	0.30	506
12	154	45	10401	775	21	24493	52	28	1518	0.20	0.29	511
13	174	43	8948	691	19	19935	53	11	618	0.25	0.30	503
14	140	44	8237	759	20	22879	40	11	472	0.18	0.26	522
15	115	44	7862	581	20	18017	35	24	899	0.20	0.29	507
16	220	45	13023	1031	19	30148	107	9	1308	0.21	0.29	508
17	139	46	9201	1007	19	28910	34	30	1105	0.14	0.23	534
18	131	45	8983	548	19	14939	47	24	1207	0.24	0.36	478
19	136	43	7867	706	19	21206	49	10	528	0.19	0.27	520
20	159	47	11525	725	19	19914	58	25	1575	0.22	0.35	482
21	166	44	10190	946	20	29324	54	12	887	0.18	0.25	526
22	142	46	10144	709	19	20550	53	23	1298	0.20	0.32	497
23	174	43	10133	888	20	26282	72	8	786	0.20	0.27	517
24	187	44	12691	1027	20	31504	64	21	1447	0.18	0.28	514
25	202	46	11814	960	22	31377	36	20	766	0.21	0.27	519
26	162	43	9509	778	20	23272	56	12	874	0.21	0.28	512
27	181	48	13279	846	20	26240	45	10	483	0.21	0.33	490
28	160	43	10201	753	21	23630	39	26	1071	0.21	0.29	508
29	199	44	11930	757	21	23798	48	18	907	0.26	0.33	493
30	100	45	5523	643	19	18460	35	10	371	0.16	0.23	538
31	101	42	5399	637	18	17444	36	11	439	0.16	0.23	535
32	82	42	5153	441	19	12887	24	25	633	0.19	0.28	515
33	111	40	6911	565	18	14700	67	24	1696	0.20	0.30	506
34	160	43	8617	785	18	22202	32	21	723	0.20	0.27	517
35	301	45	16035	1781	20	53900	56	15	874	0.17	0.23	538
36	137	43	8851	797	19	23468	57	10	814	0.17	0.27	519
37	196	42	10438	1114	18	30578	70	9	794	0.18	0.25	527
38	145	46	8439	1100	22	35842	42	13	668	0.13	0.19	556
39	110	44	6169	629	20	18804	35	11	422	0.18	0.24	530

40	210	43	11725	1193	18	33628	90	8	1076	0.18	0.25	526
41	301	44	15447	2008	19	57484	114	10	1162	0.15	0.21	546
42	170	52	13620	913	19	25943	87	21	1942	0.19	0.33	492
43	150	43	9447	799	20	24034	43	17	775	0.19	0.28	516
44	98	43	6183	533	20	16038	25	13	351	0.18	0.27	516
45	106	46	7507	546	19	15726	39	28	1145	0.19	0.31	501
46	104	44	5440	640	20	18813	36	9	357	0.16	0.22	540
47	256	43	13788	1580	19	45073	61	12	791	0.16	0.23	536
48	201	43	10794	1259	18	34889	69	10	844	0.16	0.23	535
49	174	42	10057	1194	19	34247	77	10	1002	0.15	0.22	540
50	236	44	13291	1102	20	32715	76	10	1039	0.21	0.28	512
51	117	42	7666	688	19	19253	46	28	1371	0.17	0.27	518
52	184	43	10145	717	19	20417	60	8	782	0.26	0.32	494
53	224	43	12459	1065	18	29363	72	11	858	0.21	0.29	508
54	142	42	8238	865	19	24905	64	9	888	0.16	0.24	531
55	176	44	10417	1070	20	31586	96	9	1249	0.16	0.24	531
56	137	43	7287	707	19	20912	41	13	566	0.19	0.25	526
57	81	44	4332	489	20	14821	23	12	290	0.17	0.22	540
58	152	43	9145	759	20	22718	65	9	851	0.20	0.28	514
59	179	43	10244	1346	18	37221	53	9	531	0.13	0.21	544
60	193	43	11863	970	20	28548	71	12	1286	0.20	0.28	512
61	77	43	4852	462	19	12956	23	28	684	0.17	0.26	522
62	143	43	9506	614	20	17680	58	23	1388	0.23	0.33	490
63	184	43	11557	756	19	21987	50	20	1104	0.24	0.33	489
64	197	43	10857	1066	19	31460	67	10	855	0.18	0.25	527
65	103	42	5906	606	20	17856	29	18	563	0.17	0.24	531
66	107	40	6556	582	19	17061	37	22	986	0.18	0.27	520
67	143	42	9303	563	18	15490	46	24	1163	0.25	0.36	478
68	102	43	6741	473	19	13265	33	28	970	0.21	0.32	495
69	124	43	7186	620	19	18306	32	15	503	0.20	0.28	515
70	120	43	7872	708	20	20681	43	26	1182	0.17	0.26	521
71	151	44	7770	825	19	23632	46	10	501	0.18	0.24	530
72	200	42	10892	1051	20	31771	69	9	831	0.19	0.25	527
73	132	42	7891	725	19	21103	47	9	684	0.18	0.27	520
74	123	43	8025	611	20	18200	39	11	696	0.20	0.30	505
75	210	43	11916	1192	19	34878	74	10	918	0.18	0.25	527
76	235	45	13811	1206	22	38462	48	17	863	0.19	0.26	523
77	195	42	10871	1145	19	32821	57	9	659	0.17	0.25	529
78	182	45	10451	877	20	26760	49	10	519	0.21	0.28	515
79	118	50	9066	610	18	16920	52	24	1321	0.19	0.33	490
80	205	43	11433	1198	20	35949	53	15	832	0.17	0.24	533

564

Sample 8: YQ17-29

ID	D1_int	D1_FWHM	D1_area	G_int	G_FWHM	G_area	D2_int	D2_FWHM	D2_area	R1	R2	T
1	1160	49	84923	709	46	47564	166	27	4845	1.64	0.62	360
2	1247	50	92505	712	43	45364	231	30	7351	1.75	0.64	351
3	2031	57	176889	834	60	75799	485	46	23694	2.44	0.64	350
4	1050	50	78092	514	43	34081	244	36	9235	2.04	0.64	348
5	837	54	68368	389	47	28219	200	42	8855	2.15	0.65	346
6	1263	49	91931	679	41	42309	295	33	10242	1.86	0.64	351
7	1694	53	134773	675	48	46855	378	39	15621	2.51	0.68	330
8	3451	50	261149	2114	43	140846	577	29	18059	1.63	0.62	358
9	1609	50	122125	921	42	59605	283	33	9810	1.75	0.64	351
10	1380	48	99462	735	41	46805	235	33	8341	1.88	0.64	348
11	1199	47	83411	683	41	40716	222	28	6624	1.76	0.64	351
12	1941	54	157482	928	47	66943	476	39	19886	2.09	0.64	348
13	1255	53	101571	715	43	47744	222	33	7765	1.75	0.65	347
14	2212	50	168089	1270	43	84779	389	30	12452	1.74	0.63	353
15	2701	50	208261	1522	45	104469	453	35	16966	1.78	0.63	354
16	2161	51	168852	1016	47	73232	450	40	19153	2.13	0.65	347
17	2715	59	245687	1011	61	90348	755	45	36088	2.68	0.66	341
18	3447	53	276715	1695	46	119254	612	39	25667	2.03	0.66	342
19	1148	53	92760	648	51	48161	142	30	4443	1.77	0.64	351
20	2059	47	148485	999	42	65100	376	35	14094	2.06	0.65	344
21	2360	48	169124	1275	43	84145	393	32	13371	1.85	0.63	352
22	1855	50	138796	1010	45	68248	295	30	9490	1.84	0.64	349
23	1470	49	110413	839	41	52375	340	33	12039	1.75	0.63	354
24	1804	54	145739	744	51	58331	458	44	21346	2.42	0.65	347
25	1511	58	134577	1024	40	63135	410	39	16813	1.48	0.63	356
26	2032	56	175321	889	51	67254	488	41	21168	2.29	0.66	339
27	1661	55	139135	1120	41	71195	320	34	11748	1.48	0.63	356
28	1039	49	78020	761	36	42243	209	32	7170	1.37	0.61	362
29	1410	54	115868	832	40	50939	392	41	17153	1.69	0.63	354
30	1174	52	90745	737	39	43902	247	34	8849	1.59	0.63	353
31	1855	56	158590	676	58	59550	495	44	23241	2.74	0.66	342
32	998	52	77980	421	51	32555	255	43	11689	2.37	0.64	351
33	1105	48	78477	779	37	44196	202	32	6792	1.42	0.61	365
34	1080	54	88567	499	50	38384	258	42	11491	2.16	0.64	350
35	1532	48	111847	822	43	53344	276	26	7706	1.86	0.65	347
36	2223	54	184806	1186	48	86557	396	39	16292	1.88	0.64	349
37	1901	59	170463	819	56	69786	509	44	24048	2.32	0.64	348
38	2910	55	243869	1241	54	103194	566	45	27395	2.34	0.65	345
39	790	48	52227	435	46	25949	119	26	3288	1.82	0.64	349

40	2327	58	204430	880	54	70227	552	43	25042	2.64	0.68	331
41	1805	52	135437	1118	49	77366	210	23	5161	1.61	0.62	358
42	1467	51	112450	865	44	57910	253	29	7785	1.70	0.63	354
43	1990	50	150686	956	44	62348	433	36	16633	2.08	0.66	342
44	2695	52	215635	1180	47	83761	578	39	24171	2.28	0.67	338
45	920	48	62967	556	43	34076	182	26	4976	1.65	0.62	360
46	1324	54	109015	699	46	49262	281	37	11024	1.89	0.64	348
47	763	48	53967	443	47	30404	113	23	2759	1.72	0.62	359
48	1922	49	144908	1272	38	74262	407	34	14691	1.51	0.62	359
49	1429	56	120664	748	48	54765	315	37	12468	1.91	0.64	349
50	1284	52	95693	729	48	48191	168	27	4828	1.76	0.64	348
51	2239	57	191998	1017	50	74567	521	38	21081	2.20	0.67	337
52	1271	49	95310	622	45	42307	193	31	6281	2.04	0.66	340
53	3322	54	277437	1446	54	119130	725	46	35567	2.30	0.64	349
54	3539	52	285335	1759	45	121729	893	37	35555	2.01	0.64	348
55	1206	51	89040	746	50	50999	123	25	3229	1.62	0.62	358
56	2338	59	212083	1122	56	95743	535	46	26283	2.08	0.63	352
57	812	50	60194	417	48	29032	103	28	3087	1.95	0.65	344
58	1993	52	153763	1058	46	74217	360	33	12687	1.88	0.64	350
59	1310	50	98054	713	43	45327	257	31	8522	1.84	0.65	347
60	1409	55	115624	655	52	51597	294	43	13596	2.15	0.64	350
61	2254	51	170457	1424	44	93086	380	32	13011	1.58	0.62	361
62	740	47	53676	449	48	32347	97	25	2569	1.65	0.61	365

565

Sample 9: YQ18-01a

ID	D1_int	D1_FWHM	D1_area	G_int	G_FWHM	G_area	D2_int	D2_FWHM	D2_area	R1	R2	T
1	276	42	15564	374	32	15752	62	23	1502	0.74	0.47	425
2	666	42	43171	690	32	31823	130	34	6743	0.97	0.53	401
3	385	40	22468	685	29	28189	91	28	2666	0.56	0.42	449
4	434	39	25025	564	32	25825	80	23	1925	0.77	0.47	425
5	766	41	42765	1060	32	47010	166	22	3959	0.72	0.46	433
6	526	41	28158	675	33	29507	117	22	2758	0.78	0.47	429
7	468	36	26090	533	31	23289	106	23	2645	0.88	0.50	413
8	560	40	30701	828	32	36929	100	21	2279	0.68	0.44	441
9	353	41	19312	594	31	25241	76	26	2104	0.60	0.41	453
10	452	40	25667	565	32	24883	93	25	2494	0.80	0.48	421
11	414	39	24800	740	27	28686	142	23	3496	0.56	0.44	443
12	733	42	42880	1127	33	50151	147	23	3567	0.65	0.44	439
13	264	39	13928	316	32	13702	55	21	1209	0.83	0.48	421
14	387	41	21078	475	33	20665	79	24	2026	0.81	0.48	422
15	301	39	17418	374	32	16292	67	25	1816	0.81	0.49	418
16	270	42	14039	864	21	27312	69	35	2525	0.31	0.32	495
17	835	42	47749	1669	30	69868	161	25	4260	0.50	0.39	463
18	576	41	35036	940	24	34125	174	22	4117	0.61	0.48	423
19	802	40	43377	964	33	43554	149	23	3602	0.83	0.48	423
20	538	38	31061	653	31	28088	122	24	3135	0.82	0.50	414
21	229	40	13625	325	33	14184	49	24	1242	0.70	0.47	428
22	400	40	24462	542	30	22686	110	28	3256	0.74	0.49	420
23	458	41	25185	920	30	37555	93	23	2317	0.50	0.39	465
24	742	41	41001	1500	29	61215	120	23	2895	0.50	0.39	464
25	378	40	21982	986	25	36053	116	21	2573	0.38	0.36	476
26	454	41	25972	649	32	29243	93	28	2766	0.70	0.45	437
27	521	40	29522	728	33	33427	104	21	2365	0.72	0.45	435
28	297	38	16437	462	30	19372	56	24	1407	0.64	0.44	440
29	433	39	26039	452	29	18230	163	27	4704	0.96	0.53	399
30	389	39	20928	680	25	24706	131	16	2199	0.57	0.44	442
31	695	42	45557	1585	22	53835	259	17	4682	0.44	0.44	442

566

Sample 11: YQ18-03

ID	D1_int	D1_FWHM	D1_area	G_int	G_FWHM	G_area	D2_int	D2_FWHM	D2_area	R1	R2	T
1	578	47	41765	1925	24	71630	191	14	2912	0.30	0.36	478
2	212	37	12013	633	23	21440	76	24	1937	0.33	0.34	487
3	209	39	12634	430	21	13952	85	19	1754	0.49	0.45	438
4	391	42	25269	538	29	24048	129	18	2416	0.73	0.49	419
5	147	38	8570	349	19	9400	101	26	2764	0.42	0.41	453
6	180	38	10609	285	22	9317	177	18	4650	0.63	0.43	445
7	128	35	6893	192	28	8273	33	19	948	0.67	0.43	446
8	251	39	15134	475	23	16109	175	25	4605	0.53	0.42	449
9	177	46	12623	282	29	12651	63	28	1859	0.63	0.47	429
10	132	38	7690	200	28	8511	89	21	2450	0.66	0.41	453
11	267	41	16862	513	27	21309	119	24	3114	0.52	0.41	455
12	168	40	10423	252	24	9327	112	24	3672	0.67	0.45	439
13	180	42	11793	452	21	14911	92	27	2610	0.40	0.40	458
14	375	37	21445	534	28	22654	89	28	2616	0.70	0.46	432
15	191	39	11561	253	25	8361	142	22	4063	0.76	0.48	422
16	250	36	13812	456	20	13406	153	26	4266	0.55	0.44	441
17	121	41	7598	265	25	10367	51	21	1119	0.46	0.40	460
18	385	40	23724	510	33	24853	76	23	1989	0.76	0.47	428
19	176	35	9580	289	26	11828	54	18	1211	0.61	0.42	448
20	203	48	15025	421	26	16959	88	21	2008	0.48	0.44	440
21	451	35	22076	704	27	26370	72	22	1680	0.64	0.44	441
22	117	41	7404	171	25	6212	67	18	1827	0.68	0.48	423
23	336	39	19492	668	27	26117	60	24	1519	0.50	0.41	453
24	672	40	38961	1118	31	50763	120	23	2989	0.60	0.42	450
25	515	40	30435	748	27	30724	155	19	3210	0.69	0.47	426
26	203	40	12701	271	30	11055	58	29	1753	0.75	0.50	414
27	186	41	11661	258	25	9943	88	28	2880	0.72	0.48	424
28	216	37	12347	274	31	12127	60	25	1603	0.79	0.47	426
29	185	40	11533	259	32	11512	62	18	1174	0.71	0.48	424
30	94	31	4463	138	24	4985	73	18	2070	0.68	0.39	465
31	251	43	16720	393	26	15903	75	28	2216	0.64	0.48	423
32	1750	37	86149	3686	26	135480	288	22	6808	0.47	0.38	469
33	215	36	12003	299	27	12157	49	34	1752	0.72	0.46	430
34	317	37	18073	448	28	18196	99	23	2449	0.71	0.47	429
35	362	35	19676	396	27	15754	99	26	2680	0.91	0.52	406
36	260	43	17048	421	25	16380	115	24	3088	0.62	0.47	429
37	553	43	32951	1420	30	59883	113	25	3019	0.39	0.34	485
38	351	41	22407	646	21	21310	142	22	3358	0.54	0.48	424
39	139	38	8100	188	27	7746	85	21	1940	0.74	0.46	434

40	221	42	14306	327	27	13245	85	24	2187	0.68	0.48	422
41	382	37	22084	573	27	23396	116	26	3179	0.67	0.45	434
42	258	37	14374	368	31	16212	58	28	1714	0.70	0.45	439
43	266	38	15521	387	28	15443	68	22	1605	0.69	0.48	424
44	181	41	11388	384	25	15153	80	20	1717	0.47	0.40	458
45	257	35	13956	489	28	20552	71	24	1797	0.53	0.38	466
46	247	37	14287	354	26	13748	85	26	2367	0.70	0.47	427
47	635	24	23871	321	45	22409	132	22	3085	1.98	0.48	421

567

Sample 12: YQ18-05

ID	D1_int	D1_FWHM	D1_area	G_int	G_FWHM	G_area	D2_int	D2_FWHM	D2_area	R1	R2	T
1	385	43	25629	414	28	15474	176	26	4804	0.93	0.56	387
2	189	55	14184	338	14	7426	129	58	7994	0.56	0.48	423
3	264	40	16179	168	30	5525	135	24	4219	1.57	0.62	357
4	2216	48	162748	1243	39	74174	429	36	16419	1.78	0.64	349
5	1074	41	68417	833	34	39220	250	28	7334	1.29	0.60	370
6	469	46	30021	305	38	15127	119	34	5861	1.54	0.59	373
7	1505	43	94470	1153	34	57190	271	29	8491	1.31	0.59	373
8	234	37	13408	183	25	6492	155	21	4027	1.28	0.56	386
9	285	44	19201	194	31	8825	141	27	4953	1.47	0.58	376
10	556	48	41380	466	35	22578	228	29	7072	1.19	0.58	376
11	421	49	30034	409	28	17586	121	33	4204	1.03	0.58	377
12	1173	40	66533	1089	34	50646	219	25	5774	1.08	0.54	395
13	401	47	28776	349	32	17295	132	33	4614	1.15	0.57	383
14	467	33	23958	517	25	18006	166	23	4011	0.90	0.52	404
15	373	48	27333	373	33	18863	89	24	2302	1.00	0.56	385
16	524	40	31531	415	30	17785	178	22	4188	1.26	0.59	373
17	430	45	29636	366	37	20986	91	27	2598	1.17	0.56	388
18	524	48	38973	537	32	23990	162	26	4533	0.97	0.58	378
19	503	44	34215	447	32	20582	199	25	7408	1.12	0.55	391
20	1522	36	80539	1851	29	76570	447	21	9808	0.82	0.48	421
21	515	42	33367	220	30	6966	304	22	9932	2.34	0.66	339
22	860	40	50294	1027	32	47930	226	22	5936	0.84	0.48	421
23	795	39	47386	667	33	31178	243	23	5932	1.19	0.56	386
24	1090	57	95402	1151	37	66443	247	28	7479	0.95	0.56	385
25	877	43	58014	893	31	41680	244	29	7561	0.98	0.54	395
26	1135	46	80861	431	38	23272	351	36	13277	2.63	0.69	328
27	532	35	25843	759	29	31530	123	20	2564	0.70	0.43	445
28	609	40	37518	310	29	11762	249	29	7572	1.97	0.66	341
29	501	48	35893	457	37	21353	137	22	3241	1.10	0.59	371
30	438	36	23224	607	29	26078	111	19	2936	0.72	0.44	439
31	951	38	56346	1004	30	43806	321	23	8273	0.95	0.52	405
32	604	49	43136	484	33	23857	190	29	5913	1.25	0.59	372
33	701	44	43467	558	33	25917	173	27	4902	1.26	0.59	375
34	738	46	51905	500	33	24284	271	31	9346	1.48	0.61	365
35	610	41	38715	542	31	23312	249	26	6996	1.13	0.56	386
36	523	39	30581	425	31	16702	172	27	4934	1.23	0.59	375
37	803	36	44698	730	29	31350	248	22	5881	1.10	0.55	393
38	723	37	41314	631	29	25522	245	24	6323	1.15	0.56	384
39	1071	39	63979	830	30	36979	344	20	7425	1.29	0.59	372

40	735	43	44911	398	36	17691	178	30	5693	1.85	0.66	342
41	429	39	26129	397	29	15261	214	24	5387	1.08	0.56	387
42	1175	34	60774	1114	28	43796	329	21	7522	1.05	0.54	394
43	1200	40	68882	1058	35	50178	274	22	6268	1.13	0.55	391
44	405	43	24947	371	37	17222	91	23	2248	1.09	0.56	385
45	981	37	55639	756	30	32191	337	21	7604	1.30	0.58	376
46	415	43	27785	259	31	12456	188	34	6707	1.60	0.59	372
47	1095	37	56524	1279	30	54277	252	20	5411	0.86	0.49	420
48	868	39	46265	803	33	35367	179	23	4363	1.08	0.54	396
49	936	36	48556	1059	30	45075	235	21	5510	0.88	0.49	418
50	411	38	21385	478	30	20260	93	21	2104	0.86	0.49	419
51	512	36	25424	572	29	23183	110	21	2408	0.90	0.50	414
52	869	36	43243	987	30	41739	197	21	4334	0.88	0.48	421
53	2393	36	128035	2289	28	95120	596	19	11891	1.05	0.54	393
54	1468	45	102247	1186	36	65544	278	25	7350	1.24	0.58	375
55	1427	41	89858	1196	32	55411	389	21	8524	1.19	0.58	375
56	1283	40	79790	985	31	47246	415	21	9301	1.30	0.59	375
57	1697	40	104084	1599	33	75305	418	20	9029	1.06	0.55	390
58	1413	49	107201	1117	36	61300	494	16	8482	1.27	0.61	365
59	719	38	42045	629	36	34849	173	17	3676	1.14	0.52	404
60	776	39	42739	780	33	34844	163	22	3791	1.00	0.53	402
61	1206	42	72842	928	37	47003	210	23	5084	1.30	0.58	376
62	1253	39	73386	1137	32	52025	336	20	7018	1.10	0.55	389
63	1289	46	91896	1072	40	65252	215	26	5886	1.20	0.56	385
64	1125	52	86475	943	39	55090	271	36	10493	1.19	0.57	382
65	686	43	45080	604	34	31849	110	25	2982	1.13	0.56	384
66	1648	40	101492	1321	34	64327	454	20	9671	1.25	0.58	378
67	951	44	61514	814	35	41582	198	28	5833	1.17	0.56	384
68	2076	44	140895	2053	35	108761	471	24	12006	1.01	0.54	396
69	644	41	38074	625	35	30975	146	21	3294	1.03	0.53	402
70	1475	38	81202	1515	31	66677	347	22	8225	0.97	0.52	404

568

Sample 14: YQ18-11

ID	D1_int	D1_FWHM	D1_area	G_int	G_FWHM	G_area	D2_int	D2_FWHM	D2_area	R1	R2	T
1	999	42	61508	3007	22	101733	291	15	6726	0.33	0.36	476
1	593	43	38984	1682	30	73437	142	20	3025	0.35	0.34	487
2	696	53	56897	925	36	50857	178	29	7930	0.75	0.49	417
3	704	42	45743	934	28	41122	201	22	4804	0.75	0.50	414
4	322	39	19465	475	30	21635	66	20	1423	0.68	0.46	433
5	361	42	23538	848	27	35106	87	12	1439	0.43	0.39	463
6	451	44	29810	1477	27	57795	130	20	2840	0.31	0.33	491
7	903	39	54865	1422	25	54536	313	18	6054	0.63	0.48	425
8	193	41	12250	280	31	13369	40	23	947	0.69	0.46	431
9	396	43	26116	480	33	24688	61	14	920	0.83	0.50	411
10	249	44	16912	355	28	15375	79	15	1689	0.70	0.50	415
11	782	38	42799	1056	30	44955	196	22	4554	0.74	0.46	430
12	183	59	16502	411	32	20108	59	19	1428	0.45	0.43	444
13	1010	39	60285	1253	31	59592	177	23	4231	0.81	0.49	420
14	413	59	37202	1713	26	69181	122	19	3683	0.24	0.34	487
15	600	43	39806	914	26	36257	183	19	5337	0.66	0.49	418
16	997	41	62428	1176	32	58972	151	22	3594	0.85	0.50	414
17	488	42	31888	708	33	35203	98	24	2488	0.69	0.46	432
18	1108	42	71583	1554	29	70507	288	17	5874	0.71	0.48	421
19	1534	40	91602	1916	31	87262	265	23	6414	0.80	0.49	416
20	749	43	49297	1382	29	61417	154	20	3400	0.54	0.43	444
21	1658	48	121669	2203	34	114118	352	16	8551	0.75	0.50	414
22	298	41	18810	448	29	20219	68	21	1564	0.67	0.46	430
23	1196	39	70850	2050	28	87586	216	18	4148	0.58	0.44	443
24	512	43	34027	1353	28	58959	321	19	6447	0.38	0.34	485
25	465	42	29940	585	26	23691	150	20	4202	0.79	0.52	405
26	1096	61	101633	1662	33	83854	365	24	13253	0.66	0.51	408
27	1375	44	92570	1534	30	72283	342	15	6383	0.90	0.54	395
28	1342	40	80398	1698	32	81008	305	19	6244	0.79	0.48	423
29	413	41	26260	461	29	20838	78	15	1437	0.90	0.54	395
30	724	43	47999	1135	28	48832	177	15	4007	0.64	0.48	424
31	388	40	23935	688	25	26405	132	14	2796	0.56	0.45	436
32	958	46	67934	1244	33	63580	194	26	7849	0.77	0.49	419
33	468	39	28044	801	32	37815	83	21	1805	0.58	0.41	452
34	551	42	35522	579	30	26746	127	21	3281	0.95	0.54	394
35	721	41	45362	1128	30	51894	144	20	3822	0.64	0.45	437
36	268	36	15089	408	23	14652	96	23	2687	0.66	0.47	429
37	119	51	9304	137	38	7992	8	12	107	0.86	0.53	398
38	215	47	15682	377	33	18931	74	13	1270	0.57	0.44	442

39	101	61	9490	143	30	6624	29	50	2159	0.71	0.52	405
40	163	168	39850	127	0	32	223	64	20154	1.28	0.66	339
41	543	43	35791	763	29	34459	182	14	3411	0.71	0.49	420
42	536	45	34540	934	29	40770	103	22	2382	0.57	0.44	439
43	703	44	47784	1011	25	39418	268	14	4839	0.70	0.52	405
44	428	38	25445	514	30	23892	63	24	1591	0.83	0.50	414
45	869	39	51045	1096	32	53351	132	23	3191	0.79	0.47	425
46	547	46	39112	928	28	40427	160	22	3952	0.59	0.47	428
47	530	43	35500	760	28	32431	172	19	4981	0.70	0.49	419
48	401	39	24317	568	33	28975	73	15	1733	0.71	0.44	440
49	287	44	19651	496	33	24986	73	23	2645	0.58	0.42	452
50	387	40	24222	541	30	25045	95	18	1804	0.72	0.47	425
51	712	41	44558	874	32	41590	149	23	3604	0.81	0.50	415
52	447	40	26233	606	32	28162	69	25	1820	0.74	0.47	429
53	350	34	18430	487	32	23858	42	16	689	0.72	0.43	446
54	240	40	14852	293	30	13589	59	20	1247	0.82	0.50	413
55	332	66	33580	447	37	25347	112	32	5513	0.74	0.52	404
56	1464	50	112145	2056	29	92146	547	17	14262	0.71	0.51	408

569

Sample 15: YQ18-12

ID	D1_int	D1_FWHM	D1_area	G_int	G_FWHM	G_area	D2_int	D2_FWHM	D2_area	R1	R2	T
1	449	45	28812	1108	28	46579	83	22	1915	0.41	0.37	471
2	95	46	5998	253	28	10946	20	15	457	0.37	0.34	484
3	73	45	4708	168	27	6882	33	13	681	0.44	0.38	466
4	112	45	6562	534	26	19418	22	28	653	0.21	0.25	529
5	296	43	18957	515	27	20992	68	23	1675	0.58	0.46	434
6	212	45	12781	756	28	29226	42	25	1109	0.28	0.30	506
7	177	41	10785	269	34	12811	33	25	849	0.66	0.44	440
8	670	41	40482	888	29	39975	114	22	2624	0.75	0.49	419
9	249	39	14865	312	30	14561	45	22	1049	0.80	0.49	419
10	138	38	8076	208	31	9309	28	25	732	0.66	0.45	438
11	211	39	12884	315	30	14728	38	21	931	0.67	0.45	436
12	189	44	11997	1106	24	38066	49	30	1544	0.17	0.23	535
13	244	39	13319	630	27	23521	57	23	1388	0.39	0.35	482
14	870	37	45746	1235	29	53070	141	19	2951	0.70	0.45	436
15	196	39	11852	286	30	13303	34	17	871	0.69	0.46	434
16	207	41	12316	346	30	14933	41	25	1098	0.60	0.43	443
17	172	43	9408	777	26	28988	45	25	1193	0.22	0.24	533
18	514	42	33599	908	31	43721	75	19	1521	0.57	0.43	447
19	345	37	18521	565	28	21482	70	25	1862	0.61	0.44	440
20	344	44	23154	577	30	27173	61	22	1443	0.60	0.45	438
21	641	37	36110	719	29	31544	99	23	2461	0.89	0.52	407
22	201	37	11401	349	27	13515	28	20	600	0.58	0.45	438
23	257	40	15370	572	30	24467	50	24	1281	0.45	0.37	471
24	245	39	14139	255	31	11303	37	22	843	0.96	0.54	396
25	134	42	8249	164	30	7250	22	26	591	0.82	0.51	408
26	277	40	15102	535	29	21542	44	22	997	0.52	0.40	458
27	626	42	34633	1164	30	47698	110	23	2737	0.54	0.41	456
28	232	41	14040	335	31	15511	37	25	965	0.69	0.46	432
29	246	43	14969	410	30	17871	42	28	1261	0.60	0.44	441
30	228	41	13072	715	26	26292	47	23	1125	0.32	0.32	494
31	191	40	11722	269	29	11947	30	28	890	0.71	0.48	424
32	583	37	32482	829	29	35284	96	18	1848	0.70	0.47	429
33	491	38	26862	582	31	25398	79	24	2020	0.84	0.49	416
34	345	40	18485	415	31	17395	68	22	1621	0.83	0.49	417
35	277	39	16838	577	29	24182	56	24	1466	0.48	0.40	461
36	252	39	15338	376	30	17683	46	19	944	0.67	0.45	436
37	558	41	32841	580	33	27695	84	22	1967	0.96	0.53	402
38	265	38	15312	369	30	16046	45	20	987	0.72	0.47	426
39	227	39	12817	300	31	13215	38	22	886	0.76	0.48	424

40	118	34	6224	171	28	6993	20	18	389	0.69	0.46	433
41	98	40	6040	154	28	6332	17	26	462	0.64	0.47	427
42	137	40	8402	227	30	9994	28	27	794	0.60	0.44	442
43	225	38	12122	453	26	16906	58	27	1635	0.50	0.40	461
44	212	45	12041	1049	27	38867	51	27	1440	0.20	0.23	536
45	1341	43	89843	1798	36	99042	83	24	2141	0.75	0.47	427
46	448	38	22425	1182	25	40788	125	24	3168	0.38	0.34	487
47	115	45	7612	324	28	12681	34	27	962	0.36	0.36	478
48	90	33	4582	214	25	7361	19	27	559	0.42	0.37	474
49	350	40	16657	1310	27	47441	70	25	1882	0.27	0.25	526
50	381	41	21362	1070	27	40614	84	23	2020	0.36	0.33	489
51	423	37	20401	1043	28	38937	87	22	1982	0.41	0.33	490
52	185	37	10081	399	27	15740	40	29	1211	0.46	0.37	471
53	183	40	10978	412	27	16161	33	26	928	0.44	0.39	463
54	170	39	9778	253	25	9963	42	42	1863	0.67	0.45	435
55	553	37	27700	1100	28	42095	123	24	3084	0.50	0.38	468
56	264	36	14627	625	25	23228	72	30	2253	0.42	0.36	475
57	285	40	15148	466	30	19391	46	24	1181	0.61	0.42	448
58	357	40	20080	494	31	20984	65	25	1744	0.72	0.47	428
59	236	42	11543	941	28	35448	38	24	963	0.25	0.24	531
60	129	40	6765	248	28	9825	23	26	632	0.52	0.39	462
61	352	39	20179	528	28	22292	60	22	1430	0.67	0.46	432

570

Sample 16: YQ18-13a

ID	D1_int	D1_FWHM	D1_area	G_int	G_FWHM	G_area	D2_int	D2_FWHM	D2_area	R1	R2	T
1	570	37	32362	633	28	26858	161	23	4171	0.90	0.51	409
2	368	35	20184	409	30	18465	122	25	3282	0.90	0.48	422
3	1156	43	76923	1639	26	65268	398	17	8262	0.70	0.51	408
4	2072	45	142851	3635	26	149043	571	13	11486	0.57	0.47	427
5	1351	41	82373	1868	29	81625	311	19	6213	0.72	0.48	421
6	1870	42	122038	2636	26	107159	606	17	10985	0.71	0.51	410
7	824	38	48142	1115	28	48965	196	19	4019	0.74	0.48	424
8	666	36	36670	794	28	33658	161	19	3264	0.84	0.50	414
9	295	32	14822	342	28	14736	98	25	2635	0.86	0.46	432
10	671	38	39434	876	28	37249	157	17	2903	0.77	0.50	416
11	1092	37	61665	1489	26	58415	307	17	5550	0.73	0.49	418
12	677	38	39342	791	27	33063	180	21	4075	0.86	0.51	407
13	889	38	52683	1058	27	43891	209	18	4117	0.84	0.52	403
14	758	40	47270	975	28	41523	205	17	4372	0.78	0.51	410
15	363	42	23717	497	27	19725	107	24	2698	0.73	0.51	407
16	782	46	54832	1074	26	43158	277	18	5223	0.73	0.53	399
17	496	39	30110	682	28	29564	116	26	3247	0.73	0.48	423
18	567	40	35140	773	32	37899	103	18	1984	0.73	0.47	428
19	554	38	32005	748	32	33278	123	24	3201	0.74	0.47	428
20	924	41	57605	1268	31	59873	185	20	3960	0.73	0.47	425
21	760	39	44955	1020	31	48203	136	18	2807	0.74	0.47	428
22	1315	45	91429	1830	29	81113	429	15	8886	0.72	0.50	412
23	818	39	49314	1287	26	52552	235	18	4595	0.64	0.46	430
24	394	41	24845	551	27	22723	103	18	2026	0.72	0.50	413
25	683	39	40649	850	29	37920	170	17	3005	0.80	0.50	414
26	583	38	33972	762	28	32497	155	20	3334	0.77	0.49	420
27	655	45	45047	831	29	37154	231	35	12620	0.79	0.48	425
28	979	42	62478	1122	32	54012	162	23	3997	0.87	0.52	405
29	973	41	62049	1445	28	62153	297	16	5127	0.67	0.48	423
30	889	40	49357	1683	27	66586	183	19	3762	0.53	0.41	453
31	1195	36	66545	1558	28	63487	181	19	3731	0.77	0.50	415
32	404	36	20944	792	24	26386	103	21	2330	0.51	0.42	449
33	453	36	24873	810	24	30168	114	27	3225	0.56	0.43	447
34	365	36	20294	717	26	27558	77	26	2172	0.51	0.41	456
35	416	38	24685	831	24	30806	117	23	2814	0.50	0.42	448
36	298	35	15938	592	26	20825	137	23	3348	0.50	0.40	460
37	966	37	54050	1532	27	59146	183	23	4465	0.63	0.46	432
38	721	41	45662	1073	24	32878	340	33	17347	0.67	0.48	424
39	1375	40	77150	2520	29	106362	174	22	4074	0.55	0.41	454

40	587	38	34118	1228	28	51355	93	24	2358	0.48	0.39	464
41	767	39	46710	1587	28	64519	225	19	4544	0.48	0.40	457
42	1167	39	62386	1854	29	76868	170	22	3951	0.63	0.44	443
43	420	35	22985	620	25	23352	85	22	2015	0.68	0.48	425
44	1306	34	67494	1536	27	61451	198	21	4453	0.85	0.51	411
45	460	36	25889	501	36	27761	104	9	1090	0.92	0.47	426
46	565	40	32144	592	32	27485	100	22	2301	0.95	0.52	405
47	616	41	35652	837	31	37550	131	21	2877	0.74	0.47	428
48	1290	39	78028	1578	31	75987	237	21	5294	0.82	0.49	418
49	1688	42	108345	2641	26	107255	528	17	13996	0.64	0.47	426
50	814	39	48713	1556	25	59986	247	16	4247	0.52	0.43	445
51	814	39	49557	1298	26	52298	275	17	5037	0.63	0.46	430
52	1378	41	86662	1724	28	73982	367	17	7091	0.80	0.52	406
53	675	39	39706	769	31	35046	165	26	4593	0.88	0.50	413
54	978	40	57732	1199	32	54771	213	21	4686	0.82	0.49	417
55	682	40	41377	1171	27	48860	184	17	3501	0.58	0.44	440
56	1085	38	64056	1546	31	73889	220	18	4137	0.70	0.45	436
57	1208	40	74674	2270	28	95563	324	17	5948	0.53	0.42	448
58	589	41	36591	976	31	45657	108	22	2547	0.60	0.43	445
59	1242	40	75699	1479	30	66605	299	21	6745	0.84	0.51	410
60	874	42	55990	1143	32	53679	192	21	4375	0.76	0.49	418
61	594	40	36368	812	29	35646	152	20	3243	0.73	0.48	421
62	871	36	47096	1130	28	44857	140	24	3536	0.77	0.49	417
63	1166	36	62753	1885	26	73662	210	21	4708	0.62	0.44	439
64	937	36	50356	1179	28	47288	147	22	3497	0.79	0.50	414
65	961	36	51640	1332	28	54328	145	22	3339	0.72	0.47	426
66	401	38	23533	629	28	25504	113	19	2723	0.64	0.45	434

571